Neural Correlates and Mechanisms of Sound Localization in Everyday Reverberant Settings

by

Sasha Devore

S.B. Electrical Engineering, MIT 2001
M.Eng. Electrical Engineering and Computer Science, MIT, 2005

Submitted to the Harvard-MIT Division of Health Sciences and Technology
in partial fulfillment of the requirements for the degree of

DOCTOR OF PHILOSOPHY

at the

MASSACHUSETTS INSTITUTE OF TECHNOLOGY

June 2009

Signature of Author: .....
Harvard-MIT Division of Health Sciences and Technology
May 15, 2009

Certified by: .....
Bertrand Delgutte, Ph.D.
Associate Professor of Otology and Laryngology and Health Sciences and Technology
Thesis Supervisor

Accepted by: .....
Ram Sasisekharan, Ph.D.
Edward Hood Taplin Professor of Health Sciences and Technology and Biomedical Engineering
Director, Harvard-MIT Division of Health Sciences and Technology

Neural correlates and mechanisms of sound localization in everyday reverberant settings

by

Sasha Devore

Submitted to the Harvard-MIT Division of Health Sciences and Technology
on May 15, 2009 in partial fulfillment of the requirements
for the degree of Doctor of Philosophy

Abstract

Nearly all listening environments—indoors and outdoors alike—are full of boundary surfaces (e.g., walls, trees, and rocks) that produce acoustic reflections. These reflections interfere with the direct sound arriving at a listener's ears, distorting the binaural cues for sound localization. Yet, human listeners have little difficulty localizing sounds in most settings. This thesis addresses fundamental questions regarding the neural basis of sound localization in everyday reverberant environments.

In the first set of experiments, we investigate the effects of reverberation on the directional sensitivity of low-frequency auditory neurons sensitive to interaural time differences (ITD), the principal cue for localizing sound containing low frequency energy. Because reverberant energy builds up over time, the source location is represented relatively faithfully during the early portion of a sound, but this representation becomes increasingly degraded later in the stimulus. We show that the directional sensitivity of ITD-sensitive neurons in the auditory midbrain of anesthetized cats and awake rabbits follows a similar time course. However, the tendency of neurons to fire preferentially at the onset of a stimulus results in more robust directional sensitivity than expected, suggesting a simple mechanism for improving directional sensitivity in reverberation. To probe the role of temporal response dynamics, we use a conditioning paradigm to systematically alter temporal response patterns of single neurons. Results suggest that making temporal response patterns less onset-dominated typically leads to poorer directional sensitivity in reverberation. In parallel behavioral experiments, we show that human lateralization judgments are consistent with predictions from a population rate model for decoding the observed midbrain responses, suggesting a subcortical origin for robust sound localization in reverberant environments.

In the second part of the thesis we examine the effects of reverberation on directional sensitivity of neurons across the tonotopic axis in the awake rabbit auditory midbrain. We find that reverberation degrades the directional sensitivity of single neurons, although the amount of degradation depends on the characteristic frequency and the type of binaural cues available. When ITD is the only available directional cue, low frequency neurons sensitive to ITD in the fine-time structure maintain better directional sensitivity in reverberation than high frequency neurons sensitive to ITD in the envelope. On the other hand, when both ITD and interaural level differences (ILD) cues are available, directional sensitivity is comparable throughout the tonotopic axis, suggesting that, at high frequencies, ILDs provide better directional information than envelope ITDs in reverberation. These findings can account for results from human psychophysical studies of spatial hearing in reverberant environments.

This thesis marks fundamental progress towards elucidating the neural basis for spatial hearing in everyday settings. Overall, our results suggest that the information contained in the

rate responses of neurons in the auditory midbrain is sufficient to account for human sound localization in reverberant environments.

Thesis Supervisor: Bertrand Delgutte, Ph.D.
Title: Associate Professor of Otology and Laryngology and Health Sciences and Technology

Acknowledgments

First and foremost, I would like to express my deepest gratitude to Bertrand Delgutte for his enduring confidence in me and for giving me, on the one hand, freedom to develop my research and, on the other hand, sound advice and guidance at each step of the way. His wisdom and scientific rigor have left indelible marks on my research.

My interest in auditory neuroscience originated during my studies with Barbara Shinn-Cunningham, and I am grateful to her for continuing to mentor and support me even as I left behavior for physiology. Her self-confidence, insightful comments, and tremendous enthusiasm create a fertile environment for developing scientific ideas.

The often direct but sometimes subtle influence of Ken Hancock can be found throughout this thesis. I am grateful to him for sharing both his intellectual passion and tools of the trade, and for patiently answering all of my questions and never hesitating to come running to Chamber 2 during the countless "crises" that are an inevitable part of experimental science.

I am extremely grateful to both Laurel Carney and Shig Kuwada for sharing their expertise of the awake rabbit preparation and enthusiastically welcoming me to their laboratories during the many visits it took for me to absorb the basics of the setup.

During my studies at MIT, I have also had the fortune of interacting with Chris Moore. His rapid ideas and amazing ability of simultaneously seeing the forest *and* the trees have opened my mind to new ways of thinking about the brain.

The work in this thesis would not have been possible were it not for the support of numerous research, engineering, and administrative staff members of Eaton Peabody Laboratory (EPL). Special thanks go to: Ken Hancock, Connie Miller, Mike Ravicz, Dianna Sands, Chris Scarpino, Ishmael Stefanov, and Melissa Wood.

I am fortunate for having been surrounded by so many brilliant, passionate, and caring peers. I am grateful to Antje Ihlefeld for our very fruitful discussions on all topics, and for her constant encouragement. My experience at MIT and EPL also owes much to Brad Buran, Adrian KC Lee, Xiao-Ping Liu, Ted Moallem, Tony Okobi, SR Prakash, Michael Slama, Ryuji Suzuki, Grace Wang, Bo Wen, and Courtenay Wilson.

I am grateful to Ben Guaraldi and Morgan Frank, for always forcing a smile to appear on my face.

Finally, my parents Cindy Langewisch and Vincent Devore and my sisters Rachel and Samara for their unending love and support and my dear Rafael, for never failing to believe.

Please forgive me any omissions.

Table of Contents

List of Figures

CHAPTER 1

General Introduction

Sound localization can be paramount for survival. For example, the ability to localize sound enables a predator to determine the whereabouts of prey in a visually dense environment. Moreover, sound localization can facilitate the identification of relevant sounds amidst the background of noise that is typical of our everyday listening conditions (Darwin, 2008; Kidd et al., 2005a; Shinn-Cunningham, 2008). But nearly all environments, indoors and outdoors alike, are full of boundary surfaces (e.g., walls, trees, rocks) that generate acoustic reflections. These reflections, perceived not as discrete echoes but as a unified acoustic entity termed *reverberation*, pose a challenge to accurate sound localization.

To localize sounds in the horizontal plane, listeners rely principally on two binaural, acoustic cues that result from the separation of the ears on the head (Kuhn, 1977; Shaw, 1974). The differential path-length from a sound source to the two ears gives rise to interaural time differences (ITD), whereas interaural level differences (ILD) are caused by interference of the head with the diffraction of sound waves. Accurate sound localization requires the binaural cues at a listener's ears to faithfully represent the sound source location, although listeners typically weight ITD more heavily than ILD when the sound contains low-frequency energy (Macpherson and Middlebrooks, 2002; Wightman and Kistler, 1992).

In reverberant environments, acoustic reflections interfere with the direct sound arriving at a listener's ears, distorting the binaural cues for sound localization (Hartmann

et al., 2005; Shinn-Cunningham et al., 2005a). Specifically, reverberation leads to temporal fluctuation in both ITD and ILD, dissimilarity of the signals at the two ears, and an overall reduction in the magnitude of ILDs (Ihlefeld and Shinn-Cunningham, 2004; Shinn-Cunningham and Kawakyu, 2003; Shinn-Cunningham et al., 2005a). In general, these effects become more severe with increasing distance between the sound source and the listener, as the ratio of direct to reflected sound energies (D/R) decreases.

In one of the pioneering investigations of sound localization in rooms, Hartmann (1983) demonstrated that localization accuracy for sources near the midline was largely unaffected by reverberation for impulsive sounds (i.e., 50-ms rectangularly gated tone pips), despite the degradation in ongoing binaural cues. However, with increasing reverberation i.e., decreasing D/R, localization accuracy degraded for sounds *lacking* onset transients, although localization accuracy was better for broadband noise sources than pure tones. In a later study, Rakerd and Hartmann (2005) demonstrated that masking the early portion of a broadband noise source in reverberation significantly reduces localization accuracy, with effects becoming more severe with decreasing D/R. Shinn-Cunningham et al. (2005b) demonstrated that listeners can accurately localize broadband sources near the midline in moderate reverberation, but that localization accuracy at lateral azimuths degrades with decreasing D/R. In general, behavioral studies concur that listeners have little difficulty localizing broadband sounds in moderate reverberation, although giving listeners access to the early portion of an acoustic stimulus, before the buildup of reverberation, seems to be crucial for accurate sound localization in reverberation.

Accurate sound localization in reverberant environments is often ascribed to the precedence effect or "law of the first wavefront" (Litovsky et al., 1999; Wallach et al., 1949). The precedence effect refers to the perceptual phenomenon in which a listener perceives two successive acoustic sources from disparate locations as a single fused source near the location of the leading sound. Such "localization dominance" typically breaks down at 5-10ms for impulsive acoustic sources (i.e., clicks) that do not overlap in time but can last up to 50ms for ongoing stimuli such as speech [reviewed in (Litovsky et al., 1999)].

Neural correlates of the precedence effect have been reported at virtually all stages in the auditory pathway, from the auditory nerve to the auditory cortex (Fitzpatrick et al., 1999; Litovsky and Delgutte, 2002; Litovsky and Yin, 1998; Pecka et al., 2007; Spitzer et al., 2004; Tollin et al., 2004; Yin, 1994). Typically, the time course of neural echo suppression is characterized by comparing the rate response to the lagging source to a baseline rate response obtained for an identical sound source presented in isolation.

In all of these studies, the stimuli consisted of a direct sound followed by a single reflection, which is an extreme over-simplification of everyday reverberation. For realistic ongoing sound sources in a reverberant environment, thousands of echoes contribute to the energy reaching a listener's ears over hundreds of milliseconds with considerable temporal overlap between the direct sound and the reflections. To date, no one has studied the directional sensitivity of auditory neurons using stimuli with realistic reverberation. Thus, the degree to which auditory neurons maintain robust directional sensitivity in reverberant environments is unknown.

This thesis addresses fundamental questions regarding the ability of auditory neurons to encode sound source location in reverberant environments. Using standard single-unit electrophysiological recording techniques, we characterize the effects of reverberation on directional sensitivity of binaural neurons in the auditory midbrain of both awake and anesthetized mammals, focusing on cells that are sensitive to ITD. Overall, we find that the information contained in the rate responses of ITD-sensitive IC neurons is sufficient to account for human sound localization in reverberation.

ITDs are initially coded in the auditory pathway as differences in phase-locked spike timing between auditory nerve fibers on the left and right sides of the head (Johnson, 1980; Joris, 2003; Kiang, 1965). These timing differences are transformed to a rate code by two distinct circuits in the superior olivary complex (SOC), the initial site of binaural interaction in the ascending auditory pathway (Caird and Klinke, 1983; Goldberg and Brown, 1969; Joris and Yin, 1995; Yin and Chan, 1990).

Principle cells in the medial superior olive (MSO) detect coincidences in predominately low-frequency convergent excitatory inputs from the cochlear nuclei on either side of the head (Cant and Casseday, 1986; Goldberg and Brown, 1969; Yin and Chan, 1990). The firing rate of MSO neurons, which is theoretically equivalent to a cross-correlation on the input spike trains (Colburn, 1973), is typically greatest when the binaural inputs arrive in phase (Batra et al., 1997a; Yin and Chan, 1990).

Neurons in the lateral superior olive (LSO) receive predominately high-frequency convergent excitatory input from the ipsilateral cochlear nucleus (Cant and Casseday, 1986) and inhibitory input from the contralateral cochlear nucleus via the medial nucleus of the trapezoid body. Although these subtractive circuits in the LSO are classically

associated with generating neural sensitivity to ILD (Boudreau and Tsuchitani, 1968; Tollin and Yin, 2002), a substantial fraction of LSO neurons are also sensitive to ITD (Batra et al., 1997a; Joris and Yin, 1995; Tollin and Yin, 2005). Owing to the excitatory-inhibitory interaction, the firing rate of LSO neurons is typically smallest when the binaural inputs arrive in phase (Joris and Yin, 1995; Tollin and Yin, 2005).

Most neurophysiological studies of binaural hearing have targeted the inferior colliculus (IC), the primary nucleus comprising the auditory midbrain (Aitkin et al., 1984; Hancock and Delgutte, 2004; Joris, 2003; Kuwada et al., 1987; Kuwada and Yin, 1983; McAlpine et al., 2001; Rose et al., 1966; Yin et al., 1986). The IC is an essentially obligatory synaptic station for ascending inputs to the thalamus and auditory cortex (Adams, 1979) and, as such, it receives direct and indirect inputs from both the MSO and LSO (Aitkin and Schuck, 1985; Oliver et al., 1995). While ITD tuning in the IC often mirrors its brainstem inputs (Yin and Kuwada, 1983), a substantial fraction of neurons exhibit an intermediate form of tuning that may result from convergent brainstem inputs (Agapiou and McAlpine, 2008; Batra et al., 1993; Fitzpatrick et al., 2002; McAlpine et al., 1998; Yin and Kuwada, 1983), although this form of tuning may also be partly inherited from the brainstem (Batra et al., 1997a; Batra et al., 1997b).

Neural sensitive to ITD spans the tonotopic axis in the IC (Batra, 1989; Griffin et al., 2005; Joris, 2003; Kuwada et al., 1987; Kuwada and Yin, 1983; McAlpine et al., 2001; Rose et al., 1966; Yin et al., 1986; Yin et al., 1984). Low characteristic frequency (CF) IC neurons are typically sensitive to ITD in the stimulus fine structure, while high frequency neurons are sensitive to ITD in the envelope (Joris, 2003). Most high-CF IC neurons are also sensitive to ILDs (Aitkin et al., 1972; Aitkin and Martin, 1987; Semple

and Kitzes, 1987; Stillman, 1972). Moreover, for stimuli containing naturally co-occurring binaural cues, ILD may be a more potent cue than envelope ITD (Delgutte et al., 1995).

The importance of the IC in sound localization is evident from lesion studies. Following unilateral ablation of the IC, animals show a deficit in orientating to sound sources, particularly in the hemifield contralateral to the lesion (Jenkins and Masterton, 1982; Masterton et al., 1968; Thompson and Masterton, 1978). Bilateral ablation of the IC results in a complete deficit of left-right sound source discrimination, despite the fact that hearing is still present (Masterton et al., 1968). Moreover, a case study of a single human patient with a lesion that included the right IC indicated impaired localization in the contralateral hemifield (Litovsky et al., 2002), suggesting a pivotal role of the IC in sound localization.

In this thesis, we investigate the effects of reverberation on directional sensitivity of ITD-sensitive neurons in the IC of small mammals. The initial set of experiments (Chapter 2) was done using an anesthetized cat animal model, which has been the standard in our laboratory for over 20 years. To avoid possible confounds due to the effects of anesthesia on neural processing in the IC (Kuwada et al., 1989; Ter-Mikaelian et al., 2007; Tollin et al., 2004; Torterolo et al., 2002), we developed a chronic, unanesthetized rabbit preparation. A great deal of knowledge is already available on the responses of auditory midbrain neurons in both preparations, providing a substantial knowledge base on which we build.

In Chapters 2 and 3 we characterize the effects of reverberation on the directional sensitivity of low-frequency ITD-sensitive neurons in the IC of anesthetized cats and

awake rabbits, respectively. Results show that reverberation similarly degrades the directional sensitivity of single neurons in the IC of anesthetized cats and awake rabbits, although directional sensitivity is generally better than predictions from a traditional cross-correlation model of binaural processing. We demonstrate that such neural robustness to reverberation may be mediated by onset dominance in temporal response patterns, the tendency for neurons to fire more spikes near the stimulus onset. In Chapter 4, we directly examine the role of onset dominance by using a conditioning paradigm to alter temporal response patterns in single neurons in the awake rabbit IC. In Chapter 5 we investigate the effects of reverberation on directional sensitivity of ITD-sensitive neurons in the awake rabbit IC across the tonotopic axis. Our results suggest that reverberation degrades the directional sensitivity of single neurons, although the amount of degradation depends on CF and the types of binaural cues available. In general, our findings are consistent with recent human psychophysical studies of spatial hearing in reverberation, indicating that the directional information contained in the rate responses of ITD-sensitive IC neurons is sufficient to account for human sound localization in reverberation.

CHAPTER 2

Effects of reverberation on directional sensitivity of low-frequency ITD-sensitive neurons in the inferior colliculus of anesthestized cat

This chapter has been published in *Neuron* and is included here with permission:

Devore, S., A. Ihlefeld, K.E. Hancock, B.G. Shinn-Cunningham, and B. Delgutte (2009). Accurate sound localization in reverberation is mediated by robust encoding of spatial cues in the auditory midbrain. *Neuron*, 62(1), pp 123-34.

Abstract

In reverberant environments, acoustic reflections interfere with the direct sound arriving at a listener's ears, distorting the spatial cues for sound localization. Yet, human listeners have little difficulty localizing sounds in most settings. Because reverberant energy builds up over time, the source location is represented relatively faithfully during the early portion of a sound, but this representation becomes increasingly degraded later in the stimulus. We show that the directional sensitivity of single neurons in the auditory midbrain of anesthetized cats follows a similar time course, although onset dominance in temporal response patterns results in more robust directional sensitivity than expected, suggesting a simple mechanism for improving directional sensitivity in reverberation. In parallel behavioral experiments, we demonstrate that human lateralization judgments are consistent with predictions from a population rate model decoding the observed midbrain responses, suggesting a subcortical origin for robust sound localization in reverberant environments.

Introduction

The ability to localize sound sources can be important for survival and facilitates the identification of target sounds in multi-source environments (Darwin, 2008; Kidd et al., 2005a; Shinn-Cunningham, 2008). The auditory scenes that we perceive unfold in environments full of surfaces like walls, trees, and rocks (Huisman and Attenborough, 1991; Sakai et al., 1998). When an acoustic wave emanating from a sound source strikes a boundary surface, a fraction of the energy is reflected. The reflected waves themselves generate second order reflections, with the process repeating *ad infinitum*. The myriad of temporally overlapping reflections, perceived not as discrete echoes but as a single acoustic entity, is referred to as reverberation.

Reverberation poses a challenge to accurate sound localization. To estimate the location of a sound source with low frequency energy, such as speech, human listeners rely principally on tiny interaural time differences (ITDs) that result from the separation of the ears on the head (Macpherson and Middlebrooks, 2002; Wightman and Kistler, 1992). In a reverberant environment, reflected acoustic waves reach the listener from all directions, interfering with the direct sound. Under such conditions, the ear-input signals become decorrelated (Beranek, 2004) and the instantaneous ITD fluctuates (Shinn-Cunningham and Kawakyu, 2003). Because reverberant energy builds up over time, the directional information contained in the ear-input signals has a characteristic time course, in that ITD cues represent the true source location relatively faithfully during the early portion of a sound, but become increasingly degraded later in the stimulus.

In principle, listeners could accurately localize sounds in reverberation by basing their judgments on the directional information in the uncorrupted onset of the signals

reaching the ears. Although human listeners can robustly localize sound sources in moderate reverberation (Hartmann, 1983; Rakerd and Hartmann, 2005), localization accuracy degrades in stronger reverberation (Giguere and Abel, 1993; Rakerd and Hartmann, 2005; Shinn-Cunningham et al., 2005b), suggesting that listeners are not immune to the ongoing, corrupted directional cues. To date, no one has studied the directional sensitivity of auditory neurons using stimuli with realistic reverberation. Thus, the degree to which auditory neurons maintain robust directional sensitivity in reverberation is unknown.

ITDs are initially coded in the auditory pathway as differences in relative spike timing between auditory nerve fibers on the left and right sides of the head. These timing differences are transformed to a rate code in the medial superior olive (MSO), where morphologically and physiologically specialized neurons (Grothe and Sanes, 1994; Scott et al., 2005; Smith, 1995; Svirskis et al., 2004) perform coincidence detection on convergent input from both sides of the head (Goldberg and Brown, 1969; Yin and Chan, 1990). Theoretically, the average firing rate of these coincidence detectors is equivalent to a cross-correlation of the input spike trains (Colburn, 1973).

The majority of neurophysiological studies of spatial processing have targeted the inferior colliculus (IC), the primary nucleus comprising the auditory midbrain (Aitkin et al., 1984; Delgutte et al., 1999; Joris, 2003; Kuwada et al., 1987; Kuwada and Yin, 1983; McAlpine et al., 2001; Rose et al., 1966; Stillman, 1971a; Yin et al., 1986). Multiple, parallel sound-processing pathways in the auditory brainstem converge in the IC (Adams, 1979; Oliver et al., 1995), making it a site of complex synaptic integration. Despite this complexity, the rate responses of low-frequency, ITD-sensitive IC neurons to broadband

signals with a static interaural delay resemble the responses of ITD-sensitive neurons in the MSO (Yin et al., 1986) and are well-modeled as a cross-correlation of the acoustic ear-input signals, after accounting for cochlear frequency filtering (Hancock and Delgutte, 2004; Yin et al., 1987).

Here, we investigate the effects of reverberation on the directional sensitivity of low-frequency ITD-sensitive IC neurons. Consistent with the buildup of reverberation in the acoustic inputs, we show that directional sensitivity is better near the onset of a reverberant stimulus and degrades over time, although directional sensitivity is more robust than predictions from a traditional cross-correlation model of binaural processing that is insensitive to temporal dynamics in the reverberant sound stimuli. We further show that human lateralization judgments in reverberation are consistent with predictions from a population rate model for decoding the observed midbrain responses, suggesting that robust encoding of spatial cues in the auditory midbrain can account for human sound localization in reverberant environments.

Methods

Surgical Preparation

Healthy, adult cats were anesthetized with dial-in-urethane (75 mg/kg, i.p.) and prepared for acute single-unit recording from the auditory midbrain using surgical procedures described in Hancock and Delgutte (2004). All surgical and experimental procedures were approved by the Institute Animal Use and Care Committees at both the Massachusetts Eye and Ear Infirmary and the Massachusetts Institute of Technology.

Virtual Space Stimuli

Binaural room impulse responses (BRIRs) were simulated using the room-image method (Allen and Berkley, 1979; Shinn-Cunningham et al., 2001) for a pair of receivers separated by 12 cm slightly displaced from the center of a virtual room measuring 11x13x3 meters (Fig. 2.1A). The inter-receiver distance was chosen so that the range of ITDs in the direct sound spanned the range typically experienced by cats (±360 μs, Fig. 2.1D). Because we did not include a model of the cat head in the simulations, the resulting BRIRs contained ITD but essentially no interaural level difference (ILD) cues. BRIRs were calculated for azimuths spanning the frontal hemifield (–90° to +90°) at distances of 1 and 3 m with respect to the midpoint of the receivers. Anechoic impulse responses were created by time-windowing the direct sound from the 1m reverberant BRIRs. Virtual auditory space stimuli were created by convolving the BRIRs with a 400-ms burst of exactly reproducible Gaussian broadband noise gated with 4-ms $\sin^2$ ramps (Fig. 2.1B).

Single Unit Recordings

Experimental procedures for recording activity from single units in the auditory midbrain were as described in Hancock and Delgutte (2004). When a single unit was isolated, we estimated its characteristic frequency (CF) using an automatic tracking procedure (Kiang and Moxon, 1974) and then determined the intensity threshold for diotic broadband noise. ITD-sensitivity for 200-ms broadband noise bursts (2/sec x 10 repeats) was characterized at ~15 dB above threshold. Typically, ITD was varied between ±2000μs in 200μs steps. Only ITD-sensitive units with low CFs (<2.5 kHz) were further studied with the virtual space stimuli, with responses for each of the three room conditions obtained in pseudorandom order (1/sec x 16 repeats at each azimuth).

Data Analysis

A rate-azimuth curve for each room condition was computed by averaging the number of spikes that occurred in a fixed temporal window, defined relative to stimulus onset, across all trials for each azimuth. Rate-azimuth curves were smoothed using a three point triangular smoothing filter having weights [1/6 2/3 1/6]. We computed average cumulative peristimulus time histograms (cPSTH) for each unit to obtain a metric of onset dominance in the response. Each 1 ms bin in the cPSTH represents the cumulative number of spikes up to the bin time in the anechoic PSTH. The cPSTH was computed over a 400 ms duration, with time zero corresponding to the first bin in the anechoic PSTH having an across-trial spike count distribution significantly different from that of spontaneous activity. Only azimuths that evoked mean firing rates ≥90% of the maximum rate across all azimuths were included in the average cPSTH in order to avoid including onset responses that often occur at unfavorable azimuths.

Single-Neuron Cross-Correlation Model

We used a cross-correlation model to predict reverberant rate-azimuth curves of IC units. For each unit, we fit the rate-ITD curve with a modified version of the Hancock and Delgutte (2004) cross-correlation model (Fig. 2.4A). The original model used a parabolic function to transform IACC into firing rate. We modified this transformation to be a power function of the form:

$$R(\rho) = a \cdot (\frac{1+\rho}{2})^p + b,$$

where *a, b* ,and *p* are free parameters (Coffey et al., 2006; Shackleton et al., 2005). This modification improved the model fits (as evaluated using R^2).

To predict neural responses in reverberation, we first fit the six-parameter model to each unit's rate-ITD curve using the *lsqnonlin* function in Matlab (The Mathworks, Natick, MA). We then refit the scaling parameters (*a* and *b*) to the anechoic rate-azimuth function (to compensate for differences in the duty cycle with which the measurements were made). Finally, we generated predictions of reverberant rate-azimuth curves by running the model with the appropriate virtual space stimuli as inputs. We only included units for which the goodness-of-fit (R^2) for both rate-ITD and anechoic rate-azimuth data was at least 0.75 (8/36 units excluded).

Psychophysics

Four paid human subjects with normal hearing participated in the behavioral experiment. One of the four subjects failed the preliminary training procedure and was dismissed from the experiment. Experimental procedures were approved by the Boston University Charles River Campus Institutional Review Board.

Stimuli. BRIRs were created using the same methods and room characteristics as in the physiology experiments, except that the receivers were separated by 23 cm to achieve ITDs spanning the range typically encountered by a human (±690 μs). Virtual space stimuli were created by convolving the BRIRs with random 400-ms Gaussian lowpass noise bursts (4^{th} order Butterworth filter with 2500-Hz cutoff) with 4-ms $\sin^2$ ramps.

Task. We used an acoustic pointing task to obtain a quantitative measure of stimulus laterality using the method of Best et al. (2007). Briefly, subjects adjusted the ILD of an acoustic pointer (200-Hz band noise centered at 3.0 kHz) until its perceived laterality matched that of a virtual space target. On each trial, the initial pointer ILD was randomly chosen from ±20 dB. The target and pointer were then played in alternation (500-ms interstimulus interval) until the subject indicated a match with a button press.

Data Analysis. We computed the mean ILD-match at each azimuth, for each condition, after rejecting outlying trials (defined as estimates more than ±3 standard deviations from the mean). We then fit sigmoid functions (using *lsqnonlin* in Matlab) to the individual subject responses and computed statistics using the fitted functions.

Results

Effects of reverberation on neural azimuth sensitivity

We used virtual auditory space simulation techniques (Fig. 2.1, Methods) to study the directional response properties of 36 low-frequency, ITD-sensitive neurons in the IC of anesthetized cats. The virtual space stimuli simulated the acoustics of a medium-size room (e.g. a classroom), and were designed to contain only ITD cues, without any interaural level differences or spectral cues. Stimuli were synthesized for two distances between the sound source and the virtual ears (1m and 3m) in order to vary the amount of reverberation ("moderate" and "strong"). The ratio of direct to reverberant energy (D/R) decreased with increasing distance and was largely independent of azimuth for each distance simulated (Fig. 2.1C). Reverberation did not systematically alter the broadband ITD, estimated as the time delay yielding the maximum normalized interaural correlation coefficient (IACC) between the left and right ear-input signals (Fig. 2.1D). However, increasing reverberation did cause a systematic reduction in the peak IACC (Fig. 2.1D, *inset*), indicating increasing dissimilarity in the ear-input waveforms.

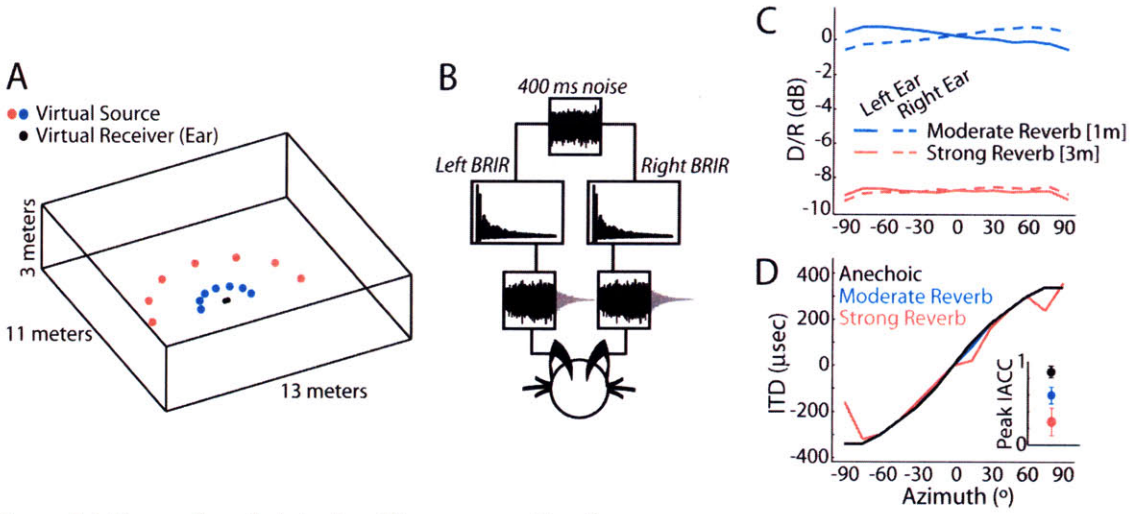

Figure 2.1 Properties of virtual auditory space stimuli.
A, Geometry of the virtual auditory environment. Reverberant binaural room impulse responses (BRIR) were simulated at two distances between source and receiver (1m and 3m). Anechoic (i.e., "no reverb") BRIR were created by time-windowing the direct wavefront from the 1m reverberant BRIR. *B,* To simulate a sound source at a given azimuth, a reproducible 400-ms broadband noise burst is convolved with the left and right BRIR and presented to the experimental subject over headphones. *C,* Direct to reverberant energy ratio (D/R) vs. azimuth for reverberant BRIRs. *D,* Broadband ITD vs. azimuth for each room condition, estimated as the time delay corresponding to the peak normalized interaural correlation coefficient (IACC). *Inset,* Peak IACC for each room condition. Error bars represent ±1 std across azimuths.

Figure 2.2A-C illustrates anechoic (i.e., "no reverb") and reverberant rate-azimuth curves for three IC units. For anechoic stimuli (Fig. 2.2A-C, black curves), the shape of the rate-azimuth curve was determined by the unit's sensitivity to ITD within the naturally occurring range (Supp. Fig. S2.1A-B), which corresponds to ± 360 µs for our virtual space simulations for cats. In many neurons, the discharge rate increased monotonically with azimuth (Fig. 2.2A-B), particularly in the sound field contralateral to the recording site, which corresponds to positive azimuths. Units with a non-monotonic dependence of firing rate on azimuth (Fig. 2.2C) generally peaked within the contralateral hemifield, consistent with the contralateral bias in the representation of ITD in the mammalian midbrain (Hancock and Delgutte, 2004; McAlpine et al., 2001; Yin et al., 1986).

In reverberation, there was an overall tendency for the range of firing rates across azimuths to decrease with increasing reverberation, although the exact dependence varied across units. Typically, the effect of reverberation was graded (Fig. 2.2A,C); however, there were units for which moderate reverberation had essentially no effect on the rate response (Fig. 2.2B). Generally, the reduction in response range primarily resulted from a decrease in the peak firing rate; increases in minimum firing rates were less pronounced.

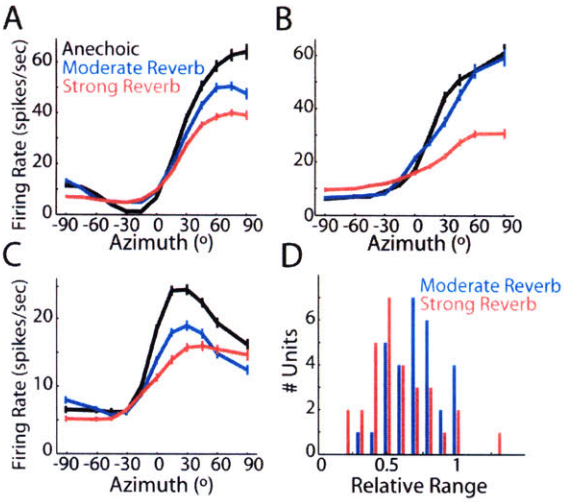

Figure 2.2 Directional sensitivity in reverberation. Anechoic and reverberant rate-azimuth curves (mean ± 1 standard error) for three IC neurons with CFs of *A*, 817 Hz; *B*, 569 Hz; *C*, 1196 Hz. *D*, Population histogram of relative range for each D/R (*moderate reverb*: n=30; *strong reverb*, n=30).

We quantified the overall compression of the rate-azimuth curves in reverberation using the *relative range*, which expresses the range of firing rates for a reverberant rate-azimuth curve as a fraction of the range of firing rates for that unit's anechoic rate-azimuth curve. In reverberation, the relative range is generally less than 1 (Fig. 2.2D) and is significantly lower for the strong reverb than for the moderate reverb condition (paired t-test, p=0.001, n=24). An information theoretic measure of directional sensitivity, which is sensitive to the variability in spike counts as well as the mean firing rates, showed a similar dependence on reverberation strength (Supp. Fig. S2.2).

Reverberation could also alter the sharpness of azimuth tuning and – for units having a best ITD within the naturally occurring range – shift the best azimuth (Supp. Fig. S2.3). However, changes in these tuning parameters occurred in either direction and were not consistently observed in all units. The most consistent effect of reverberation across our neural population was the compression of the response range.

Directional sensitivity is better near stimulus onset in reverberation

Reverberant sounds have a characteristic temporal structure that is ignored when firing rates are averaged over the entire stimulus duration as in Figure 2.2. At the onset of a sound in a reverberant environment, the energy reaching a listener's ears contains only the direct sound. Thus, the directional cues near the stimulus onset are similar for anechoic and reverberant virtual space stimuli (Fig. 2.3A-B). As reverberation builds up over time, reflections increasingly interfere with the direct sound energy at a listener's ears and the directional cues for the reverberant stimuli become more corrupted. Accordingly, we expected neural directional sensitivity to be better during the early as opposed to the ongoing portion of a sound stimulus in reverberation. Figure 2.3C-D shows rate-azimuth curves for two IC neurons computed from the early (0-50 ms), ongoing (51-400 ms), and full (0-400 ms) neural response. The rate-azimuth curves have been normalized to the maximum rate within each time period to facilitate comparison. Consistent with the build-up of reverberation, the rate-azimuth curves computed from the early response are similar across room conditions (Fig. 2.3C-D, left), whereas substantial rate compression occurs for reverberant stimuli in the ongoing response (Fig. 2.3C-D, middle). This trend holds across our sample of low-frequency ITD-sensitive neurons (Fig. 2.3E). Directional sensitivity in both moderate and strong reverberation is

significantly higher during the early as compared to the ongoing neural response epoch (paired t-test, *moderate reverb*: $p=0.007$, $n=24$; *strong reverb*: $p<0.001$, $n=25$).

Previous studies of ITD-sensitivity in the mammalian IC have reported that neural onset responses show poorer ITD-tuning than ongoing neural responses (Geisler et al., 1969). Here, we have defined the 'early' response epoch as the first 50 ms of the neural response, which is substantially longer than what is generally considered the 'onset' response of a cell. Nonetheless, to prevent non-directional early responses from biasing our results, we removed units that showed no significant change in early discharge rate across azimuth (Kruskal-Wallis test, $p>0.05$); 6/36 units were removed from the statistical analysis and are not included in Figure 2.3E.

Role of temporal response dynamics

The relative contribution of the early and ongoing responses to the directional sensitivity measured over the entire stimulus duration (Fig. 2.3C-D, right) is determined by the distribution of spiking activity over the course of the stimulus. Many low-frequency ITD-sensitive IC neurons exhibit spike rate adaptation in response to a sustained acoustic stimulus, such that firing rates are higher during the earlier portion of the stimulus and decrease over time (Ingham and McAlpine, 2004; Nuding et al., 1999; Rees et al., 1997; Stillman, 1971c). Such "onset dominance" in neural processing reduces the contribution of less-reliable ongoing reverberant stimulus energy to temporally-integrated measures of directional sensitivity.

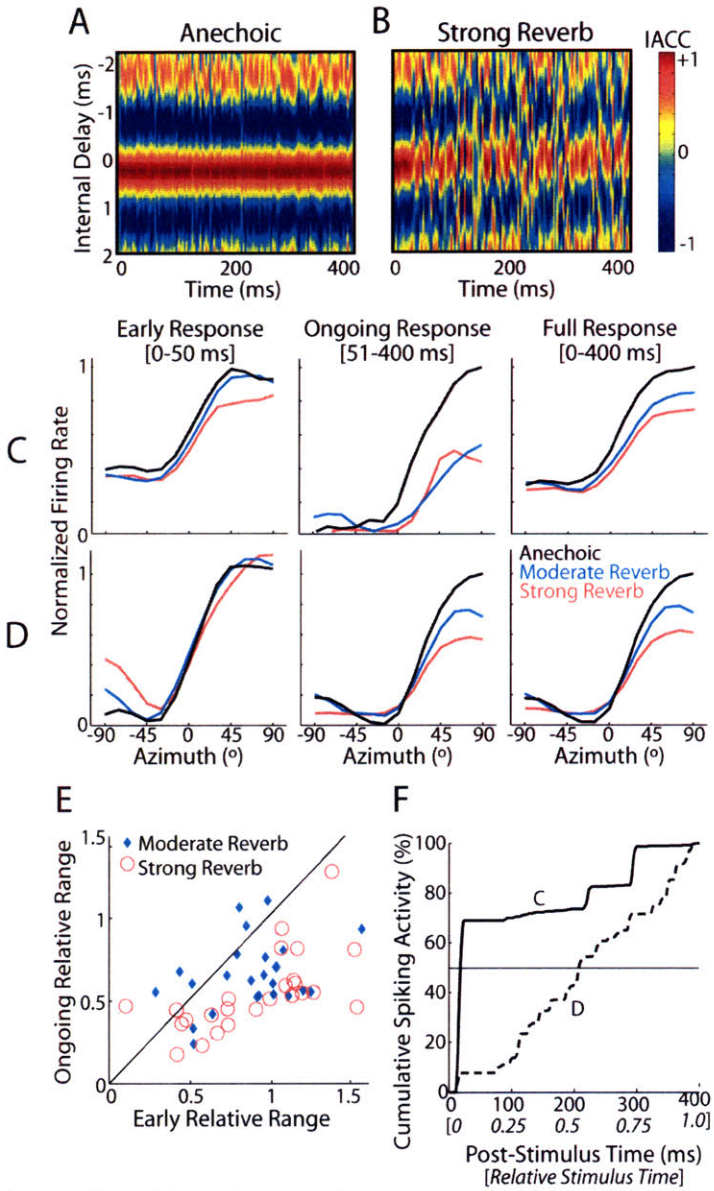

Figure 2.3 Temporal dynamics of directional sensitivity in reverberation.
A, Short-term IACC across time for the 45° *anechoic* virtual space stimulus; hot colors indicate high correlation. Ear-input signals were simulated as in Fig. 1B and subsequently bandpass filtered (4th-order Gammatone filter centered at 1000 Hz) to simulate peripheral auditory processing. Short-term IACC was computed using a sliding 4-ms window. *B,* Short-term IACC for the 45° *strong reverb* virtual space stimulus. *C-D,* Rate-azimuth curves for two IC neurons computed using the early (0-50 msec), ongoing (51-400 msec), and full (0-400 msec) neural responses. To facilitate comparison across time periods, firing rates have been normalized to the maximum firing rate in the anechoic condition, separately for each time period. Unit CFs are *C,* 747 Hz and *D,* 817 Hz. *E,* Ongoing vs. early relative range for IC neuron population. Solid line indicates identity i.e., y=x. *F,* Average cumulative peristimulus time histograms (cPSTHs) for the two neurons in panels *C* (solid line) and *D* (dashed line).

Figure 2.3F shows anechoic cumulative peristimulus time histograms (cPSTHs, see Methods) for the same two units as in Fig. 2.3C-D. A unit with strong onset dominance (Fig. 2.3F solid line) has a cPSTH that rises rapidly shortly after stimulus onset. Accordingly, the full response for this unit is determined primarily by the early response (Fig. 2.3C). In contrast, a unit that fires in a sustained manner throughout the stimulus has a more linear cPSTH (Fig. 2.3F, dashed line); in this case, the full response exhibits a stronger resemblance to the ongoing neural response (Fig. 2.3D).

To quantify onset dominance in single units, we computed T50 -- the time post stimulus onset at which the cPSTH reaches 50% of its final value (Fig. 2.3F). A strongly onset-dominated unit has a small T50 (Fig. 2.3F, solid line) while a sustained unit has a T50 near the stimulus midpoint (Fig. 2.3F, dashed line). Across the neural population, the median T50 is significantly less than 0.5 (Wilcoxon signed-rank test, $p<0.001$, $n=36$), with the interquartile range spanning [0.31, 0.47]. This suggests that early directional responses typically contribute more to the overall directional sensitivity than the more-degraded ongoing directional responses.

If the response to a reverberant stimulus were governed primarily by neural response dynamics, we would expect onset-dominated units to show better directional sensitivity in reverberation than units with a sustained response. That is, we should observe a negative correlation between T50 and relative range. However, the correlation was not significant for either condition (*moderate reverb*: $p=0.624$; *strong reverb*: $p=0.517$), suggesting that other neural properties in addition to onset dominance influence directional sensitivity in reverberation.

Comparison to a Cross-Correlation Model

Previous investigations of low-frequency ITD-sensitive IC neurons have established that the rate response to interaurally delayed broadband noise is well-described by a cross-correlation of the left and right ear-input signals, after accounting for peripheral frequency filtering and the nonlinear relationship between interaural correlation and firing rate (Hancock and Delgutte, 2004). Cross-correlation models essentially reduce all binaural processing (including interaural delays) to a change in the effective IACC computed over the entire duration of the stimulus. In general, firing rate changes monotonically with IACC in low-frequency IC neurons, although there is substantial variability in the degree of nonlinearity in the relationship (Albeck and Konishi, 1995; Coffey et al., 2006; Shackleton et al., 2005).

In a reverberant environment, reflections interfere with the direct sound wave, resulting in decorrelation of the ear-input signals [Fig. 2.1D, *inset*; see also (Hartmann et al., 2005; Shinn-Cunningham et al., 2005a)]. According to the cross-correlation model, this would *qualitatively* result in a compression of neural rate-azimuth curves, as observed in our neural data. We investigated whether a traditional cross-correlation model could *quantitatively* account for the degradation of directional sensitivity in reverberation.

We used a modified version of the Hancock and Delgutte (2004) cross-correlation model of ITD-sensitive IC neurons to generate predictions of reverberant rate-azimuth curves (see Methods). The model is a cascade of linear peripheral frequency filtering and binaural cross-correlation followed by a nonlinear transformation of IACC to firing rate (Fig. 2.4A). The model parameters were fit for each individual unit using the rate-ITD

and anechoic rate-azimuth data (Fig. 2.4B), and then fixed to predict responses to reverberant stimuli.

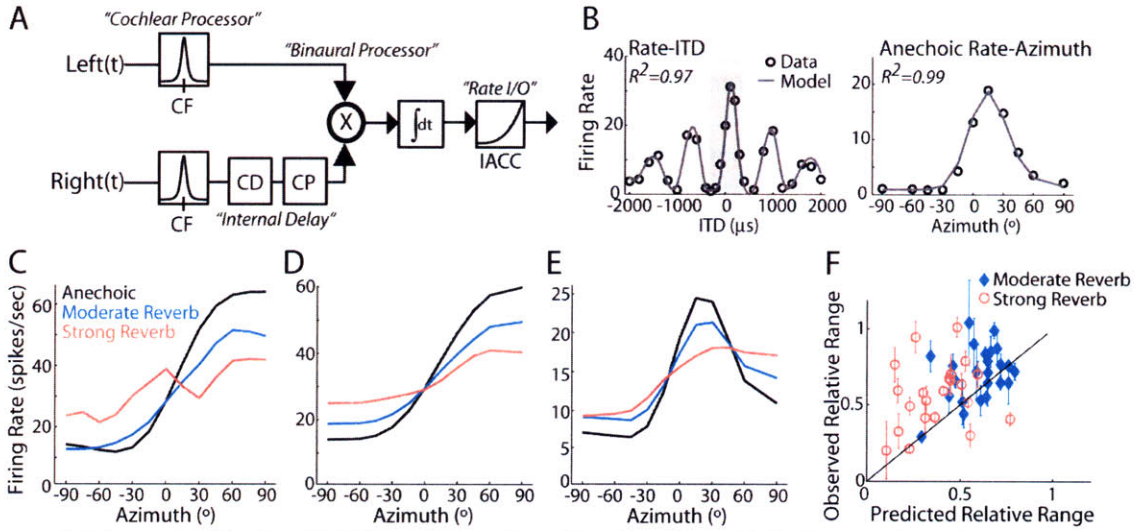

Figure 2.4 Average effective IACC poorly predicts directional sensitivity in reverberation.
A, Block diagram of the cross-correlation model, after Hancock and Delgutte (2004). Left and right ear-input signals are bandpass filtered to simulate cochlear processing. Right-ear signal is internally delayed through a combination of pure time delay (CD) and phase shift (CP), and the resulting IACC is converted to firing rate using a power-law nonlinearity. *B,* Example model fits to the rate-ITD (*left*) and anechoic rate-azimuth (*right*) data for one IC unit (CF=1312 Hz). The shaded region in the left panel delineates the range of ITDs corresponding to ±90° in the right panel. *C-E,* Model predictions of rate-azimuth curves for three IC neurons (same units as in Fig. 2A-C). For each neuron, model parameters were adjusted to minimize least-squared error between observed and predicted rate-ITD and anechoic rate-azimuth curves and subsequently fixed to generate predictions of reverberant rate-azimuth curves. *F,* Observed vs. predicted relative range across the IC neuron population. Solid line indicates identity i.e., y=x. Error bars represent bootstrap estimates of ±1 std. of relative range for observed responses.

Figure 2.4C-E shows model predictions of reverberant rate-azimuth curves for the same three IC units as in Figure 2.2A-C. As expected, the model rate-azimuth curves are qualitatively similar to the measured reverberant rate-azimuth curves in that increasing reverberation causes more compression of the response. We quantified overall differences between observed and predicted directional sensitivity using the relative range (Fig. 2.4F). Across the population, the model predicts substantial variability in the relative range, which originates from variations in both frequency tuning and the nonlinear dependence of firing rate on IACC. Accurate model predictions for individual

units would yield data points close to the identity line y=x in Figure 2.4F; however, there is a great deal of spread in the data with no significant correlation between observed and predicted relative range for either reverberation condition (*moderate reverb*: p=0.174, *strong reverb*: p=0.532). Moreover, a majority of the data points fall above the identity line, indicating that observed directional sensitivity is generally more robust (i.e., better) than model predictions. For both reverberation conditions, predicted directional sensitivity is significantly worse than observed directional sensitivity (one-tailed paired t-test, *moderate reverb*: p=0.02, n=24, *strong reverb*: p=0.005, n=24).

The cross-correlation model is not sensitive to the exact time course of short-term IACC; rather, its output depends only on the IACC averaged over the entire stimulus. In contrast, we have shown that onset dominance in neural responses emphasizes the earlier segments of the stimulus which, in reverberation, contain less-degraded directional information. Such neural processing would effectively attenuate the contribution of ongoing reverberant stimulus energy to the IACC measured at the output of the integrator in Figure 2.4A. Thus, we hypothesized that neural onset dominance could account for the inability of the model to predict directional sensitivity in reverberation.

To test the hypothesis, we examined the relationship between T50 and cross-correlation model error (defined as the difference between observed and predicted relative ranges, ΔRR). Positive values of ΔRR indicate robustness to reverberation (i.e., the cross-correlation model predicts more compression than was actually observed). Figure 2.5B shows a scatter plot of ΔRR versus T50; the filled symbols correspond to the cPSTHs plotted in Figure 2.5A. There is a significant negative correlation between the two metrics for both reverberation conditions (*moderate reverb*: r=–0.534, p=0.007;

strong reverb: r=–0.612, p=0.003). Namely, units with smaller T50 (i.e., the most onset-dominated units) tend to be more robust to reverberation relative to model predictions than units with longer T50.

Despite the correlation, the substantial spread in the data suggests that onset-dominance cannot completely account for the inability of the cross-correlation model to predict directional sensitivity in reverberation. The cross-correlation model may be a poor predictor of directional sensitivity for stimuli with dynamic interaural time differences, in general (see Discussion). Nevertheless, these results suggest that onset dominance can improve directional sensitivity in reverberation.

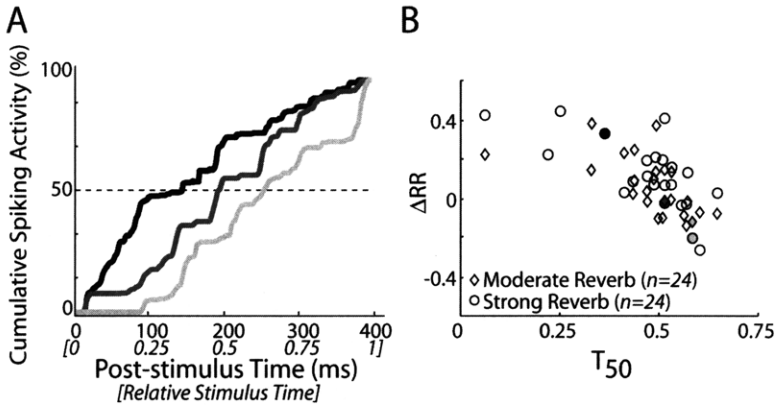

Figure 2.5 Onset dominance is related to robust directional sensitivity in reverberation.
A, cPSTHs for three IC neurons with CFs of 150 Hz (black), 741 Hz (dark gray), and 1551 Hz (light gray). T50 is defined as the time at which the cPSTH reaches 50% of its final value (intersection of cPSTH with dashed line). *B,* Model prediction error (ΔRR) vs. T50 across the IC neuron population, where positive ΔRR indicate robustness to reverberation. The two metrics are inversely correlated (*moderate reverb*: p=0.007; *strong reverb*: p=0.003). Shaded symbols correspond to the units shown in panel *A*.

Comparison to Human Psychophysics

We measured human behavioral lateralization[1] of virtual space stimuli nearly identical to those used in the neurophysiology experiments. Listeners adjusted the ILD of high-frequency narrowband noise until its perceived laterality subjectively matched that of each virtual space stimulus. Because the absolute range of pointer ILDs for azimuths spanning ±90° varied from subject to subject, we normalized the subjective lateral positions to their maximum for each subject. Figure 2.6A shows the normalized subjective lateral position as a function of stimulus azimuth. For all conditions, mean lateralization judgments vary nearly monotonically with virtual source azimuth. Listener judgments of source laterality are similar for the anechoic and moderate reverberation conditions. However, in strong reverberation, the range of lateralization judgments is noticeably compressed. This compression of perceived laterality resembles the reduction in relative range measured in single IC neurons.

[1] Because they contain only a single binaural cue, the virtual space targets (and the ILD pointer) are generally perceived on an internal interaural axis and are not externalized outside the head. Hence, they are said to be *lateralized* instead of *localized*.

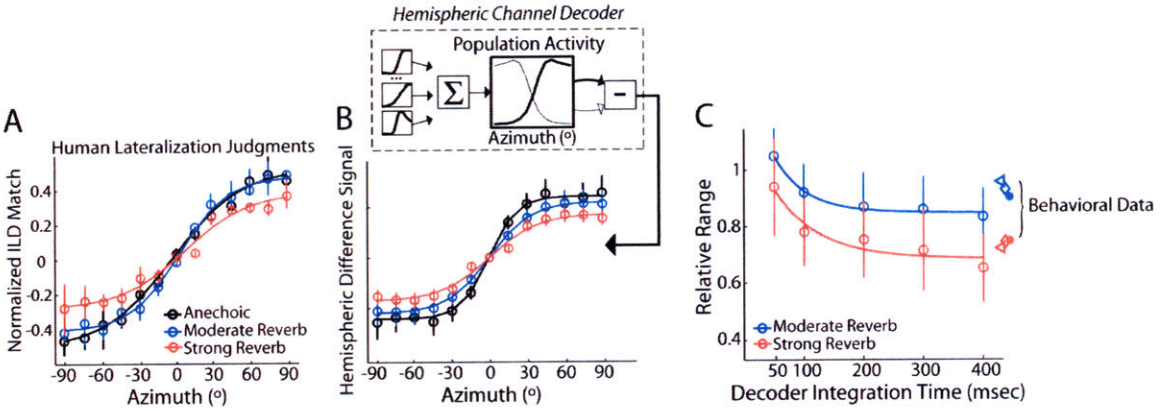

Figure 2.6 Hemispheric decoding of IC neural responses accounts for human lateralization behavior. *A,* Human lateralization judgments. Across-subject (n=3) mean (± 1 std) estimate of lateral position (i.e., normalized ILD-match) vs. stimulus azimuth. *B, Upper panel:* Schematic of the population decoding model (see text for description). *Lower panel*: Hemispheric difference signal vs. azimuth. Error bars indicate bootstrap estimates of ±1 std. *C,* Comparison of decoder and perceptual compression. Relative range of hemispheric difference signal (open circles) vs. the time interval over which firing rate is integrated in the hemispheric decoding model; solid lines indicate fits by decaying exponential. Error bars represent bootstrap estimates of ± 1 std. Relative range of human behavioral responses is plotted at the right edge of the panel (different symbols represent individual subjects).

In order to directly compare neural responses to the behavioral results, we implemented a hemispheric-difference decoding model (Hancock, 2007; McAlpine et al., 2001; van Bergeijk, 1962) using the empirically measured rate-azimuth curves from our neurophysiology experiments. The model (Fig. 2.6B, *inset*) estimates the lateral position of a sound source from the difference in the total activation between the two ICs. The choice of such a code [as opposed to a labeled line code, e.g. Jeffress (1948)] was motivated by the prevalence of monotonic rate-azimuth curves in our neural population, where a neuron's best ITD lies outside of the naturally occurring range of ITDs (Supp. Fig. 2.1C,D).

The total population activity is computed for the ipsilateral IC by summing weighted rate-azimuth curves[2] for all units in our sample of ITD-sensitive neurons. Assuming symmetry with respect to the sagittal plane in the neural activation patterns produced by sound sources located on opposite sides of the midline, the total population activity in the contralateral IC is derived by reflecting the ipsilateral population rate signal about the midline. The model output (*hemispheric difference signal*) is computed as the difference in population activity between the two ICs.

The main panel in Figure 2.6B shows the hemispheric difference signal for the anechoic and reverberant conditions. In all conditions, the hemispheric difference signal varies monotonically with stimulus azimuth. With increasing reverberation, the hemispheric difference signal becomes more compressed, as expected from the rate compression observed in individual units, and consistent with the main trend in the behavioral responses. However, for both anechoic and reverberant conditions, the hemispheric difference signal saturates more quickly for lateral source positions than the human laterality judgments (see Discussion).

We quantified compression of the hemispheric difference signal using the relative range. Figure 2.6C shows the relative range of the hemispheric difference signal (open circles) plotted as a function of the decoder integration time i.e., the time interval from stimulus onset over which we averaged the individual neuron's firing rates to compute

---

[2] The weighting factors were used to adjust for slight differences between our empirical CF distribution and that found in a larger sample of low-frequency ITD-sensitive IC neurons (Hancock and Delgutte 2004). The weighting function was $w(CF) = \frac{P_{HD}(CF)}{P_{Pr\,es}(CF)}$, where $P_{HD}(CF)$ is the lognormal distribution of CFs (with μ=6.5 and σ=0.31) fit to the Hancock and Delgutte (2004) data, and $P_{Pr\,es}(CF)$ is the empirical CF distribution in our population. Our population contained proportionally fewer neurons around 500 Hz than the Hancock and Delgutte (2004) distribution.

the hemispheric difference signal. The data are well fit by a single decaying exponential (solid curves). Because directional sensitivity is better during the earlier segment of a reverberant stimulus (Fig. 2.3E), the relative range is initially close to 1 and decreases over time, consistent with the buildup of reverberant energy in the stimulus.

The symbols at the right of Fig. 2.6C show the relative range of the lateralization estimates for individual human subjects. Both perceptual and decoder compressions show a similar dependence on reverberation strength. Quantitatively, the behavioral estimates show less compression than the hemispheric difference signal computed from the full neural response (0-400 ms), but more compression than that computed from only the early response (0-50 ms), suggesting that listener's lateralization judgments are influenced by late-arriving stimulus energy. To the extent that listeners integrate information over early and ongoing response segments, onset dominance may reduce the effective contribution of the ongoing population response.

Discussion

Our neurophysiological results show that the directional sensitivity of ITD-sensitive auditory midbrain neurons degrades over the duration of a reverberant stimulus, consistent with the buildup of reflected sound energy at a listener's ears. We further find that onset dominance in temporal response patterns emphasizes the more reliable directional information in the early response, suggesting a role for this general feature of neural processing in improving directional sensitivity in reverberant environments. By comparing neural responses with human lateralization judgments, we find that the temporally integrated population rate response forms a possible neural substrate for robust sound localization in reverberation.

Dynamics of Directional Sensitivity in Reverberation

In a reverberant environment, reflections interfere with the direct sound arriving at a listener's ears, causing the ear-input signals to become decorrelated. Thus, it is not surprising that we observed a more severe degradation in directional sensitivity with increasing reverberation for both single neurons in the auditory midbrain (Fig. 2.2D) and the cross correlation model (Fig. 2.4). However, the directional information in reverberation has a characteristic time course: it is relatively uncorrupted near the sound onset, before the arrival of reflections at a listener's ears, and becomes more degraded as reverberation builds up over time (Fig. 2.3A-B). Our results show that neural directional sensitivity parallels this temporal pattern of cues in reverberation: Sensitivity is better during the early response than during the ongoing neural response (Fig. 2.3E).

The overall directional sensitivity computed from the average rate response will depend on the distribution of spiking activity over time. Since directional information is better near the stimulus onset, a beneficial processing strategy would be to give proportionally more weight to the response near the onset of a stimulus. This could be achieved by any mechanism that reduces responsiveness in the later portions of the stimulus. A majority of neurons in our population exhibited onset dominance in their temporal response patterns, where firing rates are initially high and decay over time. When directional sensitivity is computed by integrating spike activity over time, onset dominance is a basic mechanism for emphasizing the earliest activity periods, when directional information is most reliable.

The sound stimulus used in the present experiments was a sustained noise, hence had a single onset. Many natural sounds, including human speech and animal vocalizations are characterized by prominent amplitude modulations in the 3-7 Hz range (Houtgast and Steeneken, 1973; Singh and Theunissen, 2003), which functionally create multiple "onsets" over the duration of the stimulus. Indeed, the responses of IC neurons to sinusoidally amplitude modulated (SAM) sound stimuli typically show adaptation on every modulation cycle at low modulation frequencies (Krishna and Semple, 2000; Nelson and Carney, 2007; Rees and Moller, 1983). While onsets in natural sounds are thought to be crucial for speech reception in reverberant rooms (Longworth-Reed et al., 2009), they may also provide a listener with multiple "onset-dominated" epochs over which to integrate directional information and make localization judgments (so long as the reverberation time does not exceed the period of dominant amplitude modulations in the stimulus).

Physiologically, onset-dominance in the IC could be realized through any of several neural mechanisms, including synaptic depression (Wu et al., 2002), intrinsic dynamics of active membrane channels (Sivaramakrishnan and Oliver, 2001), delayed, long-lasting inhibition (Kuwada et al., 1989; McAlpine and Palmer, 2002; Nelson and Erulkar, 1963; Pecka et al., 2007; Tan and Borst, 2007) or adaptation already present in the inputs to the IC (Smith and Zwislocki, 1975). The present physiological data do not allow us to discriminate among these possible mechanisms.

Relationship between Onset Dominance and Echo Suppression

The ability of a listener to localize sounds accurately in reverberant environments is often attributed to the precedence effect, a phenomenon in which the perceived source location is dominated by the initial portion of a stimulus (Litovsky et al., 1999). Numerous studies have reported neurophysiological correlates of classic precedence phenomena in the IC (Fitzpatrick et al., 1999; Litovsky and Yin, 1998; Pecka et al., 2007; Spitzer et al., 2004; Tollin et al., 2004; Yin, 1994). The stimuli used in these studies consisted of a leading source (representing the direct sound) followed by a lagging source (representing a single acoustic reflection). Because most of these studies used very brief stimuli, the leading and lagging sounds did not overlap in time. Such conditions are an extreme over-simplification of realistic reverberation, in which thousands of reflections contribute to the energy at a listener's ears over hundreds of milliseconds.

Typically, neurophysiological studies of the precedence effect report that responses to the lagging sound are suppressed over a range of delays between the leading and lagging sounds, consistent with the dominance of the leading sound in the perceived location. The present result suggest that onset dominance in neural responses helps

provide a robust representation of the location of sound sources in reverberation when the neural response is averaged over much longer times than the separation between individual reflections. While there is a superficial similarity between onset dominance and echo suppression, the two sets of results are not comparable because we cannot isolate the response to individual reflections as done in studies of the precedence effect.

A possible dissociation between neural echo suppression and onset dominance is suggested by the effects of anesthesia. The time course of recovery from neural echo suppression is faster in unanesthetized compared to anesthetized animals (c.f. Tollin et al. 2004; Litovsky and Yin, 1998). In contrast, ongoing experiments in our laboratory suggest that the effects of reverberation on azimuth sensitivity are comparable in the IC of awake rabbit and anesthetized cat (Devore and Delgutte, 2008). Moreover, the dynamics of spike-rate adaptation, a possible mechanism underlying onset dominance appear not to be strongly affected by anesthesia in the IC (Ter-Mikaelian et al., 2007).

While robust encoding of ITD in reverberation and neural suppression of discrete echoes each embody the seminal notion of the "law of the first wavefront" (Wallach et al., 1949), they operate on different time scales. In fact, onset dominance and neural echo suppression may contribute independently to robust encoding of azimuth in reverberant environments. The neural mechanisms underlying echo suppression in transient stimuli undoubtedly affect the neural response in the early portion of reverberant stimuli. However, there is likely an additional process, operating over longer time scales, that integrates directional information over time, emphasizing the early, reliable spatial cues over ongoing cues that are more degraded by reverberation.

Other Factors Influencing Directional Sensitivity in Reverberation

Qualitatively, the effect of reverberation on neural responses is consistent with a cross-correlation model of binaural processing (Hancock and Delgutte, 2004; Yin et al., 1987), which predicts the average firing rate of IC neurons as a function of the effective IACC of the input signals (Fig. 2.3A). However, a quantitative comparison reveals that the predicted reduction in directional sensitivity is not correlated with the observed reduction, indicating that the model does a poor job at predicting directional sensitivity in reverberation. Moreover, the observed reduction in directional sensitivity was generally less than the predicted reduction (Fig. 2.4F), suggesting that additional mechanisms not included in the model provide neural robustness to reverberation. The difference between observed and predicted directional sensitivity was systematically related to onset dominance in neural temporal responses (Fig. 2.5B); however, the relation between onset dominance and model misprediction showed a lot of scatter, suggesting that additional factors beyond neural response dynamics play a role in the model's shortcoming.

The cross-correlation model functionally reduces all processing of ear-input signals, including internal delay and reverberation, to changes in the effective interaural correlation. However, there is growing evidence that ITD-sensitive IC neurons receive convergent inputs from multiple brainstem coincidence detectors exhibiting different frequency and delay tuning (Fitzpatrick et al., 2000; McAlpine et al., 1998). Moreover, in addition to corrupting directional cues, reverberation also distorts the temporal envelopes of each ear-input signal. Temporal processing of stimulus envelope in the IC interacts with binaural processing in that manipulation of the stimulus envelope can cause changes in the firing rate of ITD-sensitive IC neurons even when IACC is unchanged (D'Angelo et al., 2003; Lane and Delgutte, 2005). Differences between model predictions

and observed responses might be explained by differences between a single effective interaural correlation computation (as assumed in the model) and the actual computation performed by the IC cell on multiple inputs with different spectral, binaural, and temporal tuning characteristics.

Comparison to Psychophysics

The present results suggest that reverberation produces similar effects on the lateralization judgments of human listeners and on the directional sensitivity of IC neurons. A direct comparison of neural responses with human behavior requires explicit assumptions about how azimuth information is decoded from the rate responses of the neural population. Two basic classes of decoding models for sound lateralization have been analyzed: labeled-line models and hemispheric channel models. In labeled-line models (Fitzpatrick et al., 1997; Jeffress, 1948; Shackleton et al., 1992), the lateral position of a sound is determined by reading out the ITD corresponding to the centroid of activity in an array of neurons tuned to different ITDs. Such models require each tuned channel to transmit a label (i.e., the best ITD) to the decoder. In contrast, a hemispheric channel model determines the lateral position of a sound source by computing the difference of activity in two broadly tuned spatial channels, each representing subpopulations of neurons that preferentially respond to sound sources in one hemifield (Hancock, 2007; McAlpine et al., 2001; Stecker et al., 2005; van Bergeijk, 1962). Consistent with previous studies (Brand et al., 2002; Hancock and Delgutte, 2004; McAlpine et al., 2001), the majority of units in our population had monotonic rate-azimuth functions (Supp. Fig. S2.1C), with best delays outside the naturally-occurring

range and almost exclusively in the contralateral hemifield (Supp. Fig. S2.1D), motivating our decision to implement a hemispheric channel decoder.

The model hemispheric difference signal was computed directly from the rate-azimuth curves measured in our sample of IC neurons. The range of the hemispheric difference signal decreased with increasing reverberation, mirroring the compression of human lateralization judgments (Fig. 2.6C). Ideally, human listeners would use only the information at the onset of the stimulus to make the lateralization judgment and would therefore be minimally affected by reverberation. The fact that lateralization judgments do show compression suggests that there may be an obligatory window of integration over which the lateral position is estimated. This possibility is intriguing, in that it suggests listeners may behave "suboptimally" given the available acoustic information. However, such behavior may be appropriate, considering that onset information can be unreliable due to masking by other sounds or internal noise. Thus, in everyday environments, optimal behavior may be to emphasize onsets, when detectable, but to also make use of ongoing information in case no onset information is available. Moreover, previous behavioral experiments have shown that human listeners are relatively insensitive to fast fluctuations in interaural correlation and appear to integrate binaural information over tens to hundreds of milliseconds when judging source direction (Grantham and Wightman, 1978). Psychophysical estimates of the length of the so-called "binaural temporal window" generally fall in the vicinity of 100 ms (Boehnke et al., 2002; Kollmeier and Gilkey, 1990). When we compared the human lateralization judgments to the hemispheric difference signal computed with different integration times (Fig. 2.6C), we found that decoder compression best matches perceptual compression for

an integration window of 100-200 ms. To the extent that lateralization judgments result from the integration of population rate responses over time, onset dominance will emphasize the early stimulus segments during this integration, as was shown for individual units (Fig. 2.3C).

The azimuth dependence of the hemispheric difference signal was shallower at lateral azimuths than that of the human lateralization judgments (c.f. Fig. 2.6A-B). However, this result is very sensitive to model assumptions including the exact distribution of CFs and best ITDs, as well as the mapping between azimuth and ITD. Moreover, species differences may also play a role since we are comparing human psychophysical data with model predictions based on cat neural data.

Hemispheric channel models have been criticized due to the lack of anatomical and physiological evidence for this type of operation, with simpler, single hemisphere rate codes offered as an alternative (Joris and Yin, 2007). With the present data, we found that the inter-channel comparison was necessary to avoid non-monotonic responses at the most lateral source positions in the population rate response of each IC.

Theoretically, Jeffress-type models become more computationally powerful for animals with larger head sizes, including humans, while hemispheric decoding models work best for smaller animals such as cats (Harper and McAlpine, 2004). Because our neural data were not amenable to a straightforward implementation of a Jeffress-type decoding model for sound localization, we cannot say whether labeled-line models can explain lateralization performance in reverberation. However, our results show that hemispheric decoding models can indeed account for human lateralization in reverberant environments.

Supplementary Methods

Information Theoretic Analysis

To quantify neural azimuth sensitivity, we estimated the mutual information (MI) between the stimulus azimuth and neural rate response (Cover and Thomas, 1991), assuming a uniform distribution of stimulus azimuths. We used a bootstrap resampling method (Chase and Young, 2005) to correct for biases in our estimates of MI due to small sample sizes. Relative information transfer (rIT) was defined as the debiased MI expressed as a fraction of the entropy of the stimulus distribution.

Characterization of Azimuth Tuning

We quantitatively characterized azimuth tuning of IC neurons by fitting each rate-azimuth curve with analytical functions, following the procedures of Smith and Delgutte (2007). Briefly, monotonic rate-azimuth curves were fit by a sigmoid function of the form $R(x) = \frac{A}{1+3^{\frac{-2(x-Az_{MS})}{HR}}} + B$, where Az_{MS} is the azimuth of maximum slope, *HR* is the half-rise, and A and B are scaling parameters. Nonmonotonic rate-azimuth curves were fit by (1) a Gaussian function of the form $R(x) = Ae^{\frac{(x-Az_{BEST})^2}{(\frac{HW}{2})}} + B$, where Az_{BEST} is the best azimuth and *HW* is the half-width and (2) a difference of Gaussians of the form $R(x) = A[e^{\frac{(x-Az_{BEST}-HR)^2}{(\frac{HR}{2})}} - e^{\frac{(x-Az_{BEST}-HR)^2}{(\frac{HR}{2})}}] + B$, where Az_{MS}, *HR*, A, and B are as defined for the sigmoid. For nonmonotonic units, we ultimately chose the function that accounted for the largest proportion of variance in the data (as quantified by R^2). Tuning parameters

were only calculated for reverberant rate-azimuth curves that had a modulation depth greater than 50% to avoid anomalous parameter values (*moderate reverb*: 5/30 excluded, *strong reverb*: 8/30 excluded).

Supplementary Results

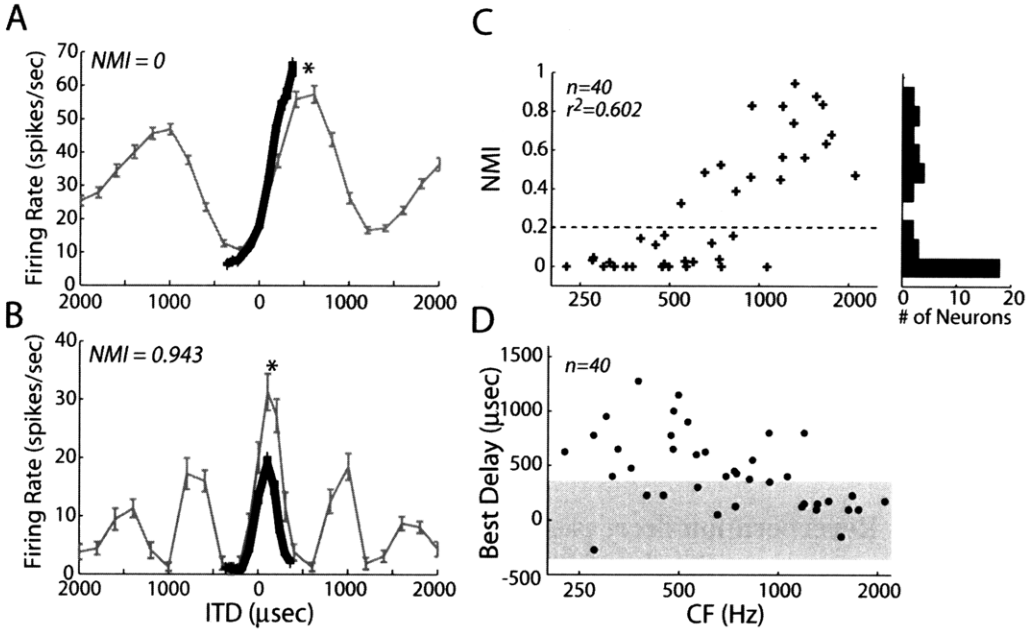

Figure S2.1 Characteristics of ITD tuning in IC neuron population.

A-B, Rate-ITD curves for broadband noise (thin gray lines) typically resemble damped sinusoids with a period approximately equal to the inverse of the neuron's characteristic frequency (CF). The anechoic rate-azimuth curves (thick black lines) parallel the noise-delay function within the range of ITDs corresponding to source azimuths in the frontal hemifield (±360 μs), consistent with the fact that ITD is the only directional cue present in the virtual space stimuli. The small differences between the two curves can be attributed to the differences in the duty cycles with which they were measured. Unit CFs are *A,* 569 Hz and *B,* 1312 Hz. *C, Left,* Nonmonotonicity index (NMI) versus CF for population of IC neurons, where $NMI = 1 - \frac{abs[r(90^\circ) - r(-90^\circ)]}{r_{max} - r_{min}}$. NMI is equal to 0 for a rate-azimuth curve that is strictly increasing or decreasing (e.g. panel *A*) and increases towards 1 as a rate-azimuth curve becomes more nonmonotonic (panel *B*). NMI is positively correlated with CF (r^2=0.602, p<0.001) such that units with CFs below 500 Hz tend to be monotonic while units with higher CFs tend to be nonmonotonic. *Right,* Histogram of NMI across IC neuron population. *D,* Best delay (BD) versus CF across IC neuron population. The BD of over half the units (25/40) lies outside the naturally occurring range of ITD (gray shaded region). BD is defined as the ITD corresponding to the peak of the rate-ITD curve, indicated by the stars in panels *A* and *B*.

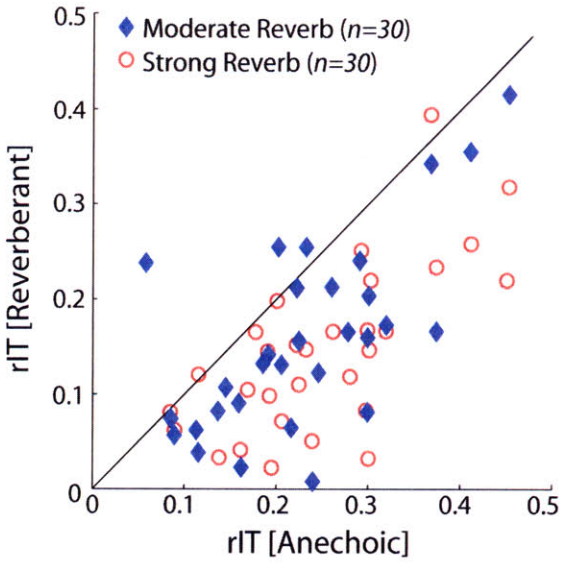

Figure S2.2 Reverberation decreases relative information transfer (rIT) between stimulus azimuth and spike count.

Scatter plot of rIT for reverberant conditions against rIT for anechoic condition across IC neuron population. Increasing reverberation leads to significant reduction in rIT (ANOVA, $F(2,69)=7.33$, $p=0.001$). Post-hoc comparisons (with Bonferroni corrections) confirm that the decrease in rIT is significant ($p<0.01$) for all pairwise comparisons between room conditions. The decrease in rIT in reverberation is significantly correlated with relative range (*moderate reverb*: $r^2=0.504$, $p<0.001$; *strong reverb*: $r^2=0.497$, $p<0.001$).

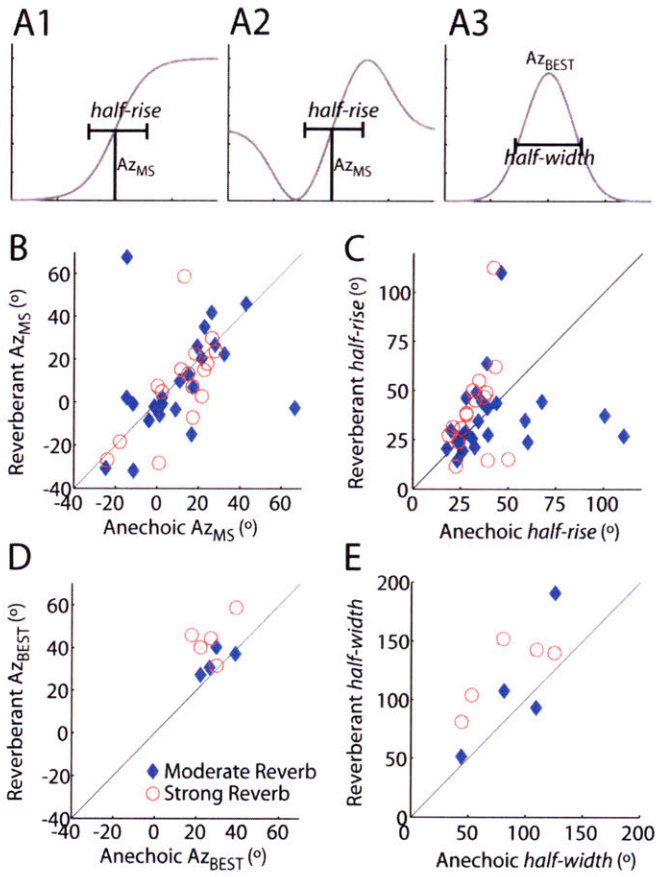

Figure S2.3 Effect of reverberation on azimuth tuning.

A, Rate azimuth curves for each unit were fit with one of three functions: *A1,* sigmoid, *A2,* difference of Gaussian, and *A3,* Gaussian. The fitted curves were used to obtain parameters characterizing azimuth tuning. *B,* Azimuth at maximum slope (Az_{MS}) for reverberant condition against anechoic Az_{MS} for IC neurons best fit by sigmoid (n=21) and difference of Gaussian (n=13) functions. Az_{MS} was relatively stable in reverberation and was significantly correlated with anechoic Az_{MS} in the *strong reverb* condition (r^2=0.427, p<0.005, n=16). The presence of two outliers resulted in a non-significant correlation for the *moderate reverb* condition (p=0.09, n=23). *C,* Reverberant versus anechoic half-rise for units with sigmoid and difference of Gaussian fits. Reverberation can cause both increases as well as decreases in half-rise. *D,* Reverberant versus anechoic best azimuth (Az_{BEST}) for nonmonotonic units with Gaussian fit (n=5). Increasing reverberation tended to shift Az_{BEST} away from the midline. *E,* Reverberant versus anechoic half-width for units with Gaussian fit (n=5). Increasing reverberation tended to increase the half-width of azimuth tuning.

CHAPTER 3

Effects of reverberation on directional sensitivity of low-frequency ITD-sensitive neurons in inferior colliculus of awake rabbit

Abstract

In Chapter 2 we demonstrated that directional sensitivity of auditory midbrain neurons in anesthetized cat degrades dynamically for reverberant stimuli. Directional sensitivity was better near the onset of a reverberant stimulus but degraded over time, paralleling the build up of reverberation over time. Anesthesia is known to alter neural response dynamics and has been shown to have profound effects on the neural processing of discrete echoes. To rule out the possibility that the results from our previous experiments were contaminated by anesthesia, we developed an awake rabbit preparation for studying single IC neurons and repeated the experiments of Chapter 2. Results demonstrate that reverberation similarly affects the directional sensitivity of single neurons in the awake rabbit and anesthetized cat IC, suggesting that, on the average, neither anesthesia nor species differences affect the neural processing of reverberation.

Introduction

Nearly all listening environments—indoors and outdoors alike—are reverberant. In reverberant environments, echoes interfere with the direct sound wave arriving at a listener's ears, distorting the spatial cues for sound localization. Because reverberation builds up over time, the source location is represented relatively faithfully during the initial portion of a sound but this representation becomes more degraded later in the stimulus. In Chapter 2 we demonstrated that the directional sensitivity of single neurons in the auditory midbrain of anesthetized cats follows a similar time course, in that sensitivity is better during the early response period and becomes degraded over time. Furthermore, we showed that onset dominance in neural response patterns can emphasize the earlier response periods, resulting in more robust directional sensitivity than expected given the average acoustic degradation in the signals.

Physiological data obtained from anesthetized preparations have come under scrutiny, owing to a growing set of investigations demonstrating profound impacts of anesthesia on neural processing at multiple levels in the auditory pathway (Kuwada et al., 1989; Tollin et al., 2004; Wang et al., 2005; Young and Brownell, 1976). Of particular importance to the topic of this thesis are investigations concerning the effects of anesthesia on the neural suppression of discrete reflections. When a pair of short-duration sounds (e.g., acoustic clicks) is presented in close succession, with the lead representing the direct sound and the lag a single echo, the neural response to the lagging sound is typically suppressed over a range of delays. Generally, the time course of suppression is quantified by the half-maximal delay—the interstimulus delay required for the neural response to the lag to reach 50% of the response to a single source. Single

neurons in the anesthetized cat auditory midbrain have an average half-maximal delay of ~35ms, although values vary from 1 to greater than 60ms in individual units (Litovsky and Yin, 1998). In contrast, neurons in the IC of unanesthetized animals typically exhibit half-maximal delays of ~10ms, with individual neurons exhibiting half-maximal delays between 1-40ms (Fitzpatrick et al., 1999; Tollin et al., 2004)(Fitzpatrick et al., 1999; Tollin et al., 2004). Although it is difficult to generalize results obtained using a single, discrete reflection to those using more complex stimuli like reverberation, these studies nevertheless suggest that the effects of reverberation on directional sensitivity of single neurons might be markedly different in the awake and anesthetized auditory midbrain.

On the other hand, not all neural response properties are altered by anesthesia. In particular, anesthesia does not have significant effects on adaptation time constants measured from the auditory midbrain of gerbils (Ter-Mikaelian et al., 2007). In Chapter 2, spike rate adaptation was implicated as one of the possible mechanisms underlying robust encoding of ITD in reverberation. Thus, it may function similarly in an unanesthetized preparation.

Because one of the central goals of our research is to elucidate the neural correlates of behavior, it is paramount to rule out the possibility that the results of our previous study were contaminated by anesthesia. To address this issue, we developed an awake (passively-listening) Dutch-belted rabbit (*Oryctolagus cuniculus)* preparation and repeated the experiments that previously done in anesthetized cat (Chapter 2).

In contrast to the aforementioned studies of echo suppression, our results suggest that directional sensitivity in reverberation is remarkably similar in neurons from awake and anesthetized IC. In particular, we demonstrate that single neurons in the awake

rabbit IC follow a similar time course of degradation as units in the anesthetized cat IC. However, we find that the proportion of neurons with non-monotonic directional responses is much higher in awake rabbit IC than anesthetized cat IC, indicating that the two species might use different neural codes for sound localization.

Methods

Surgical Preparation

Methods for recording from single neurons in the inferior colliculus (IC) of unanesthetized Dutch-Belted rabbits, (*Oryctolagus cuniculus*) were developed based on the techniques of Kuwada et al. (1987) and Nelson and Carney (2006). We performed two asceptic surgeries to prepare the rabbits (n=4) for chronic recording sessions. In both surgeries, animals were anesthetized with an intramuscular injection of acepromazine (1 mg/kg), ketamine (44 mg/kg), and xylazine (6 mg/kg). Supplemental doses of ketamine and xylazine were administered as necessary, as assessed by the onset of the pedal withdrawal and corneal reflexes. Body temperature was maintained at 37.8° throughout all surgical procedures.

In the first surgery, the skull was exposed by a midline incision and cleared free of connective tissue. A stainless steel cylinder and brass head bar were affixed to the skull using stainless steel screws and dental acrylic. The cylinder and head bar were centered on the midline with the anterior edge of the cylinder at bregma and the head bar forming a fixed angle with the tooth-orbit line. At the end of the procedure, custom ear molds were made using vinyl polysiloxane impression material (Reprosil®). Buprenorphine (Buprenex®, 0.015 mg/kg, s.c.) was administered as an analgesic for 36-48 hours post-surgery.

Animals were given at least two weeks to recover from the initial surgery before they were habituated to the experimental setup. Animals were restrained in a spandex sleeve and secured in a padded cradle. Sound stimuli were introduced by connecting acoustic drivers to the custom-fitted ear molds. The duration of daily training sessions

was gradually increased until the rabbits could sit for 2-3 hours with no signs of discomfort, typically over a period of 1-2 weeks.

Subsequently, the animals underwent a second asceptic surgical procedure in which a small (~2-3 mm diameter) craniotomy was made in the skull, centered approximately 10mm caudal and 3mm lateral to bregma. The exposed dura was treated with a topical antibiotic (Bacitracin) and the stainless steel chamber filled with sterile elastopolymer (Sammons-Preston). Additional asceptic surgeries were periodically performed to enlarge the craniotomy and to clear excessive tissue growth.

All procedures were approved by the animal care and use committees of both the Massachusetts Eye and Ear Infirmary the Massachusetts Institute of Technology.

Recording Procedures

All recording sessions took place in a double-walled electrically-shielded sound attenuating chamber. At the start of each session, the elastopolymer cap was removed and the stainless steel chamber flushed with sterile saline. A topical anesthetic (Marcaine) was applied to the craniotomy for ~5 minutes to diminish sensation upon dural penetration. Using fine forceps, we removed the dural scar tissue that had accrued since the previous recording session. A sterile 25x-gauge guide tube that protected the electrode tip was inserted 2mm below the surface of the dura using a manual manipulator.

Sound stimuli were generated by a 24-bit D/A converter (National Instruments NIDAC 4461) at a sampling rate of 50kHz and digitally filtered to compensate for the transfer function of the acoustic assemblies. The acoustic assemblies consisted of a pair of Beyer-Dynamic (DT-48) speakers attached to narrow plastic tubes that passed through

the custom-fitted ear molds. A probe-tube microphone (Etymotic ER-7C), sealed inside the sound delivery tube, measured acoustic pressure at the end of the tube. At the start of each recording session, we determined the system transfer functions using a chirp-stimulus and generated digital compensation filters.

Single units were isolated using epoxy-insulated tungsten electrodes (AM Systems) inserted through the guidetube and advanced using a remote-controlled hydraulic micropositioner (Kopf 650). The neural signal was amplified, bandpass filtered between 0.3-3kHz, and fed to a software spike detector triggering on level crossings. Spike times were saved to hard disk for subsequent analysis.

Animals were monitored on a closed-circuit video system throughout recording sessions, which typically lasted 2-3 hours but were terminated immediately if animals showed any signs of discomfort. At the end of the session, the stainless steel chamber was flushed with sterile saline, treated with topical antibiotic and resealed with sterile elastopolymer.

We typically recorded 6 days per week for up to 6 months in each IC. During the final recording session, a series of recording sites were marked by electrolytic lesions (10μA of current for 30-45 seconds) for subsequent histological verification. Because numerous penetrations were made over months, it was not possible to accurately reconstruct the position of each recording site within the IC. We instead relied on physiological criteria to define recording sites as "central nucleus-like": (1) the site fit into an orderly tonotopic progression along the dorsal-ventral axis of penetration and (2) the response was non-habituating. Units that did not meet both criteria were excluded from data analysis.

Virtual Space Stimuli

Binaural room impulse responses (BRIR) were simulated for a reverberant environment at three source-to-listener distances (0.5m, 1m and 3m) using the techniques described in Chapter 2. The parameters of the simulation, including the geometry of the virtual receivers and sources was identical to those used previously. The range of interaural time differences (ITD) corresponding to ±90° is ±360μs, covering the naturally occurring range of ITD for a Dutch-belted rabbit (Bishop et al., 2009). The BRIR did not contain azimuth-dependent interaural levels differences, because we did not include a head in the virtual simulations. Each set of ITD-only BRIR was characterized by the ratio of direct to reverberant energies (D/R), averaged across azimuths (*0.5m*: +10 dB, *1m*: 0 dB, *3m*: -9 dB). We henceforth refer to each of the three conditions as *mild, moderate*, and *strong reverb.*

Virtual space stimuli were created by convolving the normalized BRIRs with reproducible 400-ms broadband noise bursts. Stimulus intensity was computed using the filtered noise tokens.

Experimental Procedures

The search stimulus consisted of 40-Hz sinusoidally amplitude-modulated broadband noise bursts presented binaurally at a nominal level of 65 dB SPL. When a single unit was well isolated, its characteristic frequency (CF) was determined using an automatic tracking procedure (Kiang and Moxon, 1974). In earlier experiments, we determined CF by presenting a series of randomly ordered tone pips. Acoustic threshold was determined using 200-ms diotic (and occasionally contralateral) broadband noise (2/sec x 4-10

repeats). Spontaneous rate was computed from a 100-ms silent period preceding each stimulus presentation.

Noise delay functions were measured using 200-ms broadband diotic noise bursts typically presented at delays of ±2000μs in 200μs steps (2/sec x 10 trials). A unit was considered ITD-sensitive if an analysis of variance for the distributions of firing rates across ITD showed a significant effect of ITD (at the level α=0.05).

Only ITD-sensitive units were studied using the virtual space stimuli. Directional responses were obtained for the anechoic and moderate reverb conditions in pseudorandom order. We typically used 13 azimuths (15° spacing) or, occasionally, 7 azimuths (30° spacing), randomized on a trial by trial basis (1/sec x 8-15 repeats). Stimuli were presented at a level 15-20 dB above broadband noise threshold. Time permitting, we measured responses to the mild and strong reverb BRIRs.

Data Analysis

A directional response function (DRF) for each room condition was computed by averaging the number of spikes that occurred in a fixed time window across all trials for each azimuth. We defined the *early* response as [0,50ms], the *ongoing* response as [51,400ms] and the *full* response as [0,400ms]. DRFs were smoothed using a three point triangular smoothing filter having weights [1/6,2/3,1/6].

We computed the *relative range*, which is the range of firing rates for a reverberant DRF expressed as a fraction of the range of that unit's anechoic DRF. The relative range is equal to 1, by definition, for an anechoic DRF.

We computed a non-monotonicity index (NMI) for each DRF as, $NMI = 1 - \frac{abs[r(90^\circ) - r(-90^\circ)]}{\max(r) - \min(r)}$, where r represents the vector of firing rates across azimuths. The NMI is 0 for a monotonic function and increases towards 1 for non-monotonic functions.

We quantitatively characterized azimuth tuning of IC neurons by fitting each rate-azimuth curve with analytical functions, following similar procedures to Smith and Delgutte (2007). Briefly, monotonic rate-azimuth curves were fit by a sigmoid function of the form $R(x) = \frac{A}{1+3^{\frac{-2(x-Az_{MS})}{HR}}} + B$, where Az_{MS} is the azimuth of maximum slope, *HR* is the half-rise, and A and B are scaling parameters. Nonmonotonic rate-azimuth curves were fit by a Gaussian function of the form $R(x) = Ae^{\frac{(x-Az_{BEST})^2}{(\frac{HW}{2})}} + B$, where Az_{BEST} is the best azimuth and *HW* is the half-width. To be included in the analysis, we required the goodness of fit (R^2) for both anechoic and reverberant DRF to be above 0.75. Eight units (out of 94) were excluded because we couldn't obtain fits to the anechoic DRF. Of the remaining units, the following were excluded because we failed to obtain fits to reverberant DRF: *mild reverb:* 2/21, *moderate reverb:* 3/71, *strong reverb:* 2/15.

Average cumulative peristimulus time histograms (cPSTH) were computed as described in Chapter 2. Briefly, each 1 ms bin in the cPSTH represents the cumulative number of spikes up to the bin time in the anechoic PSTH. The cPSTH was computed over a 400 ms duration, with time zero corresponding to the first bin in the anechoic PSTH having an across-trial spike count distribution significantly different from that of spontaneous activity. Only azimuths that evoked mean firing rates ≥90% of the maximum

rate across all azimuths were included in the average cPSTH in order to avoid including onset responses that often occur at unfavorable azimuths.

Results

Effect of reverberation on directional sensitivity in awake rabbit IC

We obtained directional response functions (DRF) from 94 low-frequency ITD-sensitive neurons from the IC of 4 awake rabbits. The neural rate response for anechoic virtual space stimuli (Fig. 3.1, thick lines) is essentially equivalent to the rate response obtained using interaurally delayed broadband noise (Fig. 3.1, thin lines) within the naturally occurring range of ITD, confirming that ITD is the main directional cue for these stimuli. Maximum firing rates are typically elicited from sources in the hemifield contralateral to the recording site (positive azimuths), although the shape of individual DRFs ranges on a continuum from completely monotonic (Fig. 3.1A) to nonmonotonic (Fig. 3.1C).

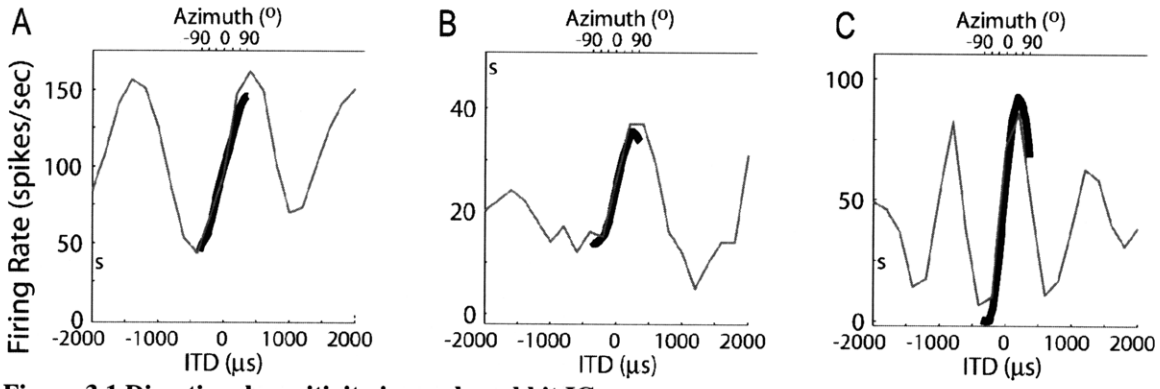

Figure 3.1 Directional sensitivity in awake rabbit IC
Noise delay functions (thin lines) and anechoic directional response functions (DRFs, thick lines) from three neurons in the awake rabbit IC. Spontaneous firing rate is indicated by the 's' symbol at the left of each panel. To facilitate comparison, virtual stimulus azimuth (top axis) has been converted to ITD (bottom axis). Unit CFs are *A*, 490 Hz; *B*, 325 Hz; and *C*, 962 Hz.

We quantified the shape of DRFs using a nonmonotonicity index (NMI, see Methods). The NMI is equal to 0 for DRF that are strictly increasing or decreasing (Fig. 3.1A) and increases towards 1 as the DRF becomes more nonmonotonic (Fig. 3.1C).

Figure 3.2 shows a scatter plot of NMI versus characteristic frequency (CF) for the awake rabbit neuron population (filled symbols). The data from anesthetized cat are superimposed (open symbols), for comparison. Despite the fact that the very low-frequency region (CF < 350 Hz) is under sampled in the rabbit preparation, there appears to be a consistent trend of increasing NMI with increasing CF. However, in the frequency range of ~400-800 Hz, there are proportionally more units with non-monotonic DRF (i.e., NMI > 0.2) in the awake rabbit neuron population (55%, 22/40) than the anesthetized cat neuron population (21.4%, 3/14). Non-monotonic DRF occur when a neuron's best delay falls within the naturally occurring range of ITD, indicating that there may be differences in the distribution of best delays across CF between the two preparations (see Discussion).

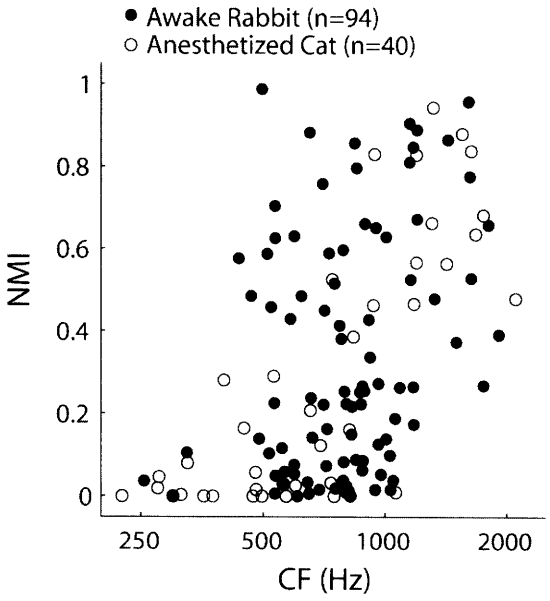

Figure 3.2 Shape of anechoic directional response functions
Nonmonotonicity index (NMI) versus CF for awake rabbit (filled symbols) and anesthetized cat (open symbols) IC neuron populations.

We obtained reverberant DRFs in 78 (out of 94) ITD-sensitive awake rabbit IC neurons using virtual space stimuli with *moderate reverb*, typical of a medium-sized

classroom. In a smaller subset of units, we obtained DRF using virtual space stimuli with *mild* and *strong reverb*, as well. Figure 3.3 shows reverberant and anechoic DRF for the same three neurons illustrated in Figure 3.1. The general effects of reverberation on DRF obtained from awake rabbit IC neurons are similar to our observations from anesthetized cat (Chapter 2). Namely, reverberation causes a compression of the range of firing rates across azimuths, both by reducing peak firing rates and increasing minimum firing rates, with increasing reverberation having more severe effects.

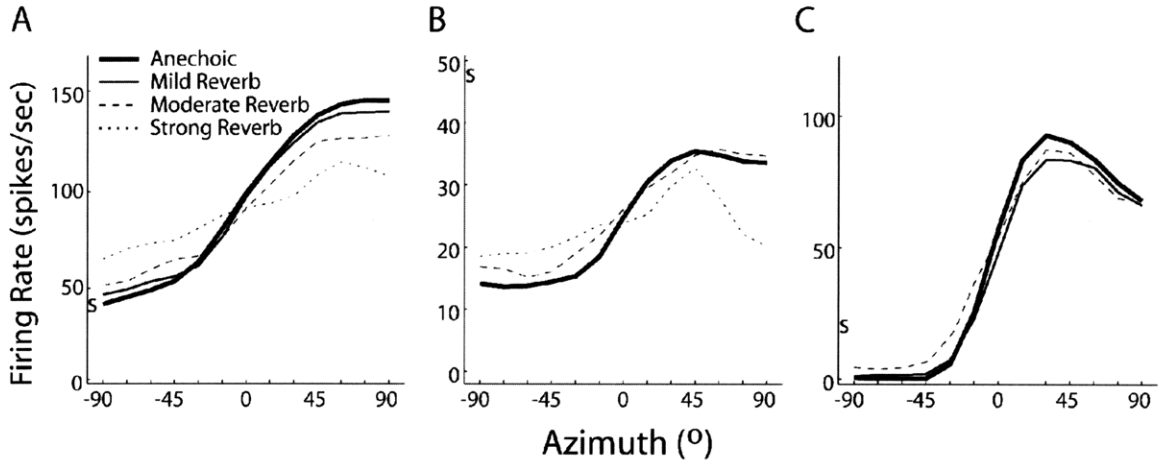

Figure 3.3 Anechoic and reverberant directional response functions
Anechoic and reverberant DRF for three awake rabbit IC neurons (same units as in Fig. 1). Spontaneous firing rate indicated by the 's' symbol at the left of each panel.

To quantify compression for individual DRF, we computed the *relative range*, the range of firing rates in a reverberant DRF expressed as a fraction of the range of firing rates in that unit's anechoic DRF. Figure 3.4 shows the distribution of relative range across the awake rabbit IC neuron population for each of the reverberation conditions. Both pairwise comparisons between successive reverberation levels show a significant decrease in relative range with increasing reverberation (*mild/moderate*: $n=22$, $p<0.001$, *moderate/strong*: $n=17$, $p<0.001$).

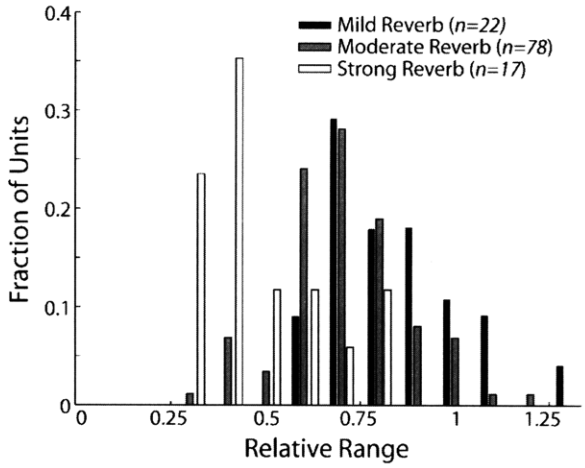

Figure 3.4 Directional sensitivity in reverberation
Distribution of relative range for each reverberation condition across the awake rabbit IC neuron population.

To quantify the effects of reverberation on DRF shape, we computed the NMI for each reverberation condition. Figure 3.5 shows scatter plots of reverberant NMI versus anechoic NMI for each of the three reverberation levels. The solid lines indicate identity i.e., y=x. At each reverberation level, the two metrics are positively correlated (*mild and moderate:* $p<0.001$, *strong:* $p=0.036$), although with increasing reverberation NMI tend to become smaller in reverberation. Statistically, the slope of the best-fitting regression line decreases with increasing reverberation (*mild:* r=0.991, *moderate:* r=0.754, *strong:* r=0.341).

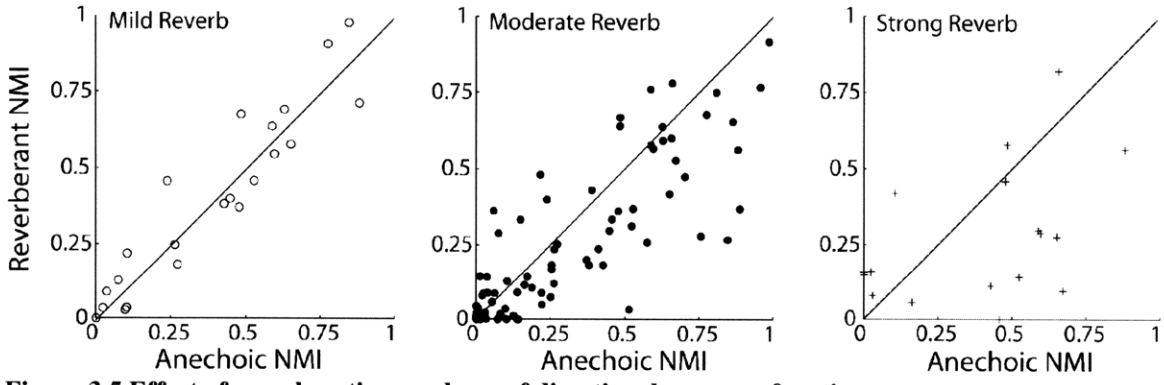

Figure 3.5 Effect of reverberation on shape of directional response functions
Reverberant NMI versus anechoic NMI across IC neuron population. Left panel, *mild reverb* (n=22); Middle panel, *moderate reverb* (n=78), Right panel, *strong reverb* (n=17).

We next quantitatively characterized the effects of reverberation on specific tuning properties of each DRF (see Methods). For non-monotonic neurons best fit by Gaussian functions, reverberation tends to cause lateral shifts in the best azimuth (Fig. 3.6A, Az_{best}) as well as an increase in the half-width of tuning (Fig. 3.6C). Both changes reduce the non-monotonicity of DRF and therefore underlie the decrease in NMI with increasing reverberation. For monotonic neurons, i.e., those best fit by sigmoid functions, reverberation has no systematic effect on the azimuth at maximum slope (Fig. 3.6B, Az_{max}); but generally causes an increase in the half-rise (Fig. 3.6D) across all reverberation levels. Both the increase in half-rise for monotonic units and the increase in half-width for non-monotonic units indicate a decrease in the sharpness of ITD tuning.

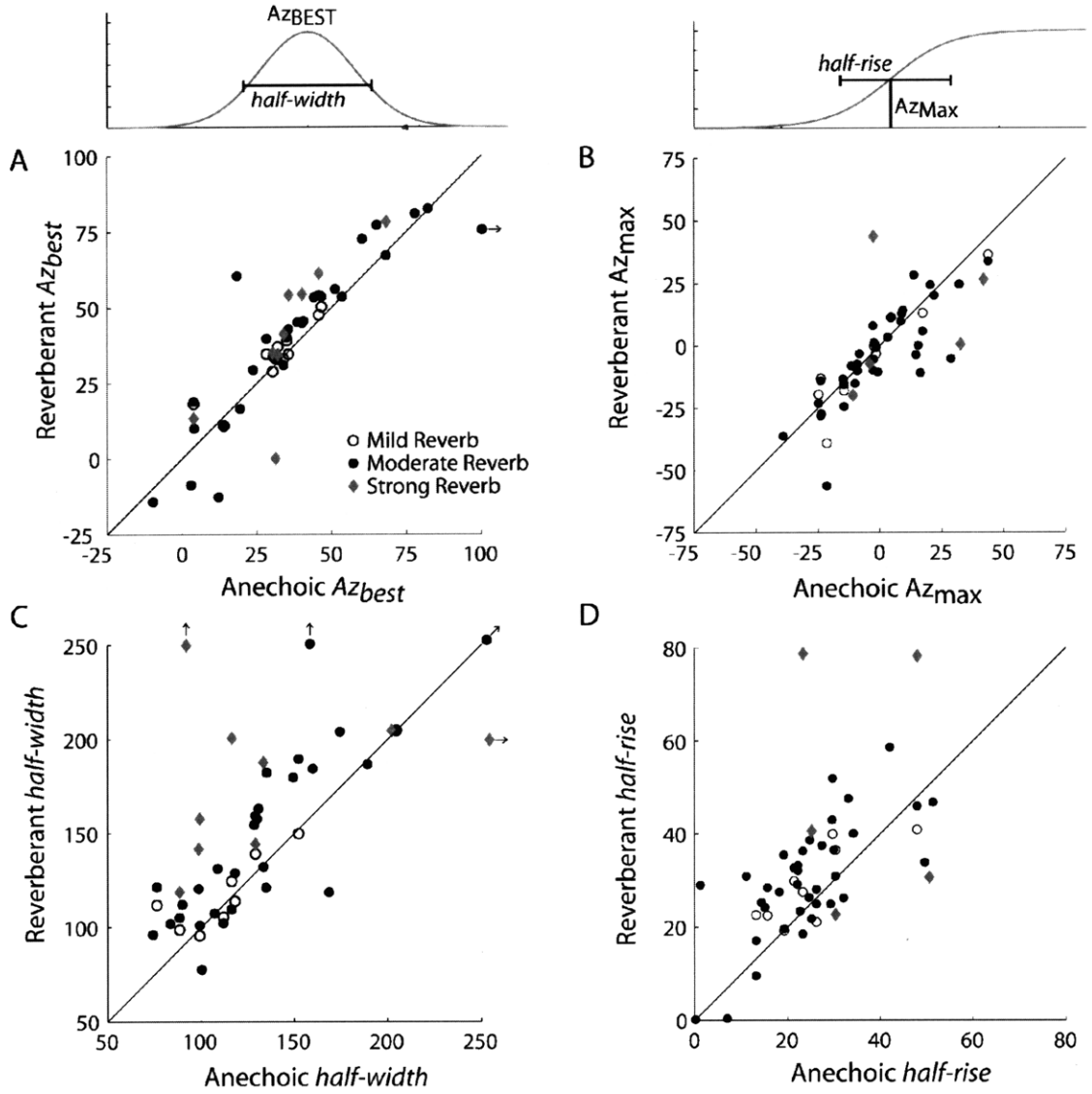

Figure 3.6 Effect of reverberation on azimuth tuning

Top, Illustration of the parameters extracted from *left,* Gaussian and *right,* sigmoid fits to anechoic and reverberant DRF. *A,* Reverberant versus anechoic best azimuth (Az_{best}) for neurons best fit by Gaussian function (mild reverb: n=10, moderate reverb: n=30, strong reverb: n=8). *B,* Reverberant versus anechoic azimuth at maximum slope for neurons best fit by sigmoid function (mild reverb: n=9, moderate reverb: n=38, strong reverb: n=5). *C,* Reverberant versus anechoic half-width for neurons best fit by Gaussian function. *D,* Reverberant versus anechoic half-rise for neurons best fit by sigmoid function.

Time course of directional sensitivity in reverberation

In Chapter 2, we demonstrated that the degradation in the neural representation of source location in reverberation is not instantaneous—the representation is better during the early portion of the stimulus which contains the uncorrupted onset. Figure 3.7 shows a

scatter plot of early (0-50ms) versus ongoing (51-400ms) relative range for each unit in the awake rabbit IC neuron population. The solid line indicates identity i.e., y=x. As observed in anesthetized cat IC, directional sensitivity is better during the early response period, as compared to the more-degraded ongoing response period. This trend holds across the rabbit IC neuron population for each of the reverberation levels[3] (one-sided paired t-test, *mild reverb*: n=21, p=0.021; *moderate reverb*: n=78, p<0.001; *strong reverb*: n=16, p=0.009).

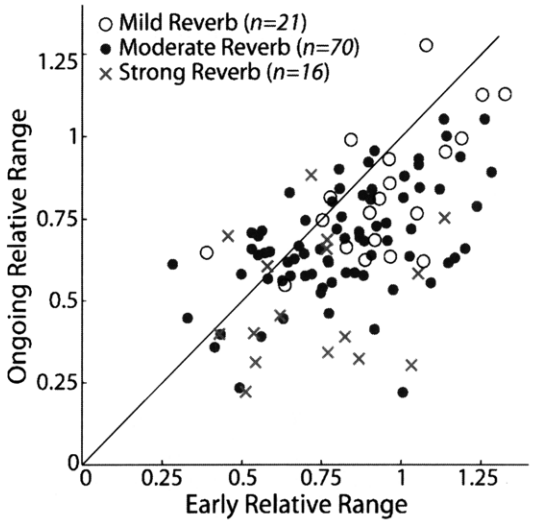

Figure 3.7 Directional sensitivity is better near the stimulus onset
A, Ongoing (51-400ms) versus early (0-50ms) relative range across the awake rabbit IC neuron population. Solid line indicates identity i.e., y=x.

The relative contribution of early and ongoing response to the overall directional sensitivity is determined the distribution of spiking activity across time. In Chapter 2, we showed that the majority of units in the anesthetized cat IC are onset dominated, i.e., firing rates are initially high and decay over time. To the extent that the computation of sound source location involves temporal integration of IC neural responses, such onset dominance emphasizes the earlier (less-degraded) neural representations. To determine

[3] As in **Chapter 2**, to prevent non-directional early responses from biasing our results, we excluded units that failed to show a significant modulation of firing rate across azimuths during the early response epoch (Kruskal-Wallis analysis of variance, p>0.05, 8/94 units excluded).

whether onset-dominance is also a feasible mechanism for improving directional sensitivity in awake rabbit, we computed the population distribution of anechoic T50—the time at which the cumulative peristimulus time histogram (cPSTH, see Methods) reaches 50% of its value at the end of the 400-ms stimulus. Figure 3.8 shows the cumulative distributions of T50 across the awake rabbit (solid line) and anesthetized cat (dashed line) IC neuron populations. Median T50 does not depend on preparation (Mann-Whitney U-test, p=0.136), nor are their significant differences between the overall distributions (Kolmogorov-Smirnov test, p=0.17), suggesting that onset dominance could play a similar role in IC of awake rabbit.

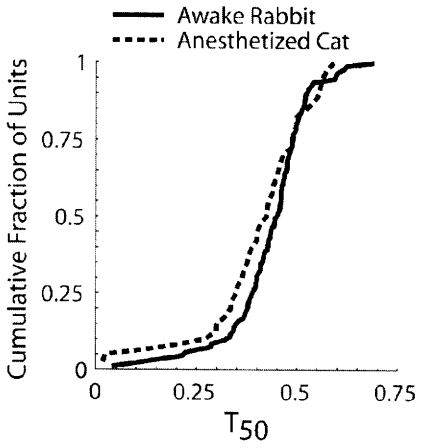

Figure 3.8 Comparison of T50 in awake rabbit and anesthetized cat IC neuron populations
Cumulative distribution of T50 across awake rabbit (solid line) and anesthetized cat (dashed line) IC neuron populations.

Comparison to Anesthetized Cat

In general, the effects of reverberation on directional sensitivity in the awake rabbit IC are qualitatively consistent with our observations from anesthetized cat (Chapter 2). To directly compare, Figure 3.9 shows the population average (± 1 std) relative range in the early, ongoing, and full neural response for both preparations at each of the common reverberation levels tested (*moderate* and *strong*). We ran separate two-way analyses of

variance on the early, ongoing, and full relative ranges using only neurons in which we obtained responses to both *moderate* and *strong reverb* (awake rabbit: n=17 neurons; anesthetized cat: n=24 neurons). For the early relative range, neither preparation nor reverberation level are significant main factors, suggesting that the response to the early segment of reverberant signals is similar across reverberation levels and between species. For both the full and ongoing relative range, reverberation level is a significant main effect but preparation is not, although there are significant interactions between the two factors (*full:* p=0.033; *ongoing:* p<0.001). In both cases, the interaction results from the fact that increasing reverberation causes a significantly larger decrease in relative range for awake rabbit IC neurons than it does in anesthetized cat (t-test, *full:* n = 40, p=0.033; *ongoing:* n=35, p<0.001), despite the fact that the distribution of relative ranges at each reverberation level are not significantly different (t-tests, P>0.11).

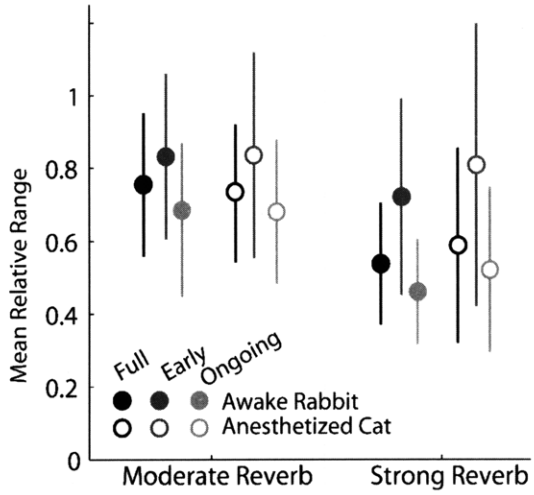

Figure 3.9 Comparison of directional sensitivity in reverberation in awake rabbit and anesthetized cat
Population average (± 1 std) relative range for each stimulus epoch (early, ongoing, full), reverberation level (moderate, strong) and preparation (awake rabbit, anesthetized cat).

All of the neurons tested in the awake rabbit IC showed a decrease in ongoing relative range from *moderate* to *strong reverb* (17 neurons) whereas in the anesthetized cat IC, 5 out of 24 neurons showed an anomalous *increase* in ongoing directional

sensitivity with increasing reverberation. The average increase in relative range for these 5 neurons was very small (0.05±0.04) compared to the average decrease observed in the remaining 19 neurons (0.21±0.16). These results suggest that responses obtained from the anesthetized cat IC show somewhat more variability than those from the awake rabbit preparation. Nevertheless, our results suggest that, on the average, reverberation has similar effects directional sensitivity of neurons from anesthetized cat and awake rabbit IC.

Discussion

Directional sensitivity is similar in awake rabbit and anesthetized cat IC

Overall, our findings suggest that the effects of reverberation on directional sensitivity of low-frequency ITD-sensitive IC neurons are similar in awake rabbit and anesthetized cat. In general, directional sensitivity is better near the onset of a stimulus but degrades as reverberant energy builds up over time. Moreover, we find that the distributions of T50—a quantitative measure of onset dominance in temporal response patterns—are similar in the two preparations, indicating that it could serve similar functional roles in emphasizing the less-degraded earlier responses. These results corroborate the findings of Ter-Mikaelian et al. (2007), who demonstrated that adaptation time constants of auditory midbrain neurons are similar in the awake and anesthetized gerbils.

Relationship to Discrete Echo Suppression

Our findings appear to contradict studies demonstrating profound differences in the neural processing of discrete echoes between awake and anesthetized animal preparations (Fitzpatrick et al., 1999; Litovsky and Yin, 1998; Tollin et al., 2004). In particular, in the present study, we found that directional sensitivity during the early stimulus epoch, where discrete echo suppression may have the most substantial impact, was not significantly different for the awake and anesthetized IC neuron populations. On the other hand, our study analyzes directional responses that are simultaneously affected by direct sound and echoes, while studies of discrete echo suppression typically analyze the response to a single, temporally isolated echo.

To resolve the differences between these types of stimuli, future investigations of discrete echo suppression should be aimed at analyzing changes in the neural response using long-duration stimuli with echoes that overlap in time with the direct sound. Indeed, a recent neurophysiological investigation of echo suppression in barn owl IC that used overlapping direct sound and echo demonstrated that the number of spikes evoked during the period of temporal overlap is independent of echo delay (Nelson and Takahashi, 2008), suggesting that the suppressive mechanisms acting on temporally isolated stimuli do not influence the neural response to simultaneous direct sound and echoes (e.g., in reverberation).

In general, the issue of whether or to what extent discrete echo suppression influences directional sensitivity in reverberation remains unresolved.

Increased Prevalence of Nonmonotonic DRF in Awake Rabbit IC: Implications for Models Sound Localization

A tangential finding of the current study was that proportionally more neurons in the awake rabbit IC have non-monotonic DRFs as compared to the anesthetized cat IC, particularly in the mid-frequency region ~400-800 Hz. Additionally, there was a paucity of units with CFs below 400 Hz in the awake rabbit IC (3.6%, 3/83 units), whereas in the anesthetized cat IC 25% (10/40) of the units had CFs below 400 Hz and the DRF are overwhelmingly monotonic (Fig. 3.2).

The increased prevalence of non-monotonic units in the awake rabbit IC could have implications for decoding models of sound localization. In Chapter 2, we demonstrated that a population rate code for sound localization based on the comparison of activity in two broadly tuned spatial channels, each representing the total activity in one IC, could account for the tendency of sound localization estimates in reverberation to shift towards

the midline (Fig. 2.6). Such hemispheric-difference decoding worked well using the anesthetized cat IC data due to the prevalence of monotonic DRFs.

Using the same algorithm described in Chapter 2 we computed hemispheric difference signals for each of the room conditions using the rabbit IC data. Figure 3.10 shows the hemispheric difference signal versus stimulus azimuth for each of the conditions; error bars represent bootstrapped estimates of ±1 std across the population. The compression in the hemispheric difference signal increases with increasing reverberation, mirroring the compression observed in individual units (Fig. 3.4). However, due to the increased prevalence of non-monotonic DRF in the awake rabbit IC, the hemispheric difference signals tend to saturate quickly at lateral azimuths, and actually exhibit modest non-monotonicies in some conditions. Consistent with the fact that reverberation causes individual DRF to become somewhat *more* monotonic (Fig. 3.5), the signals tend to saturate somewhat less rapidly at lateral azimuths in the *moderate* and *strong* reverb conditions. Nevertheless, even in the anechoic condition, for all azimuths greater than ~45°, the hemispheric difference signal yields approximately the same response, posing a challenge for the localization of stimuli at these lateral azimuths.

If our sample of rabbit IC neurons is biased towards high CFs, then we would expect the hemispheric difference signal for an unbiased sample to be more monotonic than the present data suggest, as it would be influenced by proportionally more low-CF neurons which tend to have monotonic DRF. On the other hand, if our sample *is* representative of the true underlying distribution, then the present results suggest that simple hemispheric difference decoding models might not work for this species.

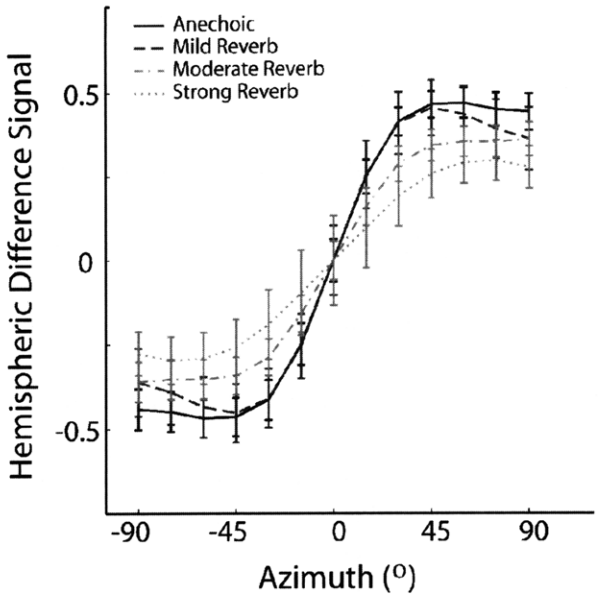

Figure 3.10 Population rate decoding in awake rabbit IC
Hemispheric difference signal as a function of virtual stimulus azimuth computed from the awake rabbit IC neural data.

The main alternative to hemispheric decoding is the Jeffress model i.e., labeled-lines codes (Jeffress, 1948). In a labeled-line model, sound location is computed from the population activity by reading out the label (e.g., ITD) of the unit that is maximally activated or by computing the ITD of the centroid across the population. The possibilities for the population readout as well as the assumptions concerning precisely what labels are transmitted are numerous; therefore, we have avoided implementing a labeled-line decoding model. However, the current neurophysiological results suggest that the Jeffress model might also be able to account for human sound localization in reverberation. Recall, the human lateralization study in Chapter 2 demonstrated that, with increasing reverberation, listener's estimate of sound location shifted towards the midline (Fig. 2.6A). If we assume that (1) neurons are labeled by their best delays and (2) sound location is computed by reading out the label of the maximally active unit, then in order for behavioral estimates of source location to shift *towards* the midline, neurons must respond more vigorously to sources *away* from the midline—a classic inverse

coding problem. The prevalence of non-monotonic DRF in the awake rabbit IC neuron population enabled us to analyze the shifts in best azimuth for a substantial number of neurons (Fig. 3.6A). The results indicated that reverberation tends to increase the best azimuth, so that neurons respond more vigorously to sources further from the midline. Such lateral shifts in best azimuth are qualitatively consistent with the behavioral results of Chapter 2, suggesting that Jeffress-type models might also be able to account for sound localization in reverberation. Of course, Jeffress models become less attractive when the proportion of monotonic DRF increases, as in the anesthetized cat IC. Resolving the issue of which decoding model works best for a particular species requires knowledge of the exact distribution of best delays and the natural range of ITDs, in addition to knowledge of sound localization behavior in that species. Lacking knowledge of the former in humans, our results suggest that both hemispheric decoding models and labeled-line models may be able to account for human lateralization behavior in reverberation, although we can not conclusively state which model works better.

Possible Explanation for the Paucity of Units with Very Low CFs in Awake Rabbit IC

An important question nevertheless remains: Why the paucity of units with very low CFs (< 350 Hz) in awake rabbit? It could be that the blind dorsal-ventral approach to the IC in the awake rabbit preparation biases us away from very low-CF neurons, whereas in the anesthetized cat preparation we visually targeted the low-CF region of the IC using a posterior approach. On the other hand, behavioral investigations of hearing in mammals have shown that the low-frequency limit for hearing in rabbits is somewhat higher than in guinea pigs or cat (Heffner and Masterton, 1980; Heffner and Heffner, 1985), suggesting that the lack of units with very low CFs in our population might partially result from a

general absence of units tuned to very low CFs. Alternatively, due to the elevated hearing thresholds at very low CFs in rabbit, there may be low CF units that simply weren't activated by the 60 dB SPL search stimulus, although such an argument can only account for the lack of extremely low-CF units (< 125 Hz). Future studies might partially resolve these issues by comparing evoked-potential neural audiograms for anesthetized cat and awake rabbit.

CHAPTER 4

Effects of conditioning on directional sensitivity of ITD-sensitive IC neurons: Probing the role of onset dominance

Abstract

Directional sensitivity of IC neurons in reverberation follows a characteristic time course, in that it is better near the onset of a stimulus and becomes more degraded over time, as reverberation builds up. Moreover, onset dominance in temporal response patterns emphasizes the earlier, less-degraded stimulus segments, resulting in more robust directional sensitivity than expected given the average acoustic degradation in the ear-input signals. Here, we use a conditioning paradigm to systematically alter temporal response patterns during the presentation of virtual space stimuli, enabling us to explicitly study the relationship between onset dominance and directional sensitivity in reverberation. Results suggest that making temporal response patterns less onset dominated typically leads to poorer directional sensitivity in reverberation, particularly during the response epochs immediately following the conditioning stimulus.

Introduction

The concept of rate codes has largely dominated the manner in which stimulus-response properties are studied in nervous system. But rate representations are inherently complicated by underlying temporal response dynamics. As first documented in the pioneering experiments of Lord Adrian in the 1920s, most sensory neurons adapt during sustained stimulation. That is, in response to a stationary, sustained stimulus, neurons typically fire an initial, high-frequency train of action potentials, followed by a gradual decline in the firing rate to a (smaller) steady state. Such temporal response dynamics poses a challenge for the coding of time-varying stimuli. The local (i.e., short-term) rate response to a stimulus feature depends on the "context" in which that feature occurs. Indeed, numerous studies have demonstrated that rate responses of neurons in the auditory midbrain to dynamic stimuli are context sensitive i.e., the rate response to a particular stimulus value (e.g., intensity) depends on the stimulus history. Examples of context sensitivity include neural echo suppression, in which the response to a simulated echo is altered by changes the properties of the leading sound source (Finlayson, 1999; Fitzpatrick et al., 1999; Litovsky and Delgutte, 2002; Litovsky and Yin, 1998; Spitzer et al., 2004; Tollin et al., 2004); dynamic range adaptation, in which the rate versus intensity curve for individual neurons can be manipulated by changing the input stimulus statistics (Dean et al., 2005); and motion sensitivity, in which the rate response to a particular binaural cue value that occurs during a dynamic motion stimulus can be profoundly altered by changing the range of simulated motion (McAlpine et al., 2000; Spitzer and Semple, 1991; Spitzer and Semple, 1993; Spitzer and Semple, 1998). The neural mechanisms underlying context sensitivity in the auditory midbrain are numerous

and include changes in the dynamics of excitation i.e., adaptation (Finlayson and Adam, 1997; McAlpine and Palmer, 2002) as well as inhibition (Finlayson and Adam, 1997; Kuwada et al., 1989; Sanes et al., 1998).

The inferior colliculus (IC), the primary nucleus comprising the auditory midbrain receives inputs from nearly all nuclei in the auditory brainstem (Adams, 1979; Aitkin and Schuck, 1985; Oliver et al., 1995; Osen, 1972). Interactions between converging excitatory and inhibitory inputs onto single IC neurons (Bock et al., 1972; Le Beau et al., 1996; Rose et al., 1963), in addition to intrinsic membrane dynamics [e.g., (Sivaramakrishnan and Oliver, 2001)], constitute some of the numerous mechanisms sculpting temporal response dynamics in the IC. Moreover, many IC units show evidence of sustained inhibition that can not be revealed by traditional extracellular recordings (Xie et al., 2007). The temporal response patterns observed across IC neurons are diverse and while many units exhibit some form of spike rate adaptation (Finlayson and Adam, 1997; Ingham and McAlpine, 2004; Nuding et al., 1999; Stillman, 1971b), other units show "sustained" or "buildup" response patterns (Nuding et al., 1999; Rees et al., 1997).

In previous work, we demonstrated that there may be an important role for temporal response dynamics in improving directional sensitivity of auditory midbrain neurons in reverberant environments. In reverberant environments, echoes interfere with the direct sound wave arriving at a listener's ears, distorting the spatial cues for sound localization. Because reverberation builds up over time, the source location is represented relatively faithfully during the initial portion of a sound but this representation becomes more degraded later in the stimulus. In Chapter 2-3, we showed

that the time course of directional sensitivity in reverberation for ITD-sensitive IC neurons qualitatively parallels the dynamics of the ear-input signals. Furthermore, we suggested that, to the extent that neural responses are onset-dominated (i.e., adapting), the earlier (less-degraded) response will be emphasized, thus serving as a simple mechanism for improving directional sensitivity in reverberation.

Here, we directly investigate the role of temporal response dynamics in sculpting directional sensitivity of individual neurons in reverberation. Namely, we use a conditioning paradigm to investigate the consequences of altering the acoustic context—and hence the local temporal response dynamics—in which a reverberant stimulus occurs. We tested the hypothesis that making a neuron less-onset dominated (i.e., by reducing the change in firing rate over the duration of the stimulus) would degrade directional sensitivity in reverberation. Consistent with our hypothesis, we find that conditioning systematically alters directional sensitivity during the early response segment (i.e., the response immediately following the conditioner). On the other hand, our results suggest that there is not a simple relationship between temporal response dynamics and directional sensitivity in reverberation measured over the entire stimulus duration. These findings highlight the complexity of neural processing that takes place at or below the level of the IC and underscore the difficulty in trying to develop simple stimulus/rate response relations.

Methods

Surgical Preparation and Recording Procedures

Methods for recording from single neurons in the inferior colliculus (IC) of unanesthetized Dutch-Belted rabbits, (*Oryctolagus cuniculus*) were as described in Chapter 3.

Acoustic Stimuli

Anechoic and reverberant stimuli were synthesized using the *anechoic* and *moderate reverb* digital filters described in Chapter 3. Virtual space stimuli were created by convolving the digital filters with reproducible 400-ms broadband noise bursts.

We used two stimulus conditions to study directional sensitivity of single neurons using the virtual space stimuli (Fig. 4.1). In the CONTROL condition, virtual space stimuli were presented in a standard stimulus-silent interval paradigm, with 600-ms of silence separating presentations of virtual space stimuli. In the CONTEXT condition, we replaced the last 200-ms of silence preceding each virtual space stimulus by a reproducible burst of dichotic broadband noises that were completely uncorrelated at the two ears. The pair of uncorrelated noise bursts (presented to the left and right ears) were created using a Gramm-Schmidt orthogonalization procedure (Culling et al., 2001). In a subset of neurons tested, the virtual space probes in the CONTEXT condition were 200-ms in duration (followed by 600 ms of silence).

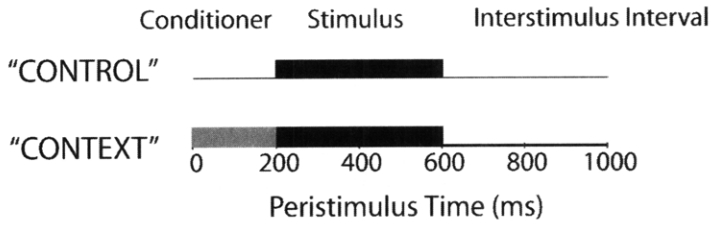

Figure 4.1 Conditioning stimulus paradigm
In the CONTROL condition (top), the virtual space stimulus is preceded by silence, whereas in the CONTEXT condition (bottom) the silent period is replaced by a 200-ms burst of broadband noise that is uncorrelated at the two ears. In a subset of experiments, the virtual space stimulus in the CONTEXT condition was 200-ms in duration, followed by 600-ms of silence.

Experimental Procedures

The search stimulus consisted of 40-Hz sinusoidally amplitude-modulated broadband noise bursts presented at a nominal level of 65 dB SPL. When a single unit was well isolated, its characteristic frequency (CF) was determined using an automatic tracking procedure (Kiang and Moxon, 1974). Acoustic threshold was determined using 200-ms diotic broadband noise (2/sec x 4-10 repeats). Spontaneous rate was computed from the spiking activity in a 100-ms silent period preceding each broadband noise presentation.

ITD-sensitivity was assessed using 200-ms broadband noise bursts typically presented at delays of ±2000μs in 200μs steps (2/sec x 10 trials). A unit was considered ITD-sensitive if an analysis of variance for the distributions of firing rates across ITD showed a significant main effect of ITD (at the level α=0.05).

Only ITD-sensitive units were studied using the virtual space stimuli. Neural responses were obtained for the four conditions (anechoic/reverb and CONTROL/CONTEXT) in pseudorandom order. We typically used 13 azimuths (15° spacing) or, occasionally, 7 azimuths (30° spacing), randomized on a trial by trial basis (1/sec x 8-12 repeats). Stimuli were presented at 15-20 dB above threshold.

Data Analysis

Neural responses were discretized into 1-ms bins. We defined the neural response latency for each neuron as the first time bin in the across-azimuth peristimulus time histogram (PSTH) showing a deflection of greater than ±2 standard deviation from spontaneous rate. A directional response function (DRF) for each room condition was computed by averaging the number of spikes that occurred during a fixed window. A *full* DRF was computed using a window starting at neural response latency, with length equal to the duration of the virtual space stimulus[4]; an *early* DRF was computed using a window starting at neural response latency, with length equal to 50-ms; and an *ongoing* DRF was computed using a window that started 50-ms after neural response latency and extended to the end of the virtual space stimulus. When analyzing response obtained in the CONTEXT condition, the analysis window was shifted forward by 200-ms to avoid including spikes elicited by the conditioner. DRFs were smoothed using a three point triangular smoothing filter having weights [1/6, 2/3, 1/6].

Quantitative analysis of DRF was done using the same metrics described in Chapter 2. Briefly, we computed a non-monotonicity index (NMI) to describe the shape of each DRF. To quantify directional sensitivity in reverberation, we computed the *relative range* for each DRF. To assess the differences in firing rate between CONTROL and CONTEXT conditions, we computed a conditioned rate index as $\frac{\bar{f}_{CONTEXT} - \bar{f}_{CONTROL}}{\bar{f}_{CONTEXT} + \bar{f}_{CONTROL}}$, where $\bar{f}$ denotes the across-azimuth average firing rate for a given stimulus condition.

---

[4] In most experiments, the virtual space stimulus was 400-ms in duration; however, in earlier experiments the duration of the virtual space stimulus was only 200-ms.

To assess changes in temporal response pattern during the virtual space stimulus we computed the ratio of early to ongoing firing rates (E/O), defined as the ratio of across-azimuth average firing rate obtained from the early (time 0-50 ms) and ongoing (time 51-end) neural response epochs. Note that the E/O is computed only from activity elicited by the virtual space stimulus in each condition, after adjusting for neural response latency.

Results

In Chapter 2 we demonstrated that onset dominance in IC neural processing emphasizes the earliest response periods to a reverberant stimulus, resulting in more robust directional sensitivity than expected given the average acoustic degradation in the ear-input signals. While the results of this study suggested a role for temporal response dynamics in sculpting reverberant directional sensitivity, the hypothesis was not directly tested. Here, we used a conditioning paradigm to investigate the effects of altering temporal response dynamics on directional sensitivity in 24 neurons from the IC of 2 awake rabbits. These neurons are a subset of the larger population studied in Chapter 3.

Effect of stimulus context on anechoic directional rate responses

The stimulus conditions, along with dot rasters illustrating the anechoic data for three neurons, are shown in Figure 4.2. In the CONTROL condition (Fig. 4.2, top row), neural responses were obtained using a standard stimulus paradigm in which trials consist of a virtual space stimulus preceded and followed by silence. In the CONTEXT condition (Fig. 4.2, middle row), the 200ms of silence preceding each virtual space stimulus was replaced by a conditioning stimulus consisting of uncorrelated broadband noise. Because the instantaneous interaural phase of uncorrelated noise varies randomly across both time and frequency, it is a spatially non-specific stimulus that can be likened to the background noise resulting from multiple, simultaneous sources of sound.

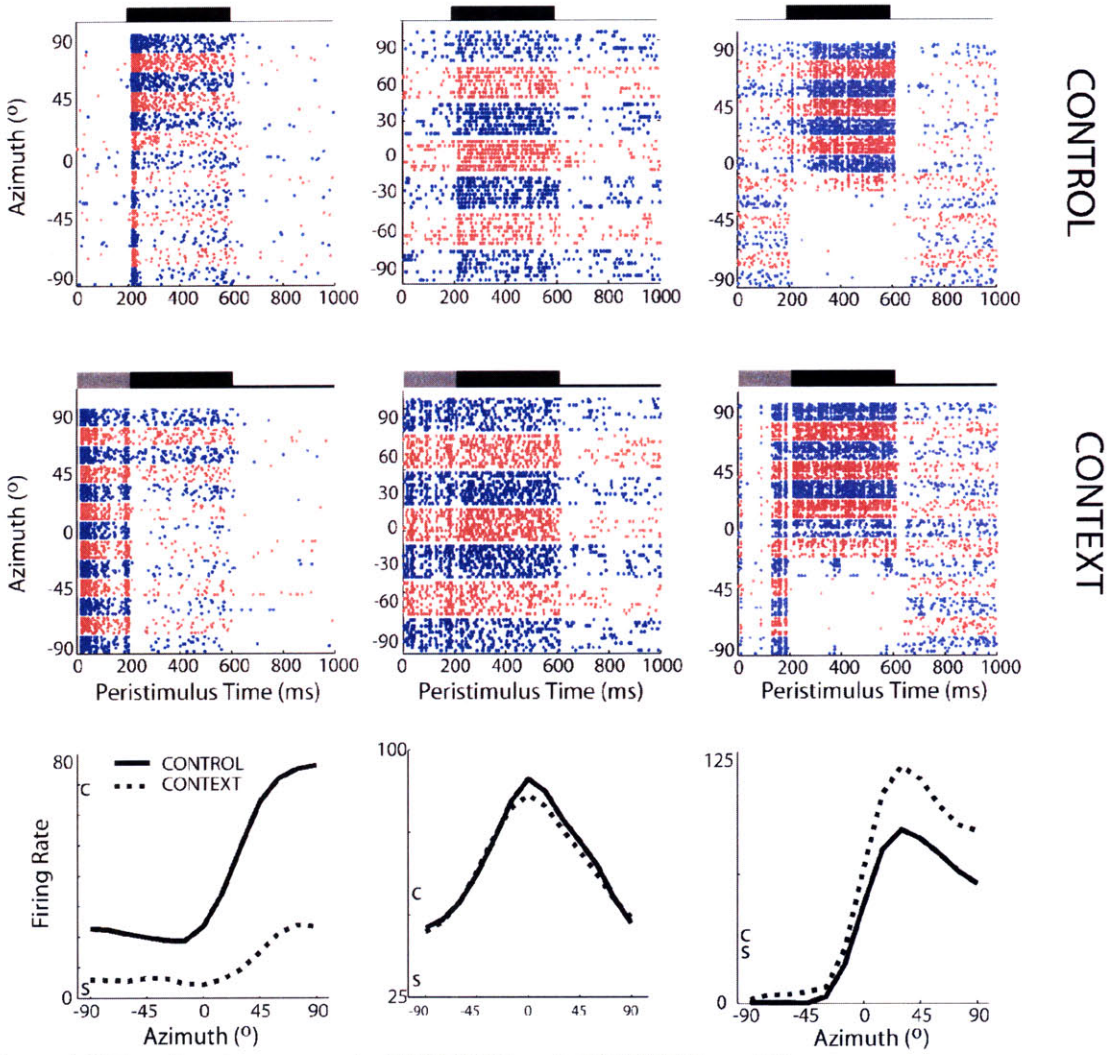

Figure 4.2 Directional responses in CONTROL and CONTEXT conditions
Representative data collected from 3 ITD-sensitive IC neurons; each column represents one neuron. *Top row*, Dot rasters illustrating activity measured anechoic CONTROL stimulus. *Middle row*, Dot rasters illustrating activity measured using the anechoic CONTEXT stimulus. *Bottom row*, Directional response functions (DRF) computed from the activity during the full virtual space stimulus (*top and middle rows,* black bars) in both CONTROL (solid lines) and CONTEXT (dashed lines) conditions.

To demonstrate that the uncorrelated noise conditioner systematically alters temporal response patterns (and hence the distribution of spiking activity over the duration of the stimulus), we computed the ratio of early to ongoing firing rates (E/O, see Methods). An E/O of one indicates that the firing rate is similar throughout the duration of the stimulus and an E/O greater than one indicates the firing rate is higher near the onset of the stimulus. Figure 4.3A shows a scatter plot of E/O obtained in the

CONTEXT condition versus the CONTROL E/O. The different symbols denote the duration of the virtual space probe in the CONTEXT condition, which determined the duration of the ongoing analysis window (see Methods). Because the effects of noise conditioning were similar for data sets analyzed using a 200-ms and 400-ms analysis window, we combined all of the data for the sake of statistical analysis. However, in all of the figures, we distinguish between the two data sets using different symbols (200-ms: filled symbols; 400-ms: open symbols).

In a majority of cells (17 out of 24), the CONTROL E/O is greater than one, indicating temporal response patterns are typically somewhat onset dominated, whereas in the CONTEXT condition E/Os are clustered around one, indicating sustained temporal response patterns. The change in E/O (ΔE/O) is highly correlated with the CONTROL E/O (Fig. 4.3B; $r=-0.982$, $p<1e-4$), consistent with the fact that noise conditioning tends to drive all E/Os toward one. Inspecting the dot rasters in the top and middle rows of Figure 4.2, it is apparent that the conditioner has the biggest influence on the neural response during early segment (e.g., first 50 ms) of the virtual space stimulus, whereas the response pattern during the ongoing segment is similar in CONTROL and CONTEXT conditions. These results suggest that the general effect of noise conditioning is to "adapt" the neural response into a steady state and therefore alter the temporal response pattern during the virtual space stimulus.

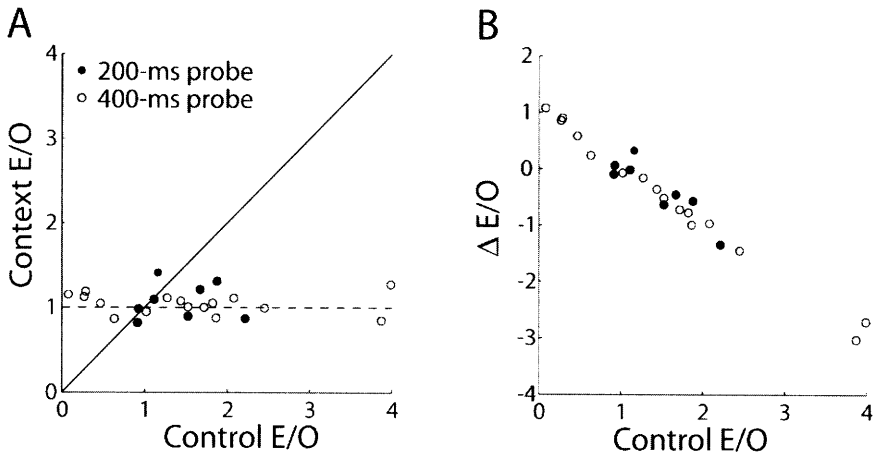

Figure 4.3 Conditioning systematically alters temporal response patterns.
A, Ratio of early to ongoing firing rates (E/O) obtained in CONTEXT condition versus CONTROL E/O. The different symbols denote the duration of the virtual space probe in the CONTEXT condition (filled symbols, 200ms; open symbols, 400 ms). *B,* ΔE/O—difference in E/O between CONTEXT and CONTROL conditions versus CONTROL E/O. The two measures are inversely correlated (r=-0.982, p<0.001).

To assess the effects of noise conditioning on directional sensitivity, we computed directional response functions (DRF) for each condition by counting the number of spikes that occurred during the virtual space stimulus, after adjusting for latency (see Methods). The bottom row of Figure 4.2 illustrates anechoic DRF obtained under CONTROL (solid line) and CONTEXT (dashed line) stimulus conditions. The firing rate elicited by the conditioner is depicted by the small 'c' at the left of each panel; spontaneous firing rate is denoted by the 's'. The conditioner reliably elicits activity from every neuron in our sample. On average, the firing rate for the noise conditioner is 62.4% (±38.1%) of the maximum firing rate observed in the CONTOL DRF.

In general, the overall shape of the DRFs was similar for both conditions (Fig. 4.2, *bottom row*). We quantified the shape of each DRF by computing a non-monotonicity index (NMI). The NMIs in CONTROL and CONTEXT conditions are highly correlated (data not shown, r=0.918, p<1e-4) and the difference is not significantly

different from zero (paired t-test, p=0.24), indicating that the noise conditioner does not significantly alter long-term directional tuning, *per se*.

The principle differences between the CONTROL and CONTEXT DRFs consist of stretching/shrinking in addition to absolute shifts along the ordinate. We hypothesized that the effect of noise conditioning on DRF firing rates would be related to the degree of onset dominance in CONTROL temporal response patterns. That is, we reasoned that onset dominated units would exhibit decreases in firing rate after noise conditioning, whereas conditioning should have little effect on the firing rate in units with more sustained response patterns.

The data in Figure 4.2-4.3 illustrate how changes in E/O are related to changes in the DRF firing rates. The unit in the leftmost column of Figure 4.2 has an adapting temporal response pattern in the CONTROL condition (Fig. 4.2, top row), and hence a large E/O. Noise conditioning adapts the response to a steady state (Fig. 4.2, middle row), so that the E/O is close to one in the CONTEXT condition. As a result of the rate adaptation, the firing rate decreases at all azimuths (Fig. 2, bottom row).

The unit in second column of Figure 4.2 has a more sustained temporal response pattern in the CONTROL condition (Fig. 4.2, top row) and therefore an E/O close to one in both CONTROL and CONTEXT conditions. The conditioner causes little rate adaptation and hence the firing rates are similar in CONTROL and CONTEXT conditions (Fig. 4.2, bottom row).

The unit in third column in Figure 4.2 illustrates one of the few neurons with an E/O less than one in the CONTROL condition. This unit has a pause/buildup type response pattern in the CONTROL condition, consisting of an onset spike followed by a

gradual buildup in activity after a brief pause. In the CONTEXT condition, the firing rate builds up during the noise conditioner so that response during the virtual space stimulus is sustained. Hence, the E/O is closer to one and the overall firing rates are higher (Fig. 4.2, bottom row).

To explicitly examine the relationship between temporal response pattern and changes in DRF firing rate across the population, we defined a conditioned rate index (see Methods), which varies between ±1, where negative numbers indicate that the average firing rate is smaller in the CONTEXT condition as compared to the CONTROL condition. Figure 4.4 shows the conditioned rate index computed from both the early (*panel A*) and the ongoing (*panel B*) response segments, plotted as a function of the CONTROL E/O. As expected, the conditioned rate index for the early response is inversely correlated with CONTROL E/O ($r=-0.83$, $p<1e-4$ such that it is positive for units with buildup-type response patterns (E/O < 1) and negative for units with onset-dominated response patterns (E/O > 1). The conditioned rate index exhibits a weaker inverse correlation with the ongoing conditioned rate index ($r=-0.573$, $p=0.003$). Moreover, the magnitude of the conditioned rate index is smaller for the ongoing response as compared to the early response segment, indicating that the effects of conditioning decay with increasing separation between the conditioning stimulus and the analysis window.

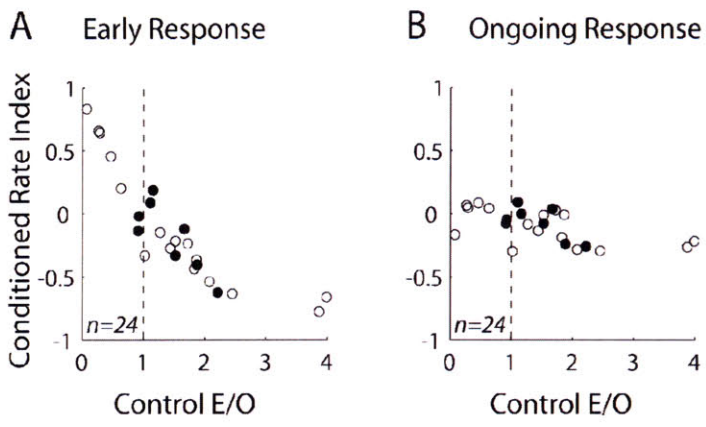

Figure 4.4 Effect of conditioning on average firing rate.
A, Conditioned rate index computed from the early response segment versus CONTROL E/O across IC neuron population. The two metrics are inversely correlated (r=-0.83, p<1e-4). The different symbols are as in Figures 4.3. *B,* Conditioned rate index computed from the ongoing response segment versus CONTROL E/O across the IC neuron population. The two metrics are inversely correlated (r=-0.573, p=0.003).

To examine the time course of conditioning, we computed the conditioned rate index in 50-ms windows, starting at the onset of the virtual space stimulus. Figure 4.5 shows line plots of the conditioned rate index as a function of analysis time interval for each of the neurons in our population. The biggest effects of conditioning are seen in the 50-ms response interval immediately following the conditioner, although the fact that the conditioned rate index does not always approach zero suggestions that conditioning can have long-term effects.

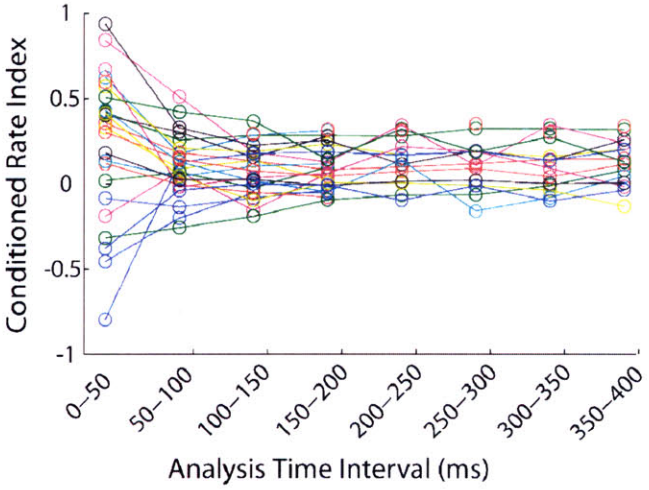

Figure 4.5 Time course of conditioning
Conditioned rate index as a function of the analysis time interval. Each curve represents one neuron in our IC sample.

Effects of noise conditioning on directional sensitivity in reverberation

Having established that noise conditioning causes systematic changes in neural rate responses, we next examined the effect of noise conditioning on directional sensitivity in reverberation.

Figure 4.6 shows anechoic (black lines) and reverberant DRF (gray lines) obtained from two IC neurons (same neurons as in left and middle columns Fig. 4.2) in both CONTROL (solid lines) and CONTEXT (gray lines) conditions. The top panels show DRF computed from the early response epoch (time 0-50 ms) whereas the bottom panels show DRF computed from the full response. The overall effects of noise conditioning on reverberant DRF are largely consistent with the changes observed for anechoic DRF. In the more onset-dominated unit (Fig. 4.6A), noise conditioning leads to decreased firing rates across azimuths (Fig. 4.6A), whereas in the sustained unit (Fig. 4.6B) noise conditioning has only minimal effects on the overall firing rate (compare dashed and solid lines).

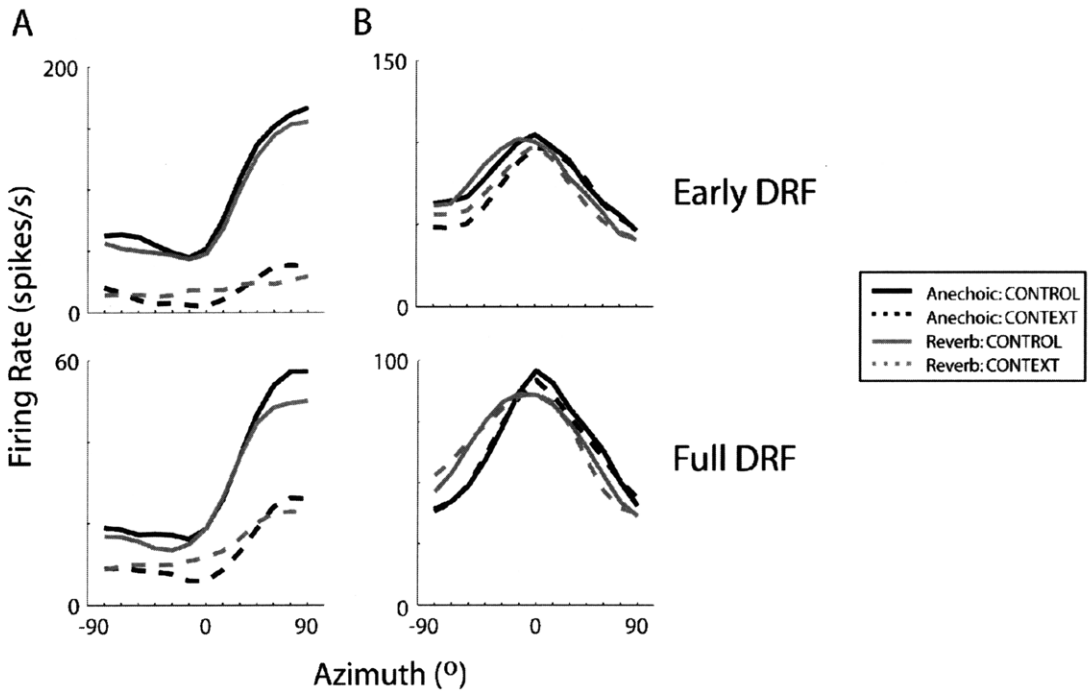

Figure 4.6 Anechoic and reverberant directional responses in CONTROL and CONTEXT conditions Anechoic (black lines) and reverberant (gray lines) DRF obtained under CONTROL (solid lines) and CONTEXT (dashed lines) conditions for two IC neurons. The top row shows DRF computed from the early response epoch, whereas the bottom row shows DRF computed from the full neural response during the virtual space stimulus.

As demonstrated in previous Chapters and illustrated by the data in Figure 4.5), reverberation causes compression of DRF, although directional sensitivity is generally better during the early stimulus epoch and degrades as reverberation builds up over time. We quantified directional sensitivity in reverberation by computing the relative range of firing rates for reverberant DRF (see Methods)[5]. Consistent with the buildup of reverberation in the acoustic inputs, the relative range computed from the early response epoch is significantly larger than the relative range computed from the ongoing stimulus epoch in both the CONTROL (paired t-test, $p=0.011$) and CONTEXT (paired t-test,

[5] The relative range is an attractive measure for quantifying directional sensitivity after conditioning, because it is insensitive to both multiplicative and additive changes in the neural response rate that occur after conditioning [see e.g., Litovsky and Delgutte (2002)].

p=0.009) conditions[6]. Moreover, in the CONTROL condition, directional sensitivity during the early response segment is correlated with E/O (data not shown, r=0.44, p=0.031), suggesting that neurons that fire more vigorously near the onset of a stimulus (i.e., onset-dominated units) are better able to signal source directional near the uncorrupted onset. Directional sensitivity during the ongoing response segment is not systematically related to E/O (p=0.33).

We hypothesized that by altering temporal response patterns with the conditioner, we would observe systematic changes in directional sensitivity in reverberation. Namely, we predicted that neurons that are highly onset dominated in the CONTROL condition would show worse directional sensitivity in the CONTEXT condition whereas units with buildup-type temporal response patterns would show improved directional sensitivity in reverberation after conditioning. Owing to the fact that conditioning has the most prominent effects on neural activity during the early response segment, we expected to observe stronger effects of conditioning during the early neural response segment.

We quantified the differences in overall directional sensitivity in reverberation by computing the difference in relative range (ΔRR) between CONTEXT and CONTROL conditions for both early and full response segments. Figure 4.7A shows ΔRR computed from the early response segment versus CONTROL E/O, where negative values along the ordinate indicate that directional sensitivity in reverberation is *worse* in the CONTEXT condition than in the CONTROL condition. Consistent with our hypothesis, ΔRR is inversely correlated with CONTROL E/O (r=-0.679, p<0.001), such that units with more onset dominated response patterns exhibit worse directional sensitivity after conditioning

---

[6] As in previous Chapters, this analysis excluded units that exhibited non-directional early responses (CONTROL, 1 unit excluded; CONTEXT, 1 unit excluded).

whereas units with buildup-type response patterns show better directional sensitivity in reverberation after conditioning.

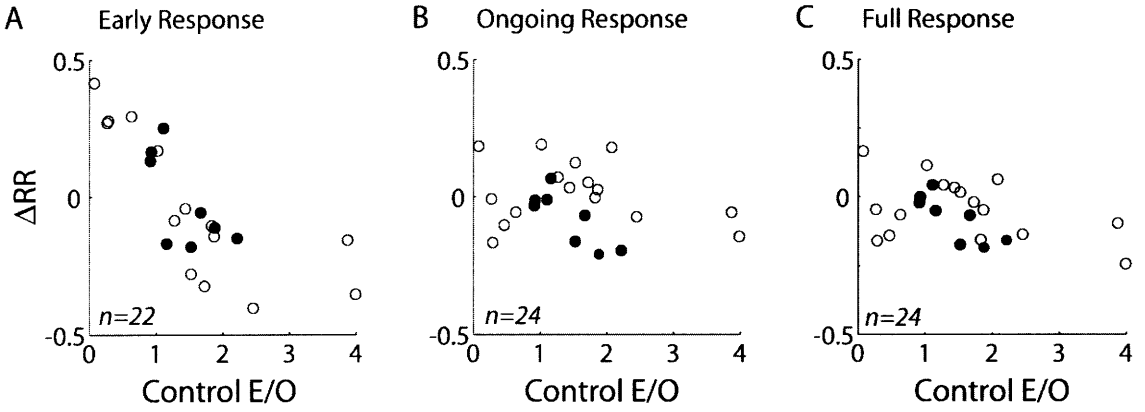

Figure 4.7 Effects of conditioning on directional sensitivity in reverberation
ΔRR—difference in relative range between CONTEXT and CONTROL conditions—versus CONTROL E/O across the IC neuron population for *A*, early response epoch, *B*, ongoing response epoch, and *C*, full response epoch. The different symbols are as in Figure 4.3.

On the other hand, there is not a systematic relationship between ΔRR and directional sensitivity measured during the ongoing neural response epoch (Fig. 4.7B, p=0.89). This result is not unexpected, considering that conditioning has milder effects on the ongoing neural response (e.g., Fig. 4.4-4.5), although the fact that ΔRR is not zero suggests that the conditioner has some influence on the neuronal response to the ongoing reverberant stimulus.

As a result of these essentially random effects of conditioning on ongoing directional sensitivity in reverberation (with respect to CONTROL E/O), when averaged over the full duration of the stimulus, the relationship between E/O and ΔRR just misses significance (Fig. 4.7C, r=0.369, p=0.076). Together, these results suggest that, contrary to our hypothesis, simply accounting for changes in neural response dynamics over the

full duration of the stimulus is not sufficient to predict changes in directional sensitivity in reverberation.

Discussion

Effect of conditioning on directional rate responses

We used a noise conditioning paradigm to study the role of temporal response dynamics in sculpting directional sensitivity in reverberation. By preceding virtual space stimuli with a broadband noise conditioner (Fig. 4.1), we were able to systematically manipulate temporal response patterns and rate responses during the virtual space stimuli (Fig. 4.3-4.4).

Consistent with previous studies of context sensitivity in the auditory midbrain, our results indicate that conditioning alters neural rate responses to virtual space stimuli (Fitzpatrick et al., 1999; Litovsky and Delgutte, 2002; Litovsky and Yin, 1998; Pecka et al., 2007; Spitzer et al., 2004; Tollin et al., 2004). In general, the changes in average firing rate after noise conditioning can largely be predicted from a neurons initial temporal response pattern (Fig. 4.4). Namely, neurons that were onset-dominated in the CONTROL condition exhibited decreased firing rates after conditioning, whereas neurons with more sustained response patterns exhibited only minor changes in firing rate after conditioning. The effects of conditioning were stronger when the analysis window was restricted to the early response segment (Fig. 4.4), indicating that the effects of conditioning are somewhat localized in time (Fig. 4.5). The reduced effect of conditioning on ongoing neural responses is not surprising, considering that the ongoing response is essentially in steady-state even in the CONTROL condition. However, despite the fact that the magnitude of the effect was reduced, the conditioner did cause long-term changes in firing rate for a substantial number neurons (Fig. 4.4B).

Role of response dynamics in mediating directional sensitivity in reverberation

By using the conditioning stimulus to systematically alter temporal response dynamics, we directly tested the hypothesis that onset dominance in temporal response patterns improves directional sensitivity in reverberation. Our results demonstrate that this simple relationship holds only during the early response segment (Fig. 4.6A), where conditioning has the strongest effects, but not when directional responses are averaged over the entire stimulus duration (Fig. 4.6B). These results suggest that accounting for changes in temporal response patterns alone is not sufficient to predict changes in directional sensitivity in reverberation.

The systematic effect of conditioning on early directional sensitivity in reverberation is intuitively related to spiking dynamics associated with onset-dominated versus buildup-type units. Onset-dominated cells fire vigorously near the onset of a stimulus; thus the uncorrupted onset of a reverberant stimulus evokes a strong response from onset-dominated cells whereas it evokes a much weaker response, if any, from buildup-type cells. On the other hand, after conditioning, both onset-dominated and buildup-type cells have been driven into a steady-state regime where they are capable of responding throughout the duration of the reverberant stimulus. Lacking the vigorous onset response after conditioning, we therefore expected directional sensitivity in reverberation to become worse in onset-dominated units. The opposite logic applies to buildup-type cells.

As explained in Chapter 2, directional sensitivity measured over the full duration of stimulus is determined by the relative contribution of the early and ongoing neural

responses. The present results showed that the conditioner causes systematic changes in the early directional sensitivity (Fig. 4.7A) but essentially random changes in ongoing directional sensitivity. In light of this finding, it is not surprising that we find such a weak relationship between overall directional sensitivity in reverberation and temporal response dynamics (Fig. 4.7C).

Nevertheless, despite the fact that the results suggest overall changes in directional sensitivity are not significantly correlated with temporal response dynamics (Fig. 4.7C), a majority of the onset dominated neurons (i.e., E/O>>1) did indeed show worse directional sensitivity after noise conditioning, as predicted. In support of this finding, Schwartz et al. (2009) recently demonstrated that spike rate adaptation—one of the possible mechanisms underlying onset dominance in the IC—can improve directional information extracted from auditory nerve spike trains across time.

Long-term changes in neural response rate after conditioning

While the present results suggest that conditioning causes systematic changes in the early response to a reverberant stimulus (Fig. 4.7A), we also found that conditioning causes changes in the ongoing directional sensitivity that are not immediately related to changes in temporal response dynamics. In general, the neural mechanisms underlying "context sensitive" changes in auditory midbrain rate responses are numerous, and include changes in the dynamics of excitation as well as inhibition (Finlayson and Adam, 1997; Kuwada et al., 1989; Litovsky and Delgutte, 2002; McAlpine and Palmer, 2002; Pecka et al., 2007; Sanes et al., 1998). The uncorrelated conditioning stimulus used in the present study might differentially activate and adapt each of the various sources of synaptic input to ITD-sensitive IC neurons, which may affect the long-term balance of excitation and

inhibition sculpting neural responses (D'Angelo et al., 2005; Ingham and McAlpine, 2005; Kuwada et al., 1989; Le Beau et al., 1996; McAlpine and Palmer, 2002; Pecka et al., 2007; Tan and Borst, 2007; Xie et al., 2007). Because reverberant stimuli are dynamic, i.e., the binaural cues are rapidly varying over time (Ihlefeld and Shinn-Cunningham, 2004; Shinn-Cunningham and Kawakyu, 2003), there is an additional level of interaction between short-term binaural cues and changes in the underlying spiking dynamics. In general, the present findings highlight the notion that the processing of ongoing dynamic stimuli (such as reverberation) in the auditory midbrain is complex and likely involves multiple sources of synaptic input. Nevertheless, our findings confirm that onset-dominance in temporal response patterns can improve directional sensitivity in reverberation, particularly during the early portion of the reverberant stimulus.

CHAPTER 5

Effects of reverberation on directional sensitivity across the tonotopic axis in the awake rabbit IC

Portions of this chapter will appear in the proceedings of the 15th International Symposium on Hearing:

Devore, S., A. Schwartz, and B. Delgutte (2009). *Effects of reverberation on directional sensitivity of auditory neurons: peripheral and central factors.* Proc. of the International Symposium on Hearing, Salamanca, Spain, 1-5 June.

Abstract

In reverberant environments, acoustic reflections interfere with the direct sound arriving at a listener's ears, distorting the binaural cues for sound localization. We investigated the effects of reverberation on the directional rate responses of single units in the inferior colliculus (IC) of unanesthetized rabbits, focusing on neurons exhibiting sensitivity to interaural time differences (ITD). Our results demonstrate that reverberation degrades the directional sensitivity of single neurons, although the amount of degradation depends on the characteristic frequency (CF) and the type of binaural cues available. When ITD is the only available directional cue, low-CF cells sensitive to ITD in fine-time structure maintain better directional sensitivity in reverberation than high-CF cells sensitive to ITD in the cochlea-induced envelope. Using recordings from primary auditory neurons, we show that this result can be attributed to the fact that reverberation degrades the directional information in interaural envelopes more so than in the fine time structure. On the other hand, when both ITD and interaural level difference (ILD) cues are available, directional sensitivity is comparable throughout the tonotopic axis, suggesting that, at high frequencies, ILDs provide better directional information than envelope ITDs in reverberation. These results are consistent with human psychophysical studies of sound localization in reverberant environments.

Introduction

Indoors and in nature alike, the auditory scenes that we perceive unfold in reverberant environments. In a reverberant sound field, reflected acoustic waves reach the listener from all directions, interfering with the direct sound at a listener's ears and distorting the binaural cues for sound localization such as interaural time and level differences (ITD/ILD). In previous work (Chapter 2-3), we demonstrated that reverberation degrades the directional sensitivity of low-frequency ITD-sensitive neurons in the auditory midbrain. Here, we extend that work by characterizing directional sensitivity in neurons across a much wider range of the tonotopic axis, maintaining our focus on neurons that are sensitive to ITD.

Neural sensitivity to ITD emerges in two distinct circuits in the superior olivary complex (SOC), the primary site of binaural interaction in the auditory brainstem (Caird and Klinke, 1983; Goldberg and Brown, 1969; Joris and Yin, 1995; Yin and Chan, 1990). Principle cells in the medial superior olive (MSO) detect coincidences in convergent excitatory inputs from the cochlear nucleus on both sides of the head (Goldberg and Brown, 1969; Yin and Chan, 1990). MSO neurons typically show "peak-type" tuning to ITD i.e., the firing rate versus ITD functions at different tonal stimulation frequencies tend to align at their peaks (Batra et al., 1997a; Yin and Chan, 1990). Neurons in the lateral superior olive (LSO) receive convergent excitatory input from the ipsilateral cochlear nucleus and inhibitory input from the contralateral cochlear nucleus via the medial nucleus of the trapezoid body. A considerable fraction of neurons in the lateral superior olive (LSO) are sensitive to ITD (Batra et al., 1997a; Joris and Yin, 1995; Tollin and Yin, 2005), although the subtractive circuits in the LSO are classically associated

with generating neural sensitivity to ILD (Boudreau and Tsuchitani, 1968). Typically, rate versus ITD functions for LSO neurons at different frequencies align at a common minima, so that LSO neurons are classified as "trough type". In practice, ITD-tuning types are not completely segregated in the brainstem. Batra et al. (Batra et al., 1997a) reported peak-type neurons in the vicinity of the LSO and trough-type neurons in the vicinity of the MSO, although such occurrences were uncommon.

The inferior colliculus (IC), the primary nucleus comprising the auditory midbrain, is an obligatory synaptic station for ascending inputs to the thalamus and auditory cortex (Adams, 1979) and, as such, it receives excitatory and inhibitory projections from nearly all nuclei in the auditory brainstem (Aitkin and Schuck, 1985; Oliver et al., 1995; Osen, 1972). Many neurons in the IC are sensitive to ITD, consistent with direct inputs from the MSO and LSO (Kuwada et al., 1987; Kuwada and Yin, 1983; Rose et al., 1966; Yin et al., 1986), although the binary classification of IC neurons as showing "peak" and "trough" type ITD-tuning is overly simplistic. IC neurons exhibit ITD-tuning along a continuum from "peak" to "trough", with many neurons showing alignment of rate versus ITD functions for different stimulation frequencies at an intermediate point between the peak and trough (Fitzpatrick et al., 2000; Fitzpatrick et al., 2002). Although "intermediate type" neurons have been located in the brainstem (Batra et al., 1997a), an alternative proposition is that "intermediate type" neurons are created locally by convergent inputs from MSO and LSO neurons onto the same IC cell (Agapiou and McAlpine, 2008; Fitzpatrick et al., 2002; McAlpine et al., 1998). Moreover, convergent brainstem inputs can also account for the fact that a fair number of IC neurons

do not exhibit an orderly alignment of rate ITD curves across frequency (McAlpine et al., 1998).

At low CFs, IC neurons are typically sensitive to ITD in stimulus fine structure while at high CFs, IC neurons are sensitive to ITD in envelopes (Batra et al., 1993; Griffin et al., 2005; Joris, 2003; Yin et al., 1984). At all characteristic frequencies (CFs), the rate response of ITD-sensitive IC neurons can altered by imposing ILDs (Batra et al., 1993; Caird and Klinke, 1987; Palmer et al., 2007), although for stimuli with naturally co-occurring binaural cues, ILD may be a more potent directional cue than envelope ITDs in high frequency neurons (Delgutte et al., 1995).

Few studies have systematically investigated ITD sensitivity across a wide range of frequencies (Caird and Klinke, 1987; Fitzpatrick et al., 2002; Joris, 2003) and, to the best of our knowledge, none of these has explicitly examined the influence of ILD that covary with ITD. Here, we use virtual auditory space (VAS) simulation techniques to characterize the effects of reverberation on the directional sensitivity of ITD-sensitive neurons in the IC of unanesthetized rabbits. We find that reverberation degrades the directional sensitivity of single neurons, although the amount of degradation depends on the characteristic frequency (CF), ITD tuning type, and the types of binaural cues available. To elucidate the role of peripheral auditory processing, we compare results from IC neurons with measures of directional information extracted from coincidence analysis of spike trains recorded from auditory nerve (AN) fibers in anesthetized cats.

Methods

Surgical Preparation and Recording Procedures

Methods for recording from single neurons in the inferior colliculus (IC) of unanesthetized Dutch-Belted rabbits, (*Oryctolagus cuniculus*) were as described in Chapter 3. All procedures were approved by the animal care and use committees of both the Massachusetts Eye and Ear Infirmary the Massachusetts Institute of Technology.

Virtual Space Stimuli

Two sets of binaural room impulse responses (BRIRs) were simulated using the room-image method (Allen and Berkley, 1979; Shinn-Cunningham et al., 2001) for a pair of receivers separated by 12 cm in the center of a virtual room measuring 11x13x3 meters. The inter-receiver distance was chosen to ensure that the range of interaural time differences measured for the BRIRs covered the naturally occurring range of ITD typically encountered by rabbits [+/-360 μs; (Bishop et al., 2009)]. BRIRs were calculated for azimuths spanning the frontal hemifield (-90° to 90°) at a distance of 1 meter with respect to the midpoint of the receivers. Anechoic impulse responses were created by time-windowing the direct wavefront from the reverberant BRIRs. In one set of BRIRs (ITD-only), we did not include a model of the head in the simulations, so that the resulting BRIRs contained ITD but essentially no ILD cues. In the second set of BRIRs (ITD+ILD), we modeled the head as a rigid sphere with a radius of 6 cm, so that the BRIRs contained both ITD and ILD cues. Figures 5.1-5.2 shows 3-D surface plots of ITD and ILD as a function of frequency and stimulus azimuth for anechoic and reverberant BRIR in both ITD-only and ITD+ILD conditions. For the anechoic ITD-only

stimuli (Fig. 5.1, *upper left*), ITD is identical across frequency channels. An undesirable, albeit minor, consequence of introducing the spherical head is that ITDs become moderately larger in the ITD+ILD stimuli (Figure 5.1, *upper right*), particularly in the lower frequency channels. In general, reverberation does not profoundly affect ITD (Fig. 5.1, *bottom row)*, although the magnitude of ITD is somewhat smaller in the lowest frequency channels. For ITD+ILD stimuli, the magnitude of ILD increases both with increasing CF and lateral position of the sound source (Fig. 5.2, *upper right*). In general, reverberation reduces the overall magnitude of ILD (Fig. 5.3 *lower right*), although the overall pattern of ILD across frequency and azimuths is similar the anechoic condition.

An additional consequence of introducing the spherical head to the simulations was that there were intensity differences between ITD-only and ITD+ILD. We wanted to preserve the intensity differences that resulted from ILD, but remove the mean level difference, so that the two sets of BRIR had equal intensity for a source at 0°. Separately for the left and right ears, we determined the scaling factor that resulted in equal-intensity anechoic ITD-only and ITD+ILD at 0°. We defined an overall scaling factor as the average across the two ears, although in practice the scaling factors for the two ears were essentially identical. Each left/right and anechoic/reverberant ITD+ILD BRIR was multiplied by this scaling factor, removing the mean level difference at 0° but preserving ILDs.

Additional sets of ITD-only BRIR were created at different distances (0.5 and 3 meters) between source and receiver. Altering the distance between source and receiver scales the intensity of the direct wavefront. We scaled each set of BRIRs so that they had the same direct-wavefront intensity (averaged across azimuths) as the 1m BRIRs. Each

ITD-only BRIR was characterized by the ratio of direct to reverberant energies (D/R) averaged across azimuths. Because ITD-only stimuli do not contain ILD, the D/R is similar across azimuths. Thus, we defined an overall D/R for each set of ITD-only BRIR by averaging across azimuths (average D/R = *0.5m*: +10 dB, *1m*: 0 dB, *3m*: -9 dB).

Virtual space stimuli were created by convolving the normalized BRIRs with reproducible 400-ms broadband noise bursts.

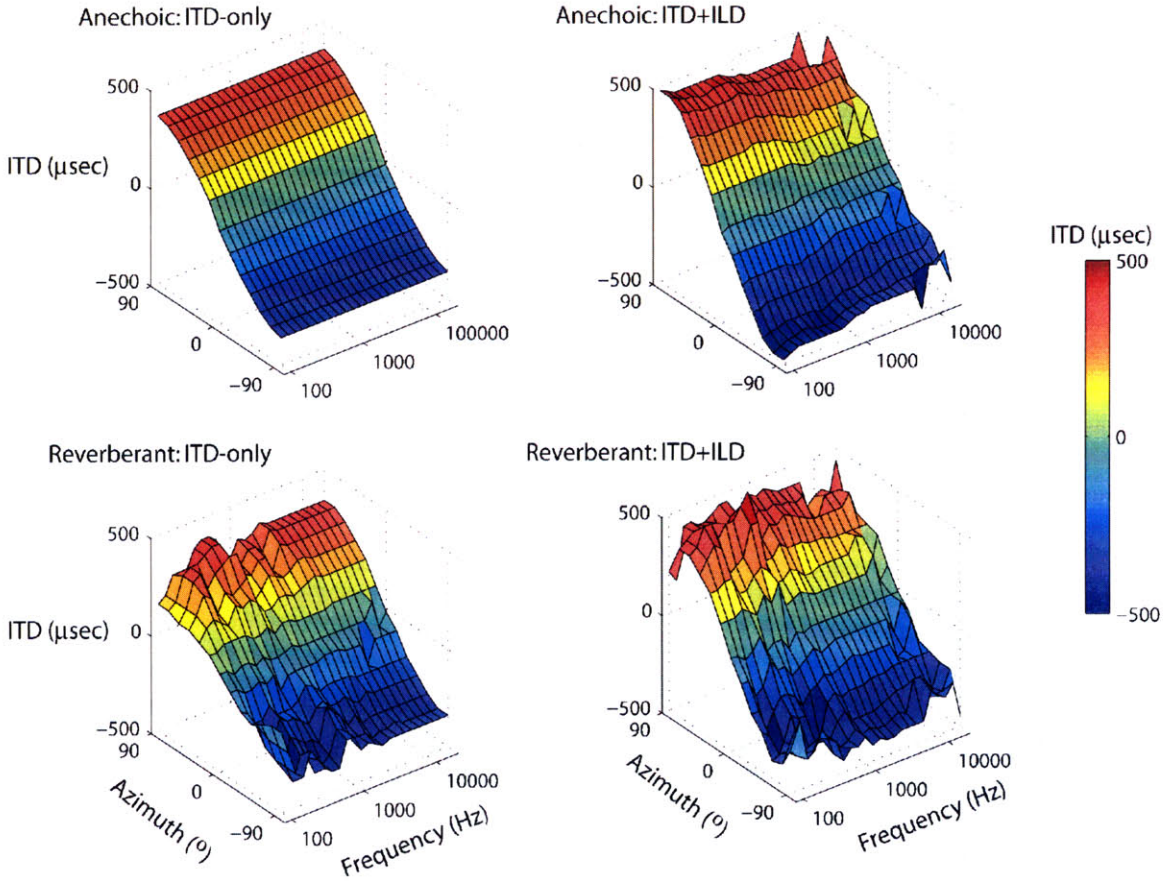

Figure 5.1 Analysis of binaural cues for virtual space stimuli: ITD
ITD as a function of frequency and virtual source azimuth for the four sets of virtual space stimuli used in the present experiments. ITD is estimated as the delay corresponding to the peak of narrowband (1/3-octave) interaural cross-correlation functions. Positive ITDs indicate that the signal at the contralateral ear is leading.

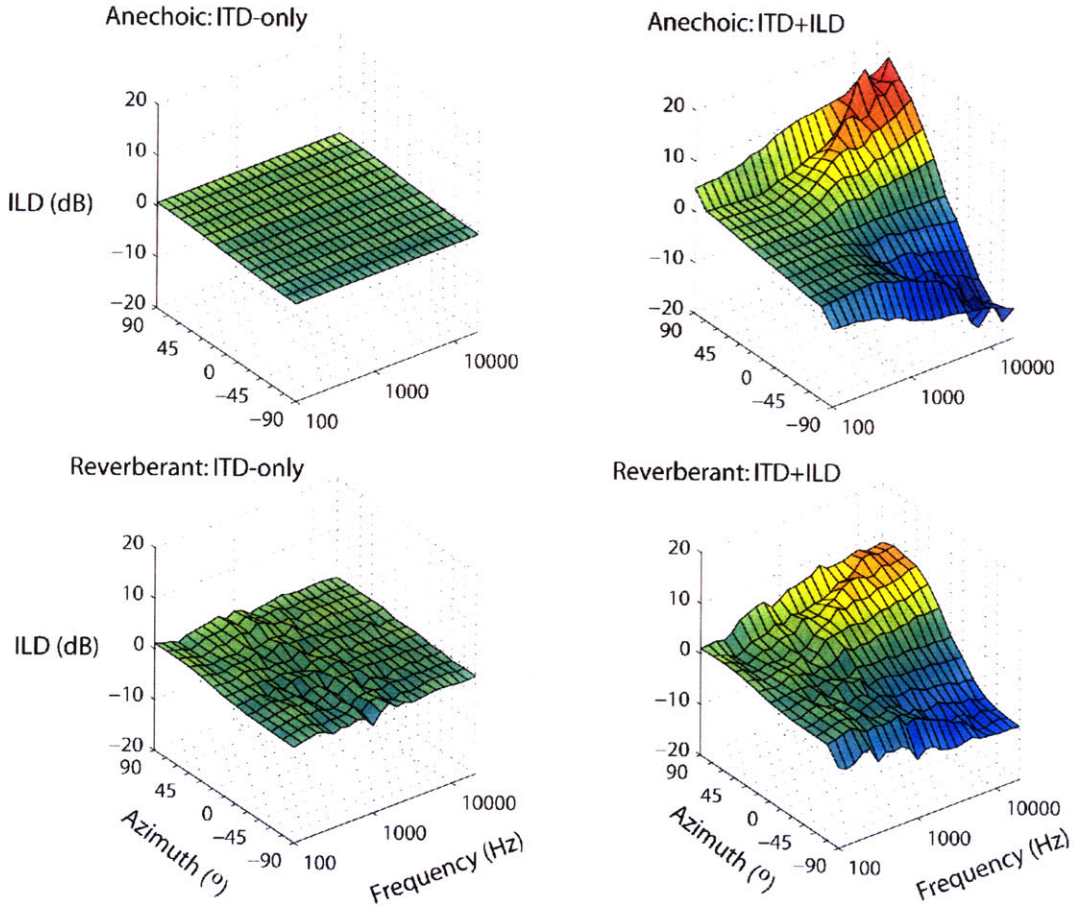

Figure 5.2 Analysis of binaural cues in virtual space stimuli: ILD
ILD computed in 1/3-octave bands as a function of filter center frequency and virtual source azimuth for the four sets of virtual space stimuli used in the present experiments. Positive ILDs indicate that the stimulus is more intense at the contralateral ear.

Experimental Procedures

Sound stimuli were generated by a 24-bit D/A converter (National Instruments NIDAC 4461) at a sampling rate of 50kHz and digitally filtered to compensate for the transfer function of the acoustic assemblies. The acoustic assemblies consisted of a pair of Beyer-Dynamic (DT-48) speakers attached to sound tubes running through the custom-fitted ear molds. A probe-tube microphone (Etymotic ER-7C), sealed inside the sound delivery tube, measured acoustic pressure at the end of the sound tube. At the start of

each recording session, we determined the system transfer functions using a chirp stimulus and generated digital compensation filters.

The search stimulus consisted of 40-Hz sinusoidally amplitude-modulated broadband noise bursts presented at a nominal level of 65 dB SPL. When a single unit was well isolated, its characteristic frequency (CF) was determined using an automatic tracking procedure (Kiang and Moxon, 1974). In earlier experiments, we determined CF by presenting a series of tone pips of different frequencies near threshold. Acoustic threshold was determined using diotic (and sometimes contralateral) broadband noise.

Characterization of ITD and ILD Sensitivity

Homophasic noise delay functions (NDFs) were measured using 200-ms broadband diotic noise bursts presented at delays of ±2000μs in 200μs steps. A unit was considered ITD-sensitive if an analysis of variance computed for the distribution of firing rates across ITD showed a significant effect of ITD (at the level α=0.05). In many neurons, we also obtained antiphasic NDFs using a similar procedure, but with the noise waveform inverted at one ear. Best ITD was defined as the ITD corresponding to the maximum response in the homophasic NDF. In a subset of neurons, we determined rate responses at best ITD as a function of the interaural cross-correlation (IACC) coefficient. We used a Gramm-Schmidt orthogonalization procedure (Culling et al., 2001) to create a pairs of 400-ms noise bursts with prescribed IACC coefficients between ±1. In all measurements, the independent variable (ITD, IACC coefficient) was randomly varied from trial to trial and we obtained at least 5 (but typically 8) repeats for each value of ITD/IACC coefficient.

ILD sensitivity was assessed using 200-ms broadband noise bursts with the same waveform at the two ears by simultaneously increasing the intensity at the contralateral ear by +ILD/2 and decreasing the intensity at the ipsilateral ear by –ILD/2, keeping the average binaural level constant. In a subset of neurons, we also characterized ILD sensitivity using 200-ms statistically uncorrelated (dichotic) noise bursts.

Characterization of Directional Sensitivity

In general, only ITD-sensitive units were studied using the virtual space stimuli, although we also characterized directional sensitivity in a small number of cells sensitive to ILD but not ITD (n=15).

Directional responses were obtained for each virtual room condition (anechoic, reverberant) and BRIR type (ITD-only, ITD+ILD) in pseudorandom order, although in earlier recording sessions we exclusively studied responses using BRIRitd. We typically used 13 azimuths (15° spacing) or, occasionally, 7 azimuths (30° spacing), randomized on a trial by trial basis. We obtained at least 8 presentations of the stimulus at each azimuth. Stimuli were presented at 15-20 dB above broadband noise threshold. Time permitting, we characterized directional sensitivity using BRIRitd with different D/Rs.

Data Analysis

Units were classified as peak, trough, or intermediate according to the shape of the homophasic NDF. To do so, we determined the three local extrema nearest 0 μs (Fig. 5.5, numbered labels). Units were first classified as either peak or trough depending on whether the middle critical point (Fig. 5.5, '2') was a local maxima (peak) or minima (trough). Next, we computed an asymmetry ratio, $\frac{abs(R_1 - R_3)}{abs(R_2 - R_1) + abs(R_2 - R_3)}$, where

R_1, R_2, and R_3 are the firing rates at the three critical points. If the asymmetry index exceeded 0.5, the unit was relabeled as intermediate, otherwise it remained in the peak or trough shape class. Example NDFs from each of the three ITD tuning shape classes can be seen in Figure 5.5.

A directional response function (DRF) for each room condition was computed by averaging the number of spikes that occurred in a 400-ms window after stimulus onset across all trials for each azimuth. DRFs were smoothed across azimuths using a three point triangular smoothing filter having weights [1/6,2/3,1/6]. The absolute range of a DRF was computed as max(r)-min(r), where r is the vector of firing rates across azimuths. We also computed the *relative range*, which is the range of firing rates for a DRF expressed as a fraction of the range of that unit's anechoic DRF. The relative range is one (by definition) for an anechoic DRF.

For conditions in which we obtained a large number of trials (>10), we quantified neural sensitivity to azimuth by estimating the mutual information (MI) between the stimulus azimuth s and neural response rate r (or, equivalently, spike count) as $MI = \sum_{s \in S} \sum_{r \in R} p(s,r) \log(\frac{p(s,r)}{p(s)p(r)})$, where $p(s)$ is the probability distribution of source azimuths (assumed to be uniform), $p(r)$ is the distribution of spike counts combined across azimuths, and $p(s,r)$ is the joint distribution of stimulus azimuth and spike count (Cover and Thomas, 1991). We used a bootstrap resampling method (Chase and Young, 2005) to correct for biases in our estimates of MI due to small sample sizes. Information transfer was defined as the debiased MI expressed as a percentage of the entropy of the stimulus distribution.

Results

We studied the effects of reverberation on the directional rate responses of single units in the IC of awake rabbits, focusing on neurons sensitive to ITD in broadband noise. Our aim was two-fold: first, to characterize the effects of reverberation on neural sensitivity to ITD across the tonotopic axis and second, to elucidate the influence of ILD on reverberant directional sensitivity. The results are presented in three sections: (1) characterization of basic ITD-sensitivity, (2) effects of reverberation on ITD sensitivity, and (3) effects of reverberation on directional sensitivity.

Basic ITD Sensitivity

We measured broadband noise-delay curves in 791 neurons in the inferior colliculi (n=6) of awake rabbits (n=4). A large fraction (60%) of the neurons we encountered were sensitive to ITD (475/791 neurons). However, this number may not be representative of the entire nucleus, as we approached the IC dorsally, resulting in a bias towards units with lower CFs. We obtained sufficient data to quantify directional sensitivity in 222 of the 475 ITD-sensitive IC neurons. The characteristic frequencies (CF) for this sample of ITD-sensitive neurons spanned 255-9600 Hz, with 52% (115/222) having CFs below 2 kHz.

Sensitivity to ITD in fine time structure versus envelope

Similar to results from anesthetized cat (Joris, 2003), we find that low-CF neurons are primarily sensitive to ITD in the fine time structure of the noise (ITD_{fs}), while high-CF neurons are sensitive to ITD in the envelope induced by cochlear filtering (ITD_{env}). ITD_{fs}- and ITD_{env}-sensitivity were distinguished by comparing noise delay functions

obtained with homophasic and antiphasic noise (Fig. 5.3A-C). Inverting the stimulus at one ear causes a 180° phase shift in fine time structure but does not alter the envelope. Thus in ITD_{fs}-sensitive cells (Fig. 5.3A), noise delay functions for A/A- stimuli show peaks and valleys that interleave with those of noise delay functions obtained with A/A stimuli, while the two noise delay functions are similar in ITD_{env}-sensitive cells (Fig. 5.3C). Both noise polarity-inverting and polarity-tolerant components can be seen in the noise delay functions of neurons with intermediate CFs, which are sensitive to a mixture of ITD_{fs} and ITD_{env} (Fig. 5.3B). Figure 4A shows the correlation coefficient between noise delay functions obtained with homophasic and antiphasic noise as a function of CF, demonstrating the transition from ITD_{fs} to ITD_{env} over a range of CFs ~0.8-2 kHz, consistent with Joris' (2003) results in anesthetized cat.

ITD_{fs}- and ITD_{env}-sensitivity can alternatively be distinguished by examining the asymmetry in rate response as a function of interaural correlation (IACC) for interaurally decorrelated noise pairs at the best delay (ITD corresponding to maximum firing rate in homophasic noise delay function). ITD_{fs}-sensitive cells (Fig. 5.3D) generally have asymmetric, monotonic rate-IACC curves that decrease as the interaural correlation coefficient is lowered from +1 (perfectly correlated) to -1 (anticorrelated), while in ITD_{env}-sensitive cells (Fig. 5.3F) the rate-IACC curve is non-monotonic and symmetric about an IACC of 0 (uncorrelated). Neurons with intermediate CFs that show a mixture of ITD_{fs}- and ITD_{env} have nonmonotonic but asymmetric rate-IACC curves (Fig. 5.3E).

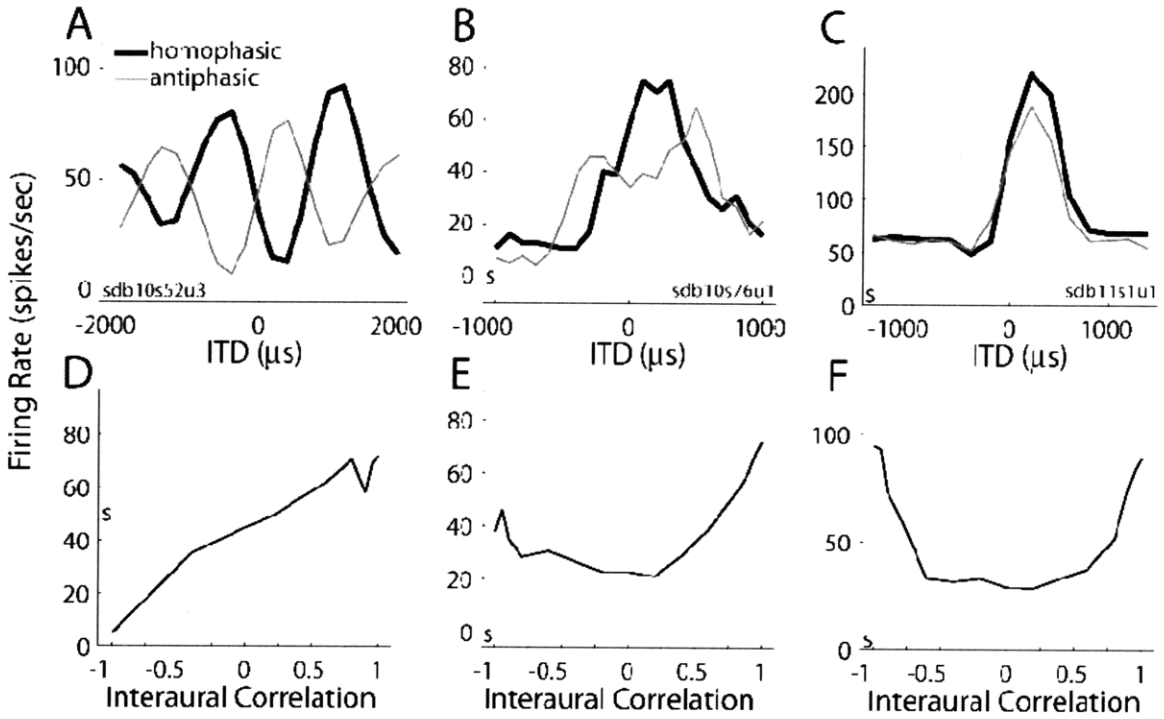

Figure 5.3 Noise delay functions across the tonotopic axis

A-C, Homophasic (black line) and antiphasic (gray line) noise delay functions for three IC neurons with CFs of *A,* 642 Hz, *B,* 1250 Hz , and *C,* 3427 Hz. *D-F,* Firing rate as a function of stimulus interaural correlation for the same three neurons in panels A-C. In all panels, spontaneous rate is indicated by the symbol at the left of each panel.

We quantified the shape of the rate-interaural correlation curves by computing a symmetry index, $\frac{abs[r(-1)-r(1)]}{\max(r)-\min(r)}$, where r is the vector of firing rates across interaural correlation coefficients. The symmetry index is 0 for asymmetric, monotonic curves (Fig. 5.3D) and reaches a maximum of 1 for symmetric, nonmonotonic curves (Fig. 5.3F). Figure 5.4B shows the symmetry index versus CF, demonstrating the transition from ITD_{fs}- to ITD_{env}-sensitivity over a range of 0.8-2.0 kHz, in corroboration with our other measurement (Fig. 5.4A).

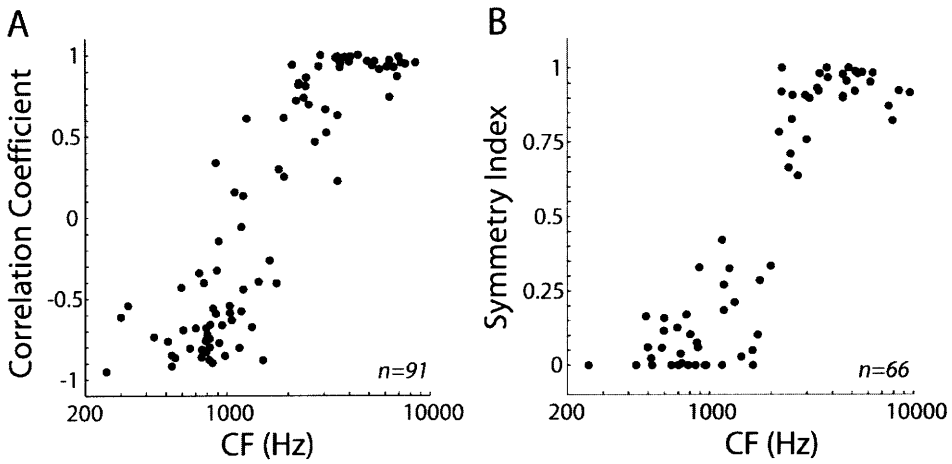

Figure 5.4 Quantifying fine-structure versus envelope ITD sensitivity
A, Correlation coefficient for homophasic and antiphasic noise delay functions versus CF for the IC neuron population. *B,* Symmetry index of rate-interaural correlation functions for IC neuron population.

We could not obtain all the necessary data to quantitatively distinguish ITD_{fs}- from ITD_{env}-sensitivity in every neuron in our population. Therefore, subsequent analyses are made on the basis of CF. We optimized the CF boundary using the data in Figure 5.4 by assuming that correlation coefficients <=0 or symmetry indices <=0.5 indicate ITD_{fs} and correlation coefficients >0 or symmetry indices>0.5 indicate ITD_{env}. A CF boundary of 2000 Hz minimized the number of classification errors; thus, we assume that neurons with CFs < 2000 Hz are primarily sensitive to ITD_{fs} and neurons with CFs > 2000 Hz primarily sensitive to ITD_{env}.

Classification based on the shape of the noise-delay function

Traditionally, ITD-sensitive neurons are classified into *peak*, *intermediate*, and *trough* phase groups by assessing the interaural phase of tonal interaural delay curves across a wide range of frequencies (Yin and Kuwada, 1983). The average of the tonal delays curves (called the composite delay curve) is similar in shape to the noise-delay function (Yin et al., 1986) and generally exhibits a prominent, symmetric peak in "peak-type" neurons, a prominent symmetric trough in "trough-type" neurons, and an asymmetric,

biphasic shape in "intermediate-type" neurons (Fitzpatrick et al., 2002). Using this feature, we developed a technique for classifying neurons into *peak*, *intermediate*, and *trough* ITD tuning shape groups based on the shape of the noise delay function (see Methods). Figure 5.5 shows noise delay functions from each tuning shape group across a wide range of CFs (top row: *peak*, middle row: *intermediate*, bottom row: *trough*). A breakdown of the units by tuning shape group is listed in Table T1, with units further separated on the basis of CF into low (< 2000 Hz) and high (> 2000 Hz) CF groups. The distribution of tuning shape class depends on CF group (X^2 test of independence, $X^2=26.31$, $p<0.001$). Namely, trough-type tuning is more common in high-CF, ITD_{env}-sensitive neurons whereas the majority of low-CF, ITD_{fs}-sensitive neurons belong to the peak-type tuning shape group. This asymmetry likely stems from the biases in CF distributions at the primary sites of binaural interaction in the MSO and LSO (Guinan et al., 1972) and is consistent with previous findings in awake rabbit obtained using interaurally delayed tones (Fitzpatrick et al., 2002).

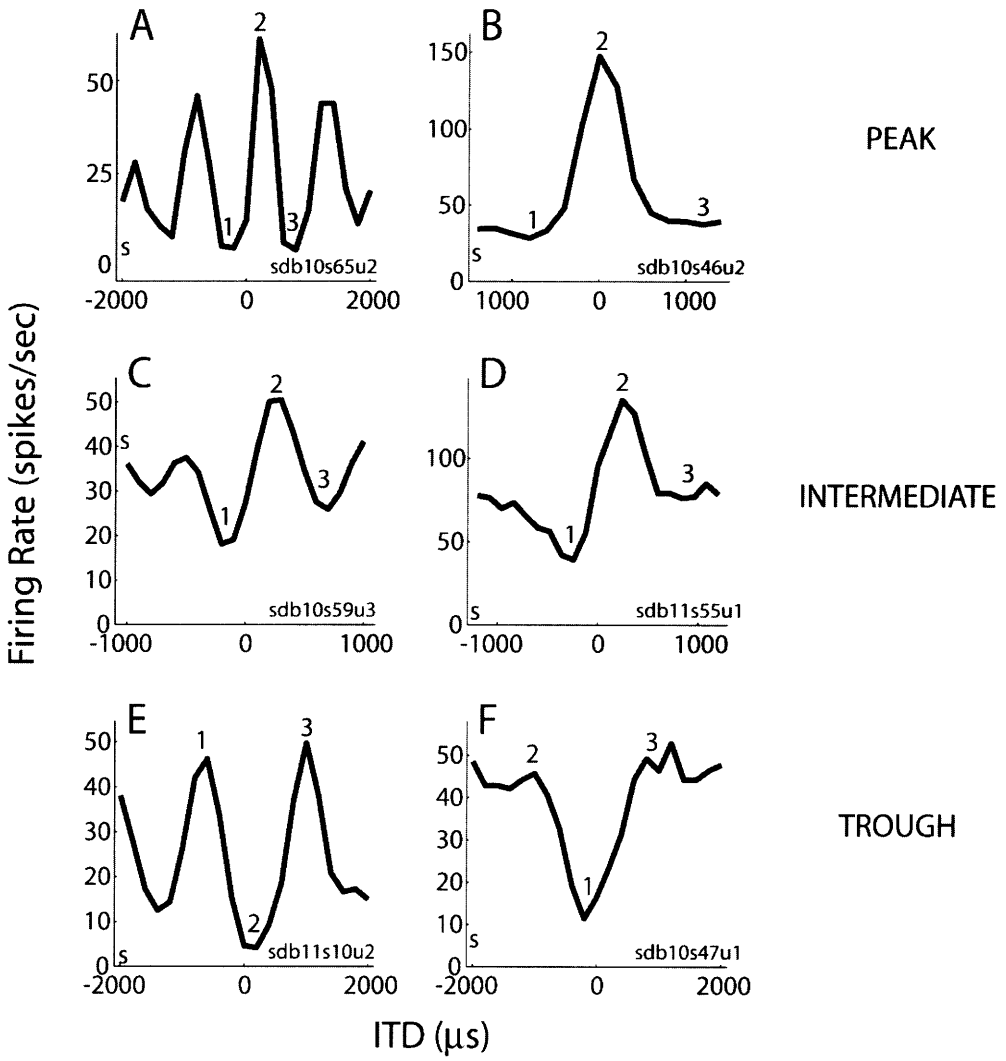

Figure 5.5 ITD tuning shape groups
Noise delay functions for low-CF (left column) and high-CF IC neurons in each of the three ITD tuning shape groups (*peak*: top row, *intermediate*: middle row, *trough*: bottom row). The numbered symbols correspond to the three local extrema used to used to determine the tuning type (see Methods). Unit CFs are *A*, 944; *B*, 6621; *C*, 1174; *D*, 6875; *E*, 564; and *F*, 3366 Hz.

Table I. ITD-sensitive neurons broken down by CF and unit type

	Peak	**Intermediate**	**Trough**	***Total***
CF < 2000 Hz	75 (69%)	18 (17%)	15 (14%)	*108*
CF > 2000 Hz	56 (49%)	20 (18%)	38 (33%)	*114*
Total	*131* (59%)	*38* (17%)	*53* (24%)	*222*

Characterization of Directional Sensitivity using ITD-only Virtual Space Stimuli

We measured rate responses as a function of virtual azimuth using ITD-only stimuli in 178 ITD-sensitive neurons. Although we use the term 'directional' to describe the responses as a function of stimulus azimuth, we are essentially characterizing ITD-sensitivity within the naturally occurring range of ITD.

Basic Properties of Anechoic Directional Response Functions

Because our ITD-only stimuli contain no ILD cues, anechoic directional response functions (DRF) are essentially equivalent to noise delay functions sampled with high resolution within the naturally occurring range of ITD (Fig. 5.6, solid lines), DRF are generally strongly modulated as a function of stimulus azimuth [mean modulation depth (± 1 std) = 0.683 ± 0.196]. In general, neurons tended to respond more vigorously to sources in the hemifield contralateral to the recording site (positive azimuths), although some neurons had nonmonotonic DRF (Fig. 5.6D,E). We quantified the shape of DRF by computing a non-monotonicity index (NMI, see Methods). Figure 5.7 shows the NMI versus CF across the IC neuron population. Aside from the tendency for units with very low CFs (< 350 Hz) to have monotonic DRF, NMI does not show a systematic dependence on CF.

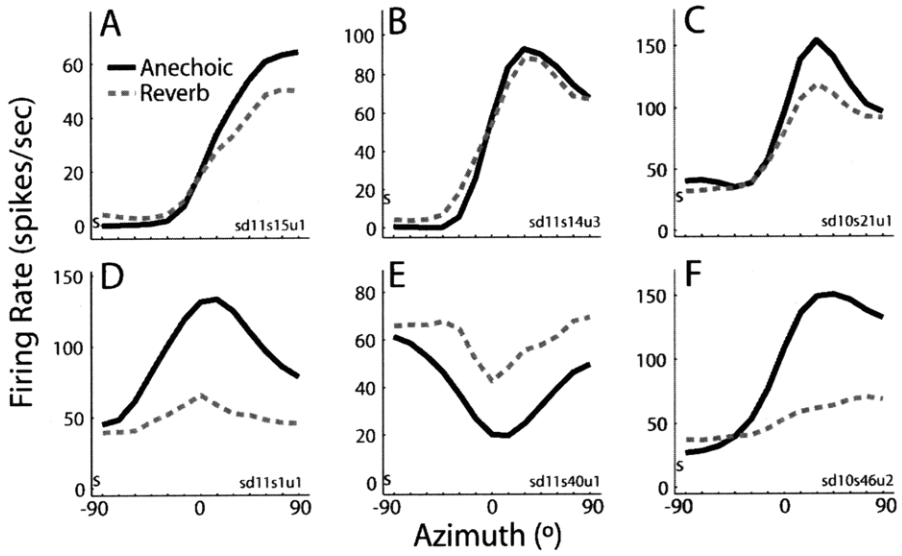

Figure 5.6 Effect of reverberation on directional rate responses
Anechoic (solid lines) and reverberant (dashed lines) directional response functions (DRFs) obtained using ITD-only virtual space simulations for six IC neurons with CFs of *A,* 606; *B,* 1154; *C,* 3427; *D,* 3660; *E,* 6621; and *F,* Hz. Spontaneous rate indicated by 's' at the left of each panel.

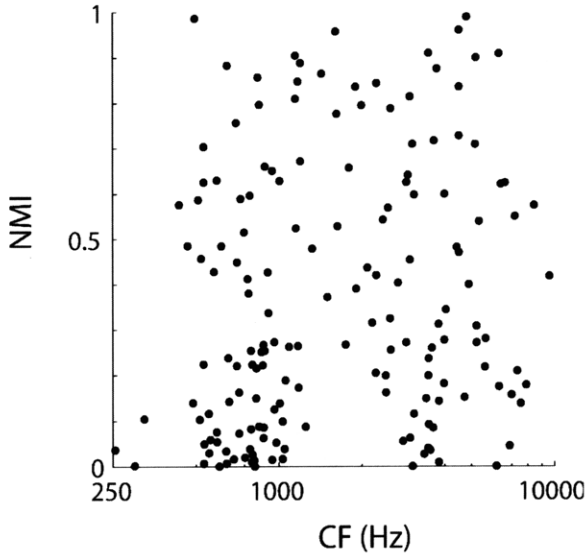

Figure 5.7 Shape of directional response functions similar at low and high CFs
Non-monotonicity index (NMI) versus CF across IC neuron population.

In those units where we obtained a sufficient number of trials (>10) at each azimuth, we quantified directional sensitivity by computing the information transfer between stimulus azimuth and spike count (see Methods). Information transfer measures the extent to which stimulus azimuth is unambiguously encoded by spike count and is

sensitive to both mean rate as well as trial-to-trial variability. Information transfer reaches a maximum of 100% when the distributions of spike counts at each azimuth are completely non-overlapping. Figure 5.8A shows information transfer as a function of CF for the sample of neurons in which we obtained an estimate of information transfer (46 out of 178 units). Information transfer does not depend systematically on CF, suggesting that neurons across a wide range of the tonotopic axis exhibit comparable sensitivity to virtual source azimuth. Consistent with results obtained in the IC of anesthetized cat (Chapter 2), we find that information transfer is highly correlated with the absolute range of firing rates across azimuths (Fig. 5.8B, r^2=0.83, n=46, p<0.001). Because we did not obtain enough trials to reliably estimate information transfer in all of the units in our sample, we quantify directional sensitivity across the entire population using the absolute range.

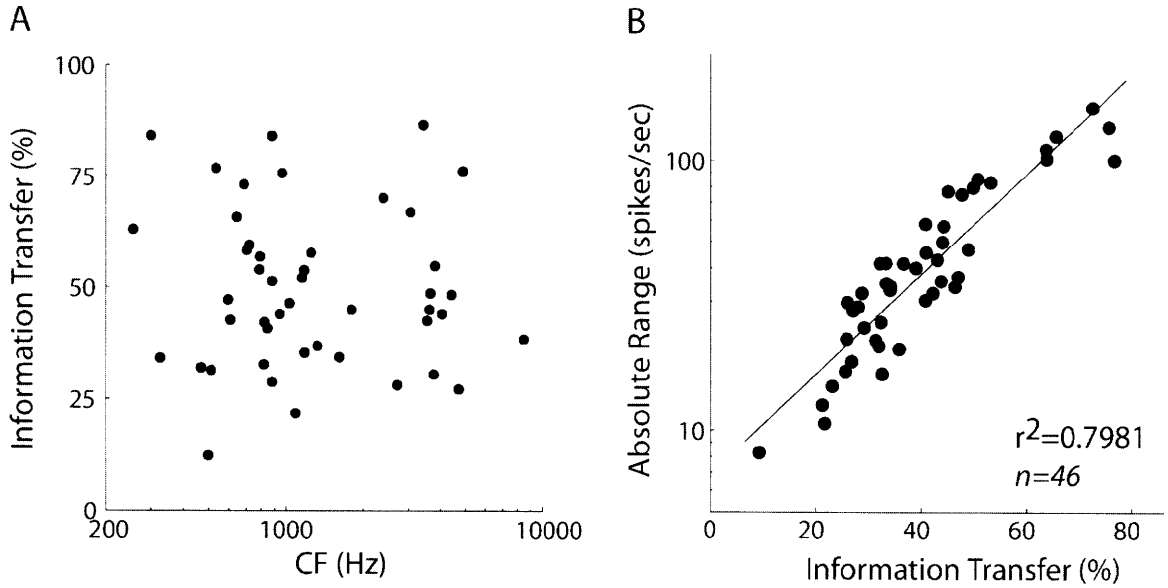

Figure 5.8 Information transfer related to absolute range of firing rates
A, Information transfer versus CF across the subset of neurons in which we obtained enough trials to reliably estimate information transfer (n=46). *B,* Driven range versus information transfer for the same population of neurons.

Figure 5.9A shows a scatter plot of absolute range versus CF for our sample of ITD-sensitive IC neurons. The solid line represents the mean absolute range within each of 6 frequency bins containing approximately equal numbers of data points. Units in the lower three CF bins are primarily sensitive to ITD_{fs} while units in the upper three bins are primarily sensitive to ITD_{env} (see Fig. 5.4). Absolute range is highly variable within each bin and there is no significant dependence of the mean absolute range on CF (ANOVA, $F(5,186)=0.36$, $p=0.875$). This finding corroborates the result obtained using information transfer and suggests that, for anechoic stimuli, comparable directional information is available in the rate responses of ITD_{fs}- and ITD_{env}-sensitive neurons.

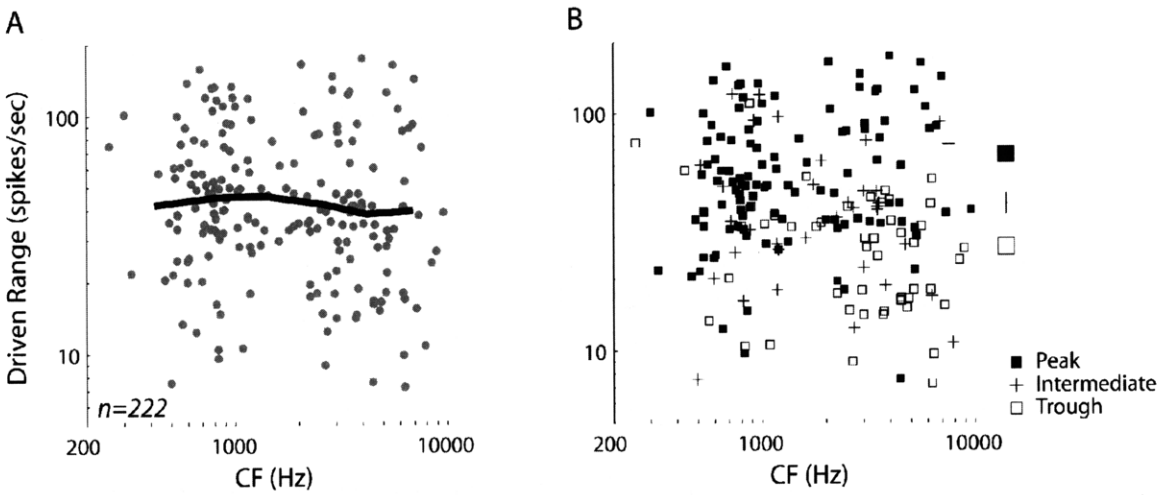

Figure 5.9 Comparable rate-based directional information across the tonotopic axis for anechoic inputs

A, Absolute range versus CF across the IC neuron population. Solid line shows mean absolute range in each of six frequency bins [edge frequencies=(250,700,950,2000,3500,5000,10000 Hz)] containing approximately equal numbers of data points. *B,* Same data as in *A* but with different symbols correspond to each ITD tuning shape class (*peak*, solid squares, n=131; *intermediate,* pluses, n=38, *trough*, open squares, n=53). The large symbols to the right of the panel illustrate the mean absolute range in each tuning shape class.

Figure 5.9B shows the same data as in Figure 5.9A, but with different symbols corresponding to each ITD tuning shape; the large symbols at the right edge of the panel represent the mean absolute range in each tuning shape group (across all CFs). Mean

absolute range depends significantly on tuning shape group (ANOVA, $F(2,219)=24.09$, $p<0.001$). Specifically, the absolute range is largest in peak-type neurons and smallest in trough-type neurons, with intermediate-type neurons falling in between (Fig. 5.9B, large symbols), although there is substantial overlap between the classes. All post hoc pairwise comparisons using Bonferroni comparisons were significant ($p<0.004$). The differences in absolute range across tuning shape groups probably results from the fact that trough-type neurons tend to be more broadly tuned to ITD than peak-type neurons (Batra et al., 1993), and supports the view that there may be fundamental differences in the mechanisms generating ITD-sensitivity in these types of units. Indeed, trough-type sensitivity is generally, although not exclusively, associated with excitatory-inhibitory coincidence detection in the LSO (Joris and Yin, 1995; Tollin and Yin, 2005), while peak-type sensitivity is associated with excitatory-excitatory coincidence detection in the MSO (Batra et al., 1997a; Yin and Chan, 1990).

Effect of Reverberation on Directional Sensitivity

Thus far, our results indicate that neurons across a wide range of the tonotopic axis are equally capable of encoding the naturally occurring range of ITD via their spike rates. However, differences between ITD_{fs}- and ITD_{env}-sensitive neurons emerge when we evaluate directional sensitivity in reverberation. We obtained DRF in 178 (out of 222) neurons using moderately reverberant ITD-only virtual space stimuli that had a direct-to-reverberant energy ratio (D/R) of 0 dB, typical of sources at a moderate distance from a listener in a classroom. In general, reverberation caused a compression of the range of firing rates (Fig. 5.6, dashed lines), such that peak firing rates were reduced and minimum firing rates increased. The compression was more pronounced in high-CF,

ITD_{env}-sensitive neurons (Fig. 5.6, bottom row), than in low-CF ITD_{fs}-sensitive neurons (Fig. 5.6, top row).

To quantify the effects of reverberation on directional sensitivity in individual neurons, we computed the *relative range*, the ratio of the range of firing rates across azimuths in reverberation to the range of firing rates in the anechoic condition. Figure 5.10A shows relative range versus CF for our neuron population; the solid line depicts the mean relative range in each of the 6 frequency bins, defined above. Although relative range is somewhat variable within each frequency bin, there is significant dependence of relative range on CF (ANOVA: $F(6,145)=14.54$, $p<0.001$). Post hoc multiple comparisons with Bonferroni corrections reveals that the relative range is significantly smaller in each of the three higher CF bins than in each of the three lower bins ($p<0.002$, all pairwise comparisons). However, the differences between bins *within* the lower three and upper three CF bins are not significant, suggesting that the decrease in relative range with increasing CF may reflect the transition from ITD_{fs}- to ITD_{env}-sensitivity.

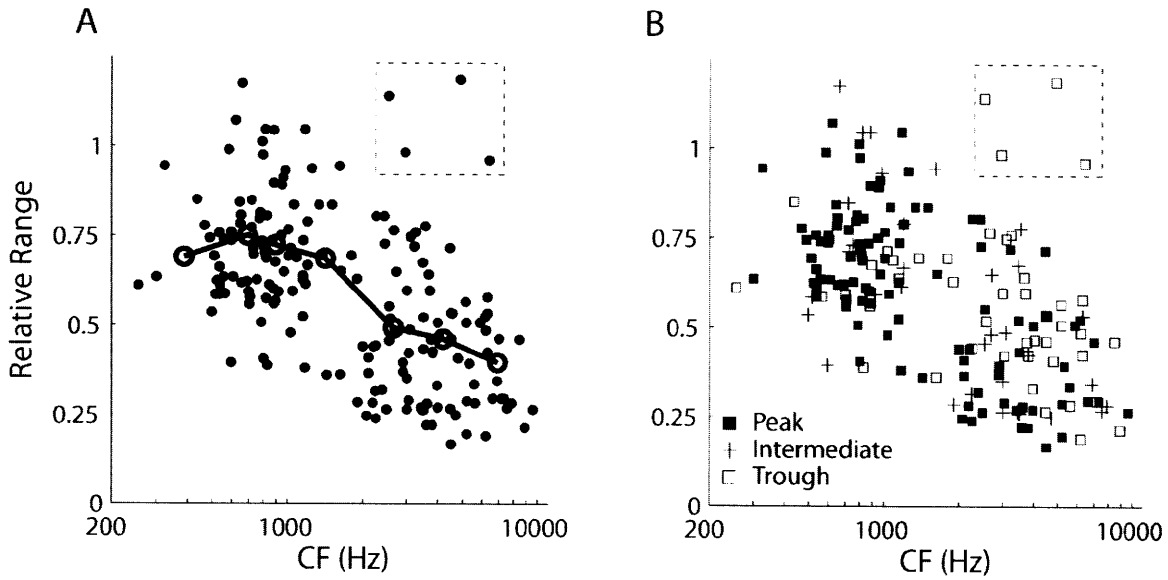

Figure 5.10 Reverberation degrades directional sensitivity more at high CFs than low CFs
A, Relative range versus CF across the IC neuron population. Solid line shows mean relative range in each of 6 frequency bins, as defined in Fig. 5. *B,* Same data as in *A* with different symbols corresponding to each ITD tuning shape class (*peak:* n=118, *intermediate:* n=37, *trough:* n=50). Dashed box encloses four outliers, discussed in text.

At both low and high CFs, there are units with relative ranges close to one, indicating that these units are robust to reverberation. At low frequencies, a relative range close to one faithfully reflects robust directional sensitivity in reverberation, that is, the anechoic and reverberant DRF are nearly identical (e.g., Fig. 5.6B). In contrast, at high CFs, reverberation can sometimes cause unexpected changes in the firing rate, resulting in a large relative range that erroneously implies robust directional sensitivity in reverberation. Figure 11 shows an example of a high-CF neuron that is unmistakably *not* robust to reverberation, but nevertheless has a relative range close to one. For anechoic inputs, this unit, which belongs to the trough-type tuning shape group, is broadly tuned to virtual azimuth (i.e., ITD) and has a small absolute range. In reverberation the response increases across all azimuths, maintaining the same absolute range so that the relative range is large. This unit is typical of the four high-CF neurons having anomalously large relative ranges (indicated by the dashed box in Figure 5.10A).

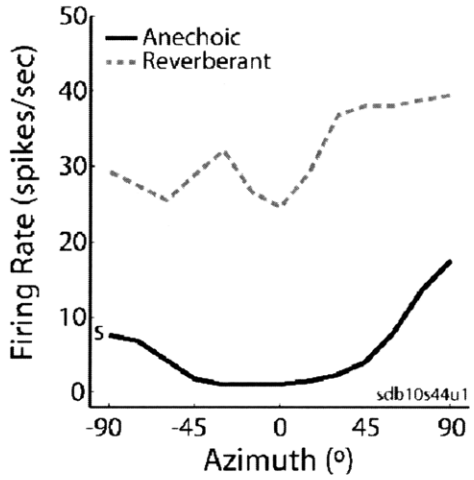

Figure 5.11 Relative range can be misleading Example of a high-CF (4900 Hz) ITD_{env}-sensitive IC neuron with an anomalously high relative range.

To explicitly examine how directional sensitivity in reverberation depends on ITD tuning shape class, Figure 5.10B shows the relative range versus CF, with different symbols representing each ITD tuning shape class. Both peak- (solid squares) and intermediate-type (pluses) units conform to the population trend in that the effect of reverberation is significantly higher at high CFs (> 2000 Hz) than at low CFs (< 2000 Hz) [*peak,* t-test, n=111, p<0.001; *intermediate*, n=35, p<0.001)]. On the other hand, the effect of reverberation is more variable in high-CF trough-type units (open squares). The fact that the absolute ranges of anechoic DRF are typically small in trough-type units renders them more susceptible to the spurious modulations in firing rate that sometimes occur in reverberation (see Fig. 5.11). Nevertheless, excluding the four outliers (indicated by the dashed box in Figure 5.10B), the relative range at higher CFs (> 2000 Hz) is significantly smaller than at lower CFs (< 2000 Hz) for trough-type units (t-test, n=42, p=0.002) as it is for the other two ITD tuning shape groups.

Effect of Lowering D/R

In some units, we measured DRF using ITD-only virtual space stimuli with different amounts of reverberation, quantified by the D/R (see Methods). Lowering D/R (i.e., increasing reverberation) typically compressed the DRF, as illustrated for the two units in Figure 5.12. Averaged across CFs, the decrease in relative range at successive D/Rs was significant (paired t-test, *10 dB/0 dB*: n=48, p=0.0128; *0 dB/-10 dB*: n=24, p<0.001), although the exact dependence of relative range on D/R varies across units. In some units, mild reverberation had essentially no effect on the rate response (e.g., Fig. 5.6B, Fig. 5.12A); in other units (Fig. 5.6D-F, Fig. 12B), directional sensitivity was degraded by even the mildest reverberation condition tested. In particular, for a given D/R, directional sensitivity is significantly worse in high CF (> 2000 Hz) ITD_{env}-sensitive neurons than in low CF (< 2000 Hz) ITD_{fs}-sensitive neurons (t-test, *+10 dB*: n=48, p=0.013; *0 dB*: n=157, p<0.001; *-10 dB*: n=24, p<0.001).

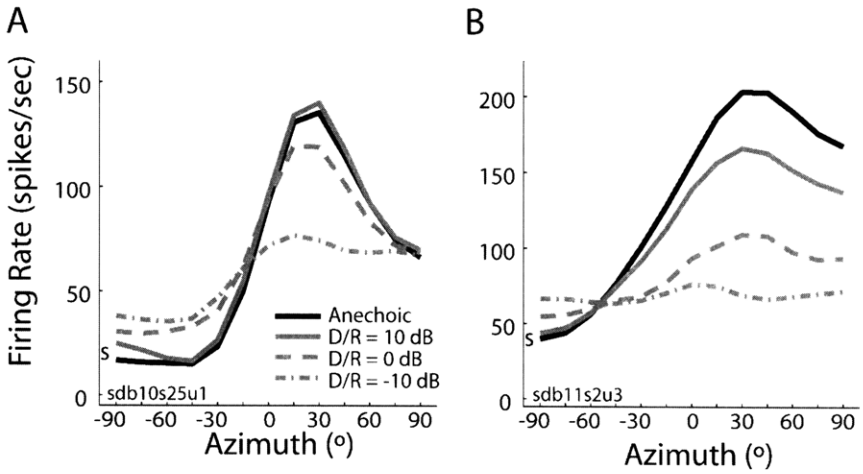

Figure 5.12 Directional sensitivity degrades with increasing reverberation
DRF obtained from *A*, low CF (707 Hz) and *B*, high CF (5593 Hz) IC neurons using virtual space stimuli with different amounts of reverberation, quantified by the direct-to-reverberant energy ratio (D/R). Spontaneous rate indicate by 's' symbol at the left of each panel.

Peripheral Factors determining ITD sensitivity in reverberation[7]

In Chapter 2, we showed that, at low CFs, compression of DRF in reverberation can be qualitatively attributed to decorrelation of the ear input signals after taking into account peripheral filtering. Here we use recordings from the AN to examine whether the disparity in the effect of reverberation for low-CF (ITD_{fs}-sensitive) and high-CF (ITD_{env}-sensitive) neurons can be explained by a similar, common type of binaural processing across all frequencies.

We recorded spike trains from auditory nerve fibers in response to both the left- and right-ear ITD-only virtual space stimuli (see Methods). Using the shuffled correlation technique (Louage et al., 2004), we implemented processing by a bank of ideal coincidence detectors receiving delayed inputs consisting of an AN fiber's responses to the left- and right-eared virtual space stimuli. Figure 5.13A,B shows shuffled cross-correlograms (SXC) for two AN fibers computed from responses to anechoic (black lines) and the 0 dB D/R (gray lines) ITD-only stimuli at 0° azimuth. The shaded region represents the range of the ITD corresponding to ±90° in the ITD-only stimuli. The SXC are normalized so that 1 corresponds to the expected normalized coincidence count for uncorrelated random spike trains. As shown by Joris (2003), SXC resemble noise delay functions from IC neurons, and reflect the phase locking of AN spikes to the quasi-periodic fine-time structure at low CFs (Fig. 5.13A) and phase locking to the aperiodic cochlear-induced envelope at high CFs (Fig. 5.13B). We quantified anechoic "directional sensitivity" by the peak height of the normalized SXC. Figure 5.9C shows anechoic SXC peak height versus CF for the AN population. The dashed line

[7] The auditory nerve data presented in this section was collected by Andrew Schwartz.

represents the least-squares regression line; the solid line from Figure 5.9A is superimposed to facilitate comparison with the IC (axis labels at right edge). In contrast to absolute range in the IC, the peak height of AN SXC *decreases* with increasing CF (Fig. 5.13C), indicating that there is additional envelope processing between the AN and IC [as suggested by Joris (2003)].

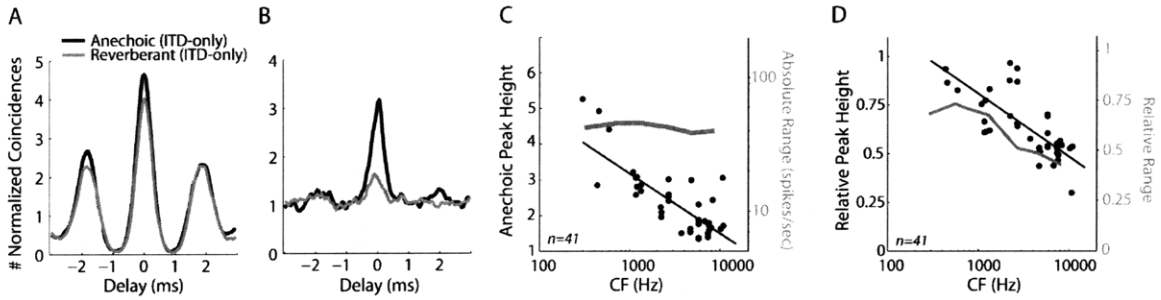

Figure 5.13 Peripheral factors determining directional sensitivity in reverberation
A, Anechoic (black line) and reverberant (gray line) shuffled cross-correlograms (SXC) computed from spike trains obtained from *A,* low CF (588 Hz) and *B,* high CF (10.7 kHz) AN fibers in anesthetized cat. Gray region represents range of ITD corresponding to ±90° in the anechoic ITD-only virtual space stimuli. *C,* Peak height of anechoic SXC versus CF across AN fiber population. Solid black line depicts best-fitting linear regression. Absolute range versus CF across IC population (gray line) reproduced from Figure 9A, for comparison (axis labeled at right). *D,* Relative peak height versus CF across AN fiber population. Solid black line depicts best-fitting linear regression. Relative range versus CF across IC neuron population (gray line) reproduced from Figure 10A, for comparison (axis labeled at right).

Similar to our observations in the IC, reverberation causes a compression of SXC that is more severe at high CFs (Fig. 5.13B) than at low CFs (Fig. 5.13A). To quantify the effects of reverberation on the SXC, we computed the relative peak height i.e., the ratio of the SXC peak height in the reverberant condition to that in the anechoic condition. We subtracted 1 from the peak height in each condition before computing the ratio, in order to remove the baseline coincidence count representing random firings. Figure 5.13D shows the relative peak height versus CF. The dashed line represents the least-squares regression line of the relative peak height versus CF data; the solid line from Figure 5.10A is superimposed to facilitate comparison (axis labeled at right edge of

panel). As with the relative range in IC neurons, the relative peak height decreases with increasing CF, although it appears that the main drop may occur at somewhat higher CFs in the AN than in the IC (Fig. 5.13D, compare solid and dashed lines). These results suggest a partial peripheral origin for the frequency-dependent effect of reverberation on ITD sensitivity in the IC.

Characterization of Directional Sensitivity using ITD+ILD

To examine the effects of reverberation in more realistic conditions, we characterized directional sensitivity in 44 ITD-sensitive IC neurons using the ITD+ILD virtual space stimuli that had an azimuth-dependent ILD in additional to ITD.

Influence of ILD on Anechoic Directional Response Functions

Figure 5.14 shows anechoic (black) and reverberant (gray) DRFs from 6 IC units obtained using ITD+ILD stimuli (dashed lines) along with responses to ITD-only stimuli (solid lines). For high-CF, ITD_{env}-sensitive neurons (Fig. 5.14, bottom row), there is a systematic, azimuth-dependent difference between anechoic DRF for ITD-only and ITD+ILD stimuli. Namely, firing rates for ITD+ILD stimuli tend to be lower than ITD-only firing rates at ipsilateral azimuths and higher at contralateral azimuths, often resulting in a larger absolute range. In other words, negative ILDs – which occur for ipsilateral sources – reduce the discharge rate, while positive ILDs – which occur for contralateral sources – enhance discharge rate over that observed in the ITD-only condition. The differences between directional responses to ITD-only and ITD+ILD stimuli were less systematic and less prominent in low-CF, ITD_{fs}-neurons (Fig. 5.14, top row).

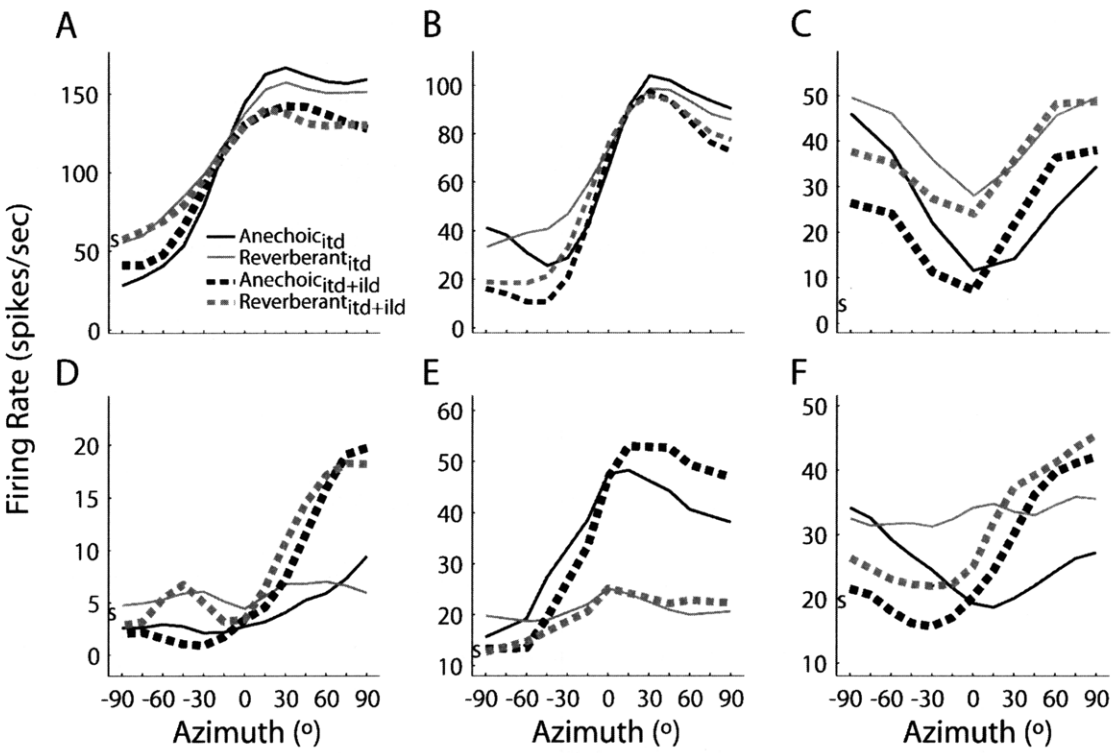

Figure 5.14 Directional response functions for ITD-only and ITD+ILD conditions
Anechoic (black lines) and reverberant (gray lines) DRF obtained from six ITD-sensitive IC neurons using ITD-only (solid lines) and ITD+ILD (dashed lines) virtual space stimuli. Unit CFs are *A,* 597; *B,* 1500; *C,* 1900; *D,* 3000; *E,* 5215; *F,* 7200 Hz. Spontaneous rate indicated by 's' symbol at the left of each panel.

To quantify the effects of ILD on the absolute range of the anechoic DRF, we defined an ILD influence index as,

$$\frac{AbsRange(DRF_{ITD+ILD}) - AbsRange(DRF_{ITD})}{AbsRange(DRF_{ITD+ILD}) + AbsRange(DRF_{ITD})}.$$

The ILD influence index takes on values between ±1 and is equal to 0 when the absolute ranges of firing rates are the same for both sets of virtual space stimuli. Figure 5.15A shows the ILD influence index versus CF, with different symbols corresponding to ITD tuning shape groups. We split the population into low (< 2000 Hz) and high (> 2000 Hz) CF groups, essentially dividing the population on the basis of ITD_{fs}- and ITD_{env}-sensitivity (see Fig. 5.4). The ILD influence index is generally positive and significantly larger in the high-CF group (one-sided t-test, n=44, $p<0.001$), indicating that ILDs that

are consistent with ITDs improve directional sensitivity at high CFs more so than at low CFs. The ILD influence index parallels the magnitude of ILD in the ITD+ILD virtual space stimuli (Fig. 5.15A, dashed line), suggesting at least a partial acoustic origin for the increasing influence of ILD with CF in the ITD+ILD condition.

The influence of ILD can also result in changes in the shape of DRF (e.g., Fig. 5.14F), in addition to changes in the absolute range of firing rates. We quantified the shape of DRF using the NMI. Figure 5.15B shows ΔNMI—the difference in NMI between ITD-only and ITD+ILD conditions—as a function of CF. Negative differences indicate that the DRF shape becomes *more monotonic* in the ITD+ILD condition. Consistent with the ILD influence index, we see the biggest effects of ILD on DRF shape at higher CFs (> 2000 Hz). In general, the NMI becomes smaller i.e., DRF become more monotonic in the ITD+ILD condition.

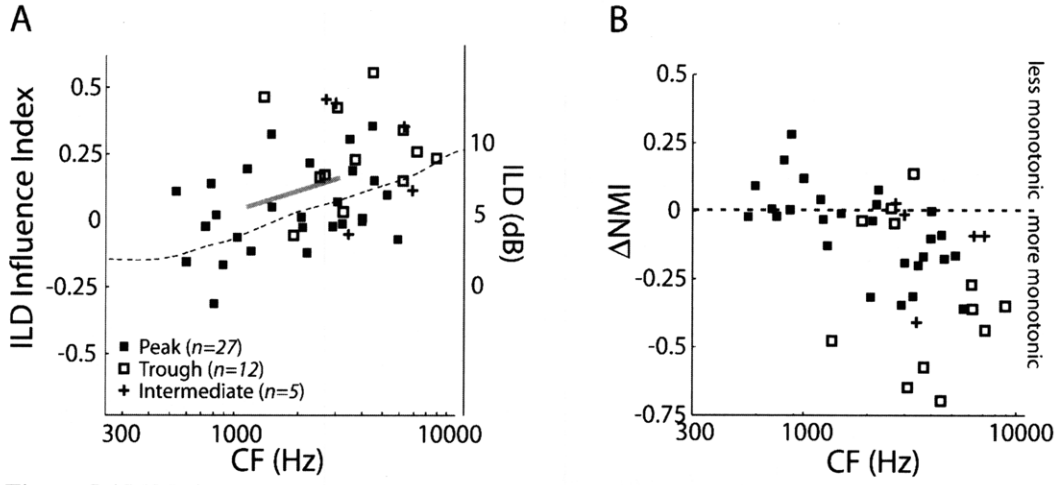

Figure 5.15 ILD increases with increasing CF

A, ILD influence index versus CF across the IC neuron population in which we obtained DRF using both ITD-only and ITD+ILD virtual space stimuli. Different symbols correspond to the ITD tuning shape classes. Thick gray line illustrates average ILD influence index in low (< 2000 Hz) and high CF (> 2000 Hz) groups. Dashed line illustrates ILD computed in 1/3-octave bands from the 90° ITD+ILD virtual space stimulus. *B,* ΔNMI, where negative differences indicate DRF becomes more monotonic in ITD+ILD condition, across IC neuron population.

Statistical analysis of ILD influence index by tuning shape class requires caution, because both the ILD influence index and the distribution of ITD tuning shape groups vary with CF. First, to avoid confounds between frequency and ITD tuning shape group, we only ran statistics on the high CF data. Moreover, we confirmed that there is no dependence of ITD-tuning shape on CF at high frequencies (Kruskal-Wallis test, X^2=2.11, p=0.348). At high CFs, the ILD influence index shows a main effect of ITD tuning shape class (Kruskal Wallis test, X^2=7.84, p=0.019). In particular, the ILD influence index is bigger in trough-type units than in peak-type units (Mann-Whitney U test: *peak/trough*, n=24, p=0.005), indicating that ILDs have a stronger influence on directional rate responses in units belong to the trough type shape groups. The difference between intermediate- and peak-type units just missed statistical significance (p=0.06), and the difference between intermediate- and trough-type units was not significant (p=0.86).

Consistent with the results obtained in the larger ITD-sensitive neuron population, we found that the absolute range of firing rates in the anechoic ITD-only DRFs depends significantly on ITD tuning shape group (Kruskal Wallis test, X^2=8.41, p=0.014). On the contrary, anechoic directional sensitivity in the ITD+ILD condition does *not* differ significantly across ITD tuning shape groups (Kruskal Wallis test, X^2=3.52, p=0.172), because the influence of ILD is strongest in trough-type units, which show the worst directional sensitivity in the ITD-only condition.

Effect of ILD on Directional Sensitivity in Reverberation

Reverberant DRFs are depicted as gray lines in Figure 5.14; solid lines represent DRF obtained using ITD-only stimuli and dashed lines represent DRF obtained using

ITD+ILD stimuli. Consistent with the results for ITD-only stimuli, reverberation generally causes a compression of DRF for ITD+ILD stimuli. In low-CF, ITD_{fs}-sensitive neurons, reverberation tends to similarly compress DRFs for both stimuli (Fig. 5.14, top row). In contrast, in high-CF neurons (Fig. 5.14, bottom row), DRF can show much less compression for ITD+ILD stimuli than for ITD-only stimuli (Fig. 5.14D,F), although in some units directional sensitivity is impoverished in both conditions (Fig. 5.14E).

Figure 5.16A,B shows the relative range plotted against CF for ITD-only and ITD+ILD stimuli, respectively, for the 44 neurons in which responses to both stimuli were measured. The gray line depicts the average relative range for CF bins above and below 2000 Hz. There is a significant interaction ($p=0.011$) between CF (low vs. high CF) and virtual space condition in a two-way ANOVA, resulting from the fact that there is a substantial improvement in directional sensitivity at high CFs, but not low CFs, when the virtual space stimuli contain both binaural cues. Consequently, directional sensitivity in reverberation is stable across the tonotopic axis for the more realistic ITD+ILD stimuli, whereas in the ITD-only condition there is significantly less information available from high-CF neurons. These results suggest that ILDs may provide more reliable directional information than ITD_{env} in reverberation.

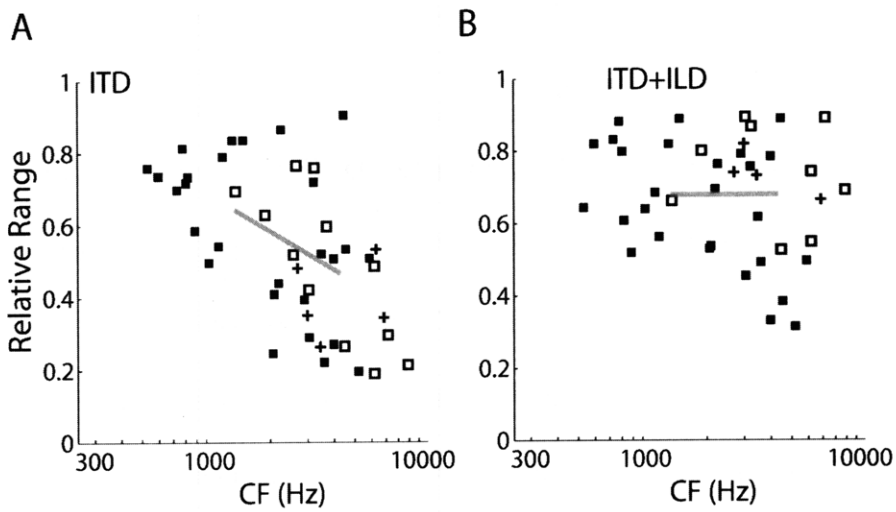

Figure 5.16 Reverberation improves directional sensitivity at high CFs in ITD+ILD condition
A, Relative range of DRF obtained using ITD-only stimuli versus CF across IC neuron population. Gray line depicts mean relative range in low (< 2000 Hz) and high-CF (> 2000 Hz) frequency groups. *B,* Relative range of DRF obtained using ITD+ILD stimuli versus CF across IC neuron population. Gray line depicts mean relative range in low (< 2000 Hz) and high-CF (> 2000 Hz) frequency groups.

As with the ILD influence index, the improvement in directional sensitivity at high CFs (between ITD-only and ITD+ILD conditions) appears to be larger for units in the trough and intermediate-type tuning shape groups. To examine this trend more closely, Figure 5.17 shows a scatter plot of ΔRR—the difference in relative range between ITD+ILD and ITD-only conditions—for each ITD tuning shape class, with units further broken down on the basis of CF. Positive values on the ordinate indicate that directional sensitivity in reverberation improves in the ITD+ILD condition. Statistical analysis of the low-CF data (Figure 5.17, solid symbols) is not possible due to the small samples sizes in each tuning shape group. On the other hand, in high-CF neurons (Figure 5.17, open symbols), the most substantial improvements are observed in neurons belonging to the trough- and intermediate-type tuning shape groups. This trend is exemplified by the three neurons in the bottom row of Figure 5.14, which belong to the intermediate-, peak-, and trough-type shape classes, respectively. In all three units, reverberation severely compresses DRF in the ITD-only condition; however, in the

ITD+ILD condition, directional rate responses are relatively robust to reverberation in the intermediate- (Fig. 5.14D) and trough-type unit (Fig. 5.14F), whereas directional sensitivity remains impoverished in the peak-type unit (Fig. 5.14E). An analysis of variance on the high CF data in Figure 5.17 confirms a significant effect of tuning shape class (Kruskal Wallis test, X^2=13.78, p=0.001); post hoc multiple comparisons with Bonferroni corrections indicates significant differences between peak/trough (p=0.002) and peak/intermediate (p=0.005) tuning shape groups, but not trough/intermediate groups (p=0.859).

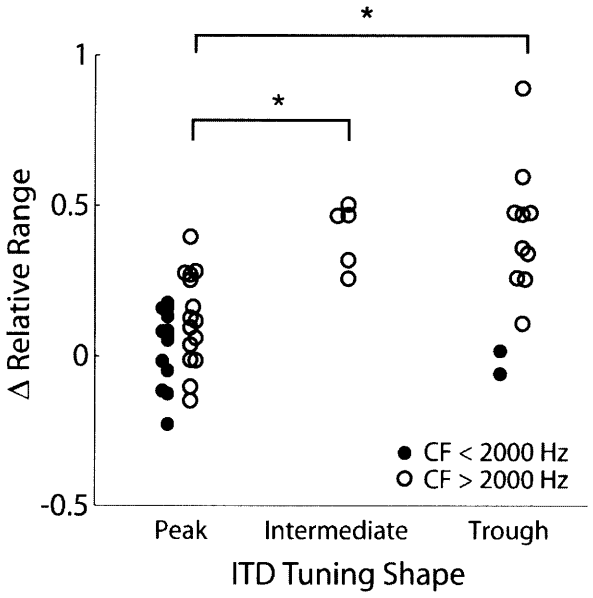

Figure 5.17 Influence of ILD in reverberation depends on ITD tuning shape group
Distribution of ΔRR in each ITD tuning shape group. Units are further divided on the basis of CF (low CF, filled symbols; high CF, open symbols). Positive differences indicate directional sensitivity improves in the ITD+ILD condition. A small horizontal scatter has been added to aid visualization. Asterisks indicate significant differences at the *p<0.005.

Directional Sensitivity in Reverberation for exclusively ILD-sensitive units

Our results suggest that ILDs may be more reliable than envelope ITDs in reverberation. As a control, we obtained DRFs using the ITD+ILD stimuli in a small population of high-CF (> 2000 Hz) cells (n=15) that were sensitive to ILD but not sensitive to ITD. Figure 5.18A-C shows DRFs obtained from three ILD-sensitive neurons, with CFs

increasing from left to right. Anechoic DRFs (black lines) typically increase monotonically with stimulus azimuth, with all 15 units preferentially responding to sources contralateral to the recording site. The panels below each set of DRFs (Fig. 5.18D-F) show noise ILD curves for each unit, obtained by adjusting the intensity in the ipsilateral ear by -ILD/2 and the contralateral ear by +ILD/2, roughly mimicking the changes that occur when a sound sources moves around the head. The vertical lines in Figure 5.18D-F delineate the range of ILD in ITD+ILD stimuli between ±90°, computed in a 1/3-octave band centered on the unit's CF. The shape of the DRF largely parallels the rate-ILD curve within this range; differences between the two curves may be caused by differences in the frequency-dependence of ILD between the virtual space stimuli and broadband noise.

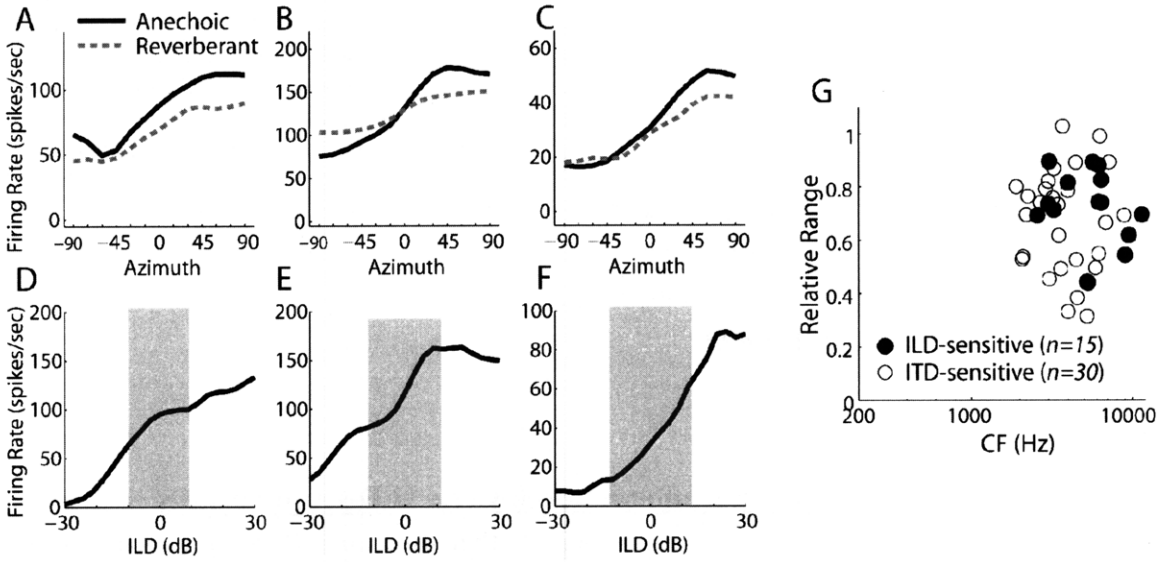

Figure 5.18 Directional response functions for neurons sensitive only to ILD
A-C, Anechoic (solid) and reverberant (dashed) DRF obtained using the ITD+ILD stimuli in three IC neurons that were sensitive to ILD but not ITD. Unit CFs are *A,* 3250; *B,* 5292; and *C,* 11500 Hz. *D-E,* Firing rate versus ILD obtained using broadband noise for the same three IC neurons in panels *A-C.* The gray shaded region indicates the naturally occurring range of ILD in the anechoic ITD+ILD VAS stimuli, computed in a 1/3-octave band centered at the unit's CF. *G,* Relative range versus CF for the exclusively ILD-sensitive neuron population (solid symbols) and high-CF ITD-sensitive neuron population (open symbols).

Similar to our observations for the ITD-sensitive neuron population, reverberation typically compresses the range of firing rates in ILD-sensitive neurons. The compression of firing rates in the reverberant DRF probably results from the reduced magnitude of ILD in reverberation (Fig. 5.2). Figure 5.18G shows the relative range versus CF across the ILD-sensitive neuron population (solid symbols), with the relative range data from the high-CF ITD-sensitive neuron population overlaid as small, open symbols. On the average, directional sensitivity in reverberation does not differ between the two populations of neurons (t-test, n=44, p=0.874), supporting the notion that, at high CFs, ILDs provide reliable directional information in reverberation.

Gradient of ILD Sensitivity Across Tuning Shape Groups

In general, our results suggest that neurons in the intermediate- and trough-type ITD tuning shape groups show a stronger influence of ILD than neurons in the peak-type tuning shape group. An alternative way to reveal the gradient of ILD-influence across tuning shape groups is illustrated in Figure 5.19, which shows anechoic DRFs from 4 high-CF IC neurons obtained using correlated (solid lines) and uncorrelated (dashed lines) noise stimuli. The first three panels in Figure 5.19 show DRFs for ITD-only (black) and ITD+ILD (gray) stimuli from ITD-sensitive neurons belonging to the peak, intermediate, and trough-type tuning shape groups, respectively. The rightmost panel shows DRFs obtained using ITD+ILD stimuli from a high-CF neuron that was sensitive to ILD but not sensitive to ITD. We did not obtain DRFs using ITD-only stimuli in this unit, as it was not sensitive to ITD. In each of the three ITD-sensitive neurons, uncorrelating the ITD-only input signals leads to a complete compression of the DRF, as expected (Fig. 5.19A-C, dashed black lines); that is, it abolishes directional sensitivity.

The same holds true for uncorrelated ITD+ILD stimuli in the peak-type neuron (Fig 5.19A), indicating that ITD is key determinant of directional sensitivity in this unit. On the other hand, uncorrelating the ITD+ILD input signals causes less compression of the DRF in the intermediate-type unit (Fig. 5.19B) and essentially no compression of the DRF in the trough-type unit (Fig. 5.19C). The effects (or lack thereof) of uncorrelating the ITD+ILD input signals are similar in the trough-type unit and exclusively ILD-sensitive unit (Fig. 5.19D), suggesting that intensity differences, rather than timing differences, at least partially mediate directional sensitivity in the intermediate- and trough-type units. The gradient in the influence of ILD across ITD tuning shape class is generally consistent with presumed differences in the brainstem circuitry generating ITD-sensitivity for the different tuning shape groups (see Discussion).

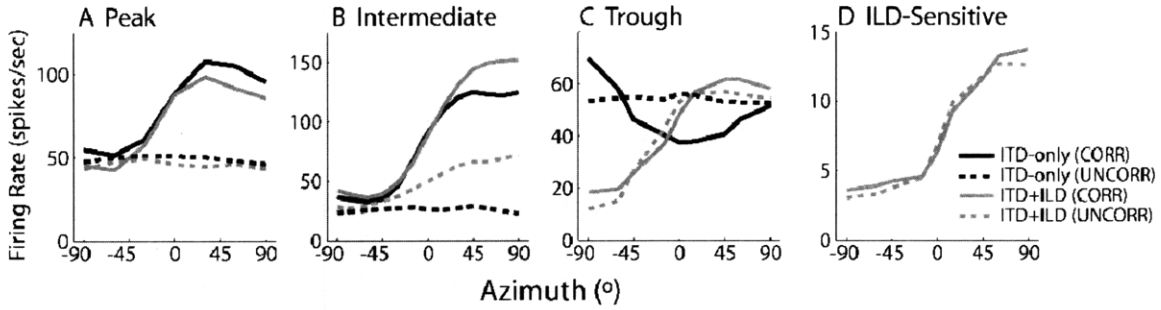

Figure 5.19 Influence of ILD depends on ITD tuning shape group
DRF obtained using correlated (solid lines) and uncorrelated broadband noise (dashed lines) for ITD-only (black lines) and ITD+ILD (gray lines) conditions. Units belonged to the following ITD tuning shape groups: *A,* peak; *B,* intermediate; *C,* trough; and *D,* not sensitive to ITD but sensitive to ILD.

Discussion

In a reverberant environment, echoes and reflections interfere with the direct sound arriving a listener's ears, distorting the binaural cues for sound localization. Consistent with previous observations in anesthetized cat (Chapter 2), reverberation degrades directional sensitivity in ITD-sensitive IC neurons by compressing the range of firing rates across azimuths, although the amount of degradation depends on the CF and the types of binaural cues available. When the virtual space stimuli contain only ITD cues, directional sensitivity in reverberation is significantly worse in high-CF ITD_{env}-sensitive neurons than in their low-CF ITD_{fs}-sensitive counterparts. However, directional sensitivity at high CFs can be significantly improved when the virtual space stimuli contain both ITD and ILD cues, suggesting that, at high CFs, ILDs prominently contribute to directional sensitivity in reverberation. Here, we discuss the two sets of results, focusing on the mechanisms underlying directional sensitivity for each type of binaural cue. We conclude by discussing how these neurophysiological results can account for observations from recent human psychophysical investigations of spatial hearing in reverberation.

Reverberation degrades ITD_{env} more than ITD_{fs}

Similar to the results obtained by Joris (2003) in anesthetized cat, we showed that low-CF IC neurons in the awake rabbit IC are primarily sensitive to ITD_{fs}, while high-CF neurons are primarily sensitive to the envelope ITDs. For anechoic stimuli, we found that the directional sensitivity of high-CF ITD_{env}-sensitive neurons is comparable to that of low-CF ITD_{fs}-sensitive neurons. However, directional sensitivity in reverberation is significantly worse in the high-CF ITD_{env}-sensitive neurons. Moreover, these trends held true for neurons in all of

the ITD tuning shape groups, suggesting that reverberation has similar effects on excitatory-excitatory and excitatory-inhibitory coincidence detection.

To examine the contribution of peripheral processing to these IC results, we used ideal coincidence detectors to extract ITD-based directional information from spike trains recorded from cat AN fibers with the ITD-only stimuli. Unlike what we observed in the IC, we found that, for anechoic stimuli, directional information decreased with increasing CF in the auditory nerve. This phenomenon has been observed previously, both in physiological investigations (Joris, 2003) as well as in an analysis using an auditory nerve model (Macpherson and Middlebrooks, 2002) and suggests that there must be additional processing of envelopes (or selective degradation of fine-structure information) between the AN and the IC (Joris, 2003).

On the other hand, similar to the trend observed in the IC, we found that reverberation caused an increasing reduction in the relative peak height of the shuffled cross-correlation with increasing CF, suggesting a partial peripheral origin for the IC results. Consistent with Joris' (2003) observation that the transition from ITD_{fs} sensitivity to ITD_{env} sensitivity occurs at higher CFs in the AN than in the IC, we found that the degradation in directional sensitivity produced by reverberation seemed to occur at higher CFs in the AN than in the IC, although more AN data are needed to reach a definitive conclusion (compare dashed and solid lines in Fig. 5.13D). The fact that the effect of reverberation covaries with the transition from ITD_{fs} to ITD_{env} in both structures is evidence that it is not an effect of frequency, *per se*; rather, it suggests that reverberation degrades directional coding more so for envelopes than fine-time structure. The difference in transition frequency between the AN and the IC may be accounted for by additional degradation in fine structure coding

between the AN and the binaural processor in the auditory brainstem (Joris, 2003) or in emergence of ITD_{env}-sensitivity at lower CFs (Agapiou and McAlpine, 2008).

Although differences in species (cat versus rabbit) and state (anesthetized versus awake) need to be considered when interpreting the two sets of results, the similarity of AN fiber tuning properties in cat and rabbit (Borg et al., 1988) helps validate the cross-species comparison. Moreover, our observations are consistent with Sayles and Winter's (2008) finding that reverberation degrades neural sensitivity to envelope pitch cues more severely than fine structure cues in the anesthetized guinea pig cochlear nucleus.

Influence of ILD on directional sensitivity

Our second set of IC results demonstrates that, at high CFs, directional sensitivity in reverberation can be significantly improved when VAS stimuli contain ILD as well as ITD cues (c.f. Fig. 5.16A,B), suggesting that ILDs may be more reliable than envelope ITDs in reverberation. Given that the ILD influence index parallels the magnitude of ILD in the virtual space stimuli (Fig. 5.15A, dashed line), we would expect ILD to be of even greater importance in more realistic head-related transfer functions, which can exhibit ILDs up to ±30 dB in species with directional pinnae (Bishop et al., 2009; Musicant et al., 1990).

At low CFs, the influence of ILD on directional sensitivity was not systematic and less prominent than at high CFs (Fig. 5.14A-C), probably due to the fact that the magnitude of the ILD is small at low frequencies (Fig. 5.2). The fact that the ITD and ITD+ILD stimuli give rise to similar directional sensitivity at low CFs suggests that the differences in the range of ITD for the two sets of stimuli (Fig. 5.1) were of minor consequence and can be ignored.

In general, the results suggest that directional sensitivity at low CFs is primarily governed by ITD while at high CFs, ILDs play an essential role. Neural sensitivity to ITD

and ILD appear to be governed by different stimulus properties. ITD sensitivity is completely dependent on the correlation of the waveforms at the two ears (Fig. 5.19, compare black solid and dashed lines); on the other hand, ILD sensitivity is very robust to manipulations of interaural correlation (Fig. 5.19, *right panel*). Nevertheless, ILD-sensitivity also degrades in reverberation (Fig. 5.18); we can attribute this degradation to the overall decrease in the magnitude of ILD in reverberation (Fig. 5.2, *right column*). Directional sensitivity in the exclusively ILD-sensitive neuron population is similar to what we observed in our high-CF ITD-sensitive neuron population (Fig. 5.18G), supporting the claim that the improvement in directional sensitivity at high CFs is due to the greater reliability of ILDs as compared to envelope ITDs in reverberation.

A shortcoming of the current study is that we obtained ITD+ILD DRF at only one D/R; thus, we do not know whether the current findings generalize to conditions with more (or less) extreme reverberation. Future studies might aim to extend the present findings by characterizing the influence of ITD and ILD on directional sensitivity in a variety of reverberant environments.

Mechanisms mediating influence of ILDs at high CFs

The influence of ILD on directional responses at high CFs was not uniformly distributed across the neuron population: The magnitude of both the ILD influence index and the improvement in directional sensitivity in reverberation (ΔRR) depended significantly on ITD tuning shape group. In particular, the improvement was largest for neurons in the trough- and intermediate-type tuning shape groups and smallest for neurons in the peak-type group (Fig. 5.17). The gradient in influence of ILD across ITD tuning shape groups provides clues as to the underlying mechanism.

For anechoic stimuli, trough-type neurons showed the poorest directional sensitivity in the ITD-only condition (Fig. 5.10B, open squares), but the strongest influence of ILD (Fig. 5.15A), resulting in more robust directional sensitivity in reverberation for ITD+ILD as opposed to ITD-only stimuli. Neurons in the trough-type tuning shape group are thought to receive input from the LSO (Batra et al., 1993). Subtractive excitatory-inhibitory (EI) binaural interactions in the LSO are classically associated with computation of ILDs (Boudreau and Tsuchitani, 1968), although many LSO neurons are also sensitive to ITD (Batra et al., 1997a; Joris and Yin, 1995; Tollin and Yin, 2005). The likely origin of ILD sensitivity in trough-type neurons, and hence the mechanism improving directional sensitivity in the ITD+ILD condition, is the EI interaction that occurs already in the auditory brainstem. However, we can not rule out the possibility that ILD-sensitivity is also created *de novo* within the IC (Li and Kelly, 1992).

Peak-type neurons exhibited superior directional sensitivity in the ITD-only condition (Fig. 5.10B, solid squares), but were only mildly influenced by ILD [Fig. 5.15A; see also (Caird and Klinke, 1987)]. Thus, high-CF peak-type neurons were typically poorly tuned to source azimuth in reverberation in both VAS stimulus conditions (Fig. 5.16A,B). Peak-type ITD-sensitivity is generally, although not exclusively, associated with excitatory-excitatory (EE) coincidence detection in the MSO (Batra et al., 1997a; Yin and Chan, 1990).

In principle, EI interactions in the brainstem can produce tuning to ITD that is as precise as tuning produced by EE interactions (Breebaart et al., 2001; Tollin and Yin, 2005). However, in practice we find that neurons associated with the EI interaction

(trough-type) are typically more poorly tuned to ITD than neurons associated with the EE interaction (peak-type) [see also (Batra et al., 1993)], while the opposite is true with respect to ILD (Caird and Klinke, 1987). More provocatively, it may be the case that ITD-sensitivity in trough-type neurons is simply an epiphenomenon of the EI interaction, given that it is overwhelmed by naturally co-occurring ILD [present results, see also (Delgutte et al., 1995; Joris and Yin, 1995)].

Intermediate-type neurons exhibit features associated with both peak- and trough-type neurons. For anechoic stimuli, intermediate-type neurons can be as directionally sensitive as peak-type neurons in the ITD-only condition (Figure 5.9B); however, they are also strongly influenced by ILD and therefore show improved directional sensitivity in reverberation in the ITD+ILD condition (Figure 5.16A,B). These observations suggest that the intermediate-type neurons may receive convergent input from both ITD- and ILD-sensitive neurons in the brainstem. Indeed, it has been shown that intermediate-type neurons can be created through the convergence of MSO and LSO inputs onto single IC cells (Agapiou and McAlpine, 2008; Fitzpatrick et al., 2002; Shackleton et al., 2000). Moreover, there is physiological evidence that ITD-sensitive IC neurons receive convergent input from multiple brainstem coincidence detectors (Batra et al., 1993; McAlpine et al., 1998) as well as anatomical evidence that inputs from the MSO and LSO overlap within tonotopic bands in the IC(Loftus et al., 2004; Oliver et al., 1995). Of course, we cannot exclude the possibility that intermediate-type neurons are created through dual EE/EI interactions in single neurons in the auditory brainstem (Batra et al., 1997b) nor the possibility that the ILD sensitivity is created *de novo* in the IC (Li and Kelly, 1992). The most general interpretation of our results is that intermediate-type

ITD-tuning is created through dual, although not necessarily segregated, EE and EI binaural interactions, that produce sharp sensitivity to ITD and that spares directional sensitivity in reverberation.

Caution must be taken in interpreting the results using the ITD tuning shape groups. First, it is entirely plausible that peak-type neurons in the IC actually receive input from trough-type neurons in the brainstem that have been inverted through inhibitory synapses in e.g., the DNLL and vice versa. However, the fact that we found highly significant differences between these two classes of neurons suggests that we are justified in distinguishing between them on the basis of ITD tuning shape. Second, the classification of neurons into the *intermediate* category is based on a parameter that varies continuously (*asymmetry ratio*, see Methods). We chose a relatively strict criterion value for the asymmetry index. In particular, this meant that some neurons assigned to the *peak-type* class had small but non-zero asymmetry indices. If we assume that asymmetry in noise delay functions results from convergent inputs onto single IC cells (Agapiou and McAlpine, 2008), then we might expect some neurons in our peak-type category to show an influence of ILD. Indeed, as shown in Figure 5.17, there is a modest population of *peak-type* cells that show improved directional sensitivity in the ITD+ILD condition.

In general, our data suggest that, at high CFs, ILDs convey more reliable directional information than envelope ITDs in reverberation. Thus, it would be advantageous for high-CF ITD_{env}-sensitive neurons to be tuned to ILD as well as ITD. An important functional consequence of interaction of convergent ITD- and ILD-sensitive inputs in the IC or, more loosely, dual EE/EI interactions, is the significant

improvement of directional sensitivity in reverberation. An important future step will be to establish the origin of the ILD-sensitive directional response components onto IC cells in awake rabbit.

Comparison with Human Psychophysics

The present neurophysiological results parallel those of human psychophysical studies of spatial hearing in reverberant environments. Rakerd and Hartman (2006) found that ITD discrimination thresholds for 1/3-octave noise bands degrade more rapidly with increasing reverberation at high frequencies (2850 Hz) than at low frequencies (715 Hz), consistent with our observation that reverberation causes more severe compression of DRF in high-CF, ITD_{env}-sensitive IC neurons than in low-CF ITD_{fs}-sensitive neurons. Rakerd and Hartmann further found that, for reverberant noise bands, ITD-discrimination degraded when they introduced a small ILD in opposition to the ITD, suggesting that ILD has an important influence on localization in reverberation. Rakerd and Hartmann observed effects of ILD at both low and high frequencies, while the influence of ILD on neural responses was most prominent in high-CF, ITD_{env}-sensitive neurons. The two sets of results may be reconciled if, as suggested by Fig. 15A, the influence of ILD on neural responses is determined by the magnitude of the ILD. Since Rakerd and Hartmann used the same ILDs at low and high frequencies, similar effects are expected for the two frequency bands in their experiment. In contrast, the ILD in our experiments were determined by a rigid sphere model for the head; therefore, the magnitude of the ILD increased with frequency. Nevertheless single-unit experiments using stimuli with opposing ITD and ILD are needed to better understand the relationships between our results and those of Rakerd and Hartmann.

In a different study, Kiggins et al. (2005) demonstrated that sound localization accuracy in a reverberant room was similar for low-pass (0.5-1.0 kHz) and high-pass (4-8

kHz) pink noise, although accuracy tended to be slightly worse in the high-pass conditions at lateral azimuths. Likewise, we find comparable directional sensitivity across the tonotopic axis using the ITD+ILD stimuli (Fig. 5.16B). The parallel between the two studies suggests that our observation that ILD-sensitivity at high-CFs is comparable to ITD_{fs}-sensitivity at low-CFs is *not* an artifact of our particular simulated reverberant room or the VAS simulation techniques employed. Unlike our study, which used simulated reverberation and a simplified spherical head model, the Kiggin's study used head-related transfer functions obtained using an acoustic mannequin in a real room. Of course, despite these simple parallels, it is not possible to relate the firing rate of single neurons to the perceived azimuth from behavioral studies without making explicit assumptions about the neural code for sound localization. An important future avenue for research is to test whether models that incorporate the observed effects of reverberation on directional sensitivity of single neurons are able to successfully account for psychophysical performance.

The duplex theory of sound localization (Rayleigh, 1907) stipulates that listeners use ITD at low frequencies and ILD at high frequencies. The present results, which represent one of the few investigations of ITD sensitivity across a wide range of CFs using a common set of stimuli, suggest that, in the anechoic condition, ITD_{env}-sensitivity at high CFs can rival that based on fine-time structure at low CFs. However, the low perceptual weight given to high-frequency ITD_{env} cues in sound localization by most human listeners (Macpherson and Middlebrooks, 2002) may result from the fact that ITD_{env} cues are less reliable than ILD cues in reverberant listening conditions.

CHAPTER 6

General Conclusions and Discussion

The central focus of this thesis was to investigate connections between the effects of everyday room reverberation on the neural representation of sound localization cues in the mammalian auditory midbrain and the localization behavior of human listeners. Overall, we found that reverberation degrades the directional sensitivity of single neurons, although onset dominance in temporal response patterns serves as a simple mechanism for improving directional coding near stimulus onsets, when the directional information is most reliable. Moreover, the striking parallels between our neurophysiological findings and the localization performance of human listeners suggests that the information contained in neural rate responses at the level of the auditory midbrain is sufficient to account for human spatial hearing in reverberation.

Time course of directional sensitivity in reverberation

In Chapters 2 and 3, we demonstrated that the time course of neural directional sensitivity in reverberation qualitatively parallels the buildup of reverberation in the acoustic inputs, such that it is better near the stimulus onset and becomes more degraded over time. Thus, as neural responses are integrated over longer time periods, ongoing reverberation increasingly contaminates the neural response, resulting in worse directional sensitivity. To assess the extent to which perceptual judgments of sound location are corrupted by ongoing reverberation, we implemented a hemispheric difference decoding model to

predict localization estimates using the data obtained from the neurophysiological experiments. We found that human judgments of sound source location—obtained in parallel behavioral experiments—matched the output of the decoder using an integration window of approximately 150 msec. While these findings demonstrate the sufficiency of a temporally integrated hemispheric decoding mechanism, it is plausible that other readouts, such as a labeled line code (Jeffress, 1948; Takahashi et al., 2003), might also account for the behavioral results.

The present results suggest several key areas for future research in neurophysiology as well as psychophysics. First, perhaps fortuitously, our findings corroborate previous studies using very different behavioral tasks that derived similar windows for temporal integration in the binaural system (Boehnke et al., 2002; Kolarik and Culling, 2009; Kollmeier and Gilkey, 1990). To establish the validity of our findings, future research efforts should be made to develop behavioral localization experiments that directly test the temporal integration hypothesis. For example, one could generate a set of reverberant binaural room impulse responses in which the delay between the direct sound and first echo is digitally manipulated, so as to provide the listener with shorter and longer uncorrupted onsets. By analyzing the compression of localization judgments as a function of the length of the uncorrupted onset, one could derive a model-free estimate of the integration window.

Furthermore, in the present study, human behavior was exclusively compared to neural rate responses obtained from the auditory midbrain. Although our findings suggest that rate information contained at this level of the auditory pathway is sufficient to account for human behavior, we have not demonstrated a necessary role for processing

at the level of the midbrain. That is, given that the midbrain receives direct, monosynaptic projections from the primary sites of binaural interaction in the brainstem (Adams, 1979; Aitkin and Schuck, 1985; Glendenning and Masterton, 1983; Loftus et al., 2004; Oliver et al., 2003; Oliver et al., 1995), it may be the case that behavioral judgments can be decoded on a similar timescale from rate responses obtained in these lower auditory stations. In order to establish the significance of midbrain processing and understand the transformations that take place beyond the initial site of binaural interaction, future efforts should be aimed at characterizing the effects of reverberation in auditory stations *below* the midbrain.

Along similar lines, the neural circuits that implement the decoding algorithms presumably lie downstream of the auditory midbrain (Stecker et al., 2005). The neural signals upon which these circuits operate have therefore undergone both thalamic and cortical processing beyond what was currently observed at the level of the auditory midbrain. Thus, another important area for future research will be to characterize the effects of reverberation on directional sensitivity in higher auditory centers. Decoding models can then be implemented using neural responses obtained from these higher auditory centers, giving further insight into the relevant timescale of temporal integration for sound localization in reverberation.

In the present study, we uncovered evidence for temporal integration in sound localization by using a modeling approach to directly compare neural responses to human behavior. In general, our study demonstrates that key insights into the mechanisms mediating basic auditory behavior (such as e.g., sound localization) can be made when complimentary approaches are combined. Future efforts at furthering our understanding

of the effects of reverberation on directional sensitivity should be guided by a similar, complimentary approach.

Understanding the computations performed by ITD-sensitive IC neurons

In Chapter 2, we demonstrated that a standard cross-correlation model of binaural processing typically predicted worse directional sensitivity in reverberation than observed in individual IC neurons. Moreover, we showed that such robustness to reverberation was systematically related to onset dominance in temporal response patterns, suggesting a simple mechanism for improving directional sensitivity in reverberation. An obvious area for future research would be to extend the cross-correlation model so that it is sensitive to temporal dynamics, in addition to the binaural properties of the input stimulus. The membrane-dynamics-based models of Cai et al. (1998a; 1998b) might provide a good starting point, although an inherent complication in using such multi-parameter models is the risk of overfitting individual responses. Of course, these problems can be avoided given a solid understanding of the anatomy and physiology; thus, modeling efforts should necessarily be physiologically constrained [e.g., (Hancock and Delgutte, 2004; Nelson and Carney, 2004)].

In Chapter 4, we developed a direct test of the onset dominance hypothesis by using a conditioning paradigm to alter temporal response patterns in individual neurons. Consistent with our hypothesized role for onset dominance in the neural processing of reverberation, results showed that making temporal response patterns less onset-dominated resulted in worse directional sensitivity in reverberation, particularly during the response epoch immediately following the conditioner. An intriguing direction for

future research is to explore the role of onset dominance in robust directional coding in reverberation using acoustic stimuli with multiple acoustic onsets, such as e.g., natural speech and other amplitude modulated sounds.

Alternatively, one can take a step back and reexamine the notion of robust coding of ITD in reverberation. In this thesis, we explored the possibility that temporal dynamics of spiking responses may partly underlie robust directional sensitivity in reverberation. However, robust encoding of ITD in reverberation could be achieved not only by mechanisms that emphasize onsets in neurons tuned *near* the source location but also by mechanisms that reduce the ongoing "noise" seen by neurons tuned *away* from the source location. Such noise reduction would prevent a neuron from firing to echoes that originate from favorable directions when the direct sound is coming from an unfavorable source location. Rucci and Wray (1999) proposed a model for noise reduction in the barn owl auditory pathway that results from convergent and lateral inhibitory connections onto single neurons in the barn owl's auditory space map. Future research efforts aimed at developing more accurate computational models of IC neuron responses in reverberation might make use of similar features.

Integration of multiple binaural cues

In Chapter 5 we extended our investigations of directional sensitivity in reverberation to include ITD-sensitive neurons across the tonotopic axis. We demonstrated that reverberation degrades envelope ITD cues more than fine structure ITD cues. However, for realistic stimuli containing both ITD and ILD, directional sensitivity is comparable across the tonopic axis, suggesting ILDs are more reliable than envelope ITDs in

reverberation. Moreover, we demonstrate that the influence of ILDs on directional sensitivity in reverberation depends on the shape of the noise delay function. Namely, neurons with trough-shaped noise delay functions, which indicate excitatory-inhibitory binaural interactions, show the biggest influence of ILDs while neurons with peak-shaped noise delay functions, which indicate excitatory-excitatory binaural interactions, show the least influence of ILDs. Neurons with asymmetric noise delay functions, which may indicate a combination of both types of binaural interactions, also exhibit prominent influences of ILD. In general, these results emphasize the importance of excitatory-inhibitory binaural interactions, and hence the ILD-processing pathway, for spatial hearing in reverberation.

Similar to the issues raised by the experiments of Chapters 2 and 3, an important question raised by this study is whether these results can be explained by processing *prior* to the auditory midbrain, or if they emerge only at the level of the auditory midbrain. Two key areas for future research are (1) to establish the effects of reverberation on directional rate responses at the primary site of binaural interaction in the brainstem and (2) to develop neurophysiological methods for teasing apart the various sources of input to individual IC neurons. The former experiments are relatively straightforward, and would involve only basic changes to the current experimental setup. Experiments in the latter category are more difficult and have classically been approached using both pharmacological manipulation as well as lesion techniques (Davis, 2002; Davis et al., 1999; Kelly and Kidd, 2000; Kelly and Li, 1997; Kidd and Kelly, 1996; Li and Kelly, 1992; Pollak et al., 2003; Pollak et al., 2002; Sally and Kelly, 1992; van Adel et al., 1999). Future efforts might combine these standard methods with recently developed

techniques for in vivo optogenetic control of neural circuits (Han and Boyden, 2007; Han et al., 2009; Huber et al., 2008; Liewald et al., 2008; Tsai et al., 2009; Zhang et al., 2008) to bring a modern approach to functional studies of integration at the level of the auditory midbrain. Moreover, such studies will also be important for constraining computational models that seek to describe the interactions taking place in the auditory midbrain.

Sound localization in realistic listening conditions

This thesis addressed fundamental questions regarding the effects of everyday room reverberation on the ability of individual neurons and human listeners to signal the location of a single, isolated sound source in everyday reverberant settings. Yet, in the real world, it is rare that a listener actually performs such a simple task. The real task faced by the auditory system in parsing the unfolding acoustic scene is to localize and identify the information-content of relevant sound sources, amidst the background hum of the multiple, simultaneous sources typical of our everyday listening environments. The most remarkable feat of the auditory system is not that we can localize and identify single sound sources in reverberation, but that we can localize and selectively attend to single sound sources in reverberation amidst the interference of the complex acoustic background (Kidd et al., 2005b). A first step towards elucidating the neural basis of such real world auditory behavior will be to extend the current experimental paradigms to study how reverberation affects the encoding of multiple, simultaneous sources of sound. Using the complimentary approaches already developed in this thesis, decoding models can be further refined to perform more appropriate auditory behaviors. While, ultimately, complex auditory perception most likely arises from cortical processing, the auditory

midbrain is nevertheless an obligatory station in the ascending pathway to cortex (Adams, 1979). Thus, to fully understand the computations performed at higher levels we must continue to study the transformations that take place along the way.

References

Adams, J. C. (1979). Ascending projections to the inferior colliculus. J Comp Neurol *183*, 519-538.

Agapiou, J. P., and McAlpine, D. (2008). Low-frequency envelope sensitivity produces asymmetric binaural tuning curves. J Neurophysiol *100*, 2381-2396.

Aitkin, L. M., Blake, D. W., Fryman, S., and Bock, G. R. (1972). Responses of neurons in the rabbit inferior colliculus. II. Influence of binaural tonal stimulation. Brain Research *47*, 91-101.

Aitkin, L. M., Gates, G. R., and Phillips, S. C. (1984). Responses of Neurons in the Inferior Colliculus to Variations in Sound-Source Azimuth. J Neurophysiol *52*, 1-17.

Aitkin, L. M., and Martin, R. L. (1987). The representation of stimulus azimuth by high best-frequency azimuth-selective neurons in the inferior colliculus of the cat. J Neurophysiol *57*, 1185-1200.

Aitkin, L. M., and Schuck, D. (1985). Low frequency neurons in the lateral central nucleus of the cat inferior colliculus receive their input predominantly from the medial superior olive. Hearing Research *17*, 87-93.

Albeck, Y., and Konishi, M. (1995). Responses of neurons in the auditory pathway of the barn owl to partially correlated binaural signals. J Neurophysiol *74*, 1689-1700.

Allen, J. B., and Berkley, D. A. (1979). Image method for efficiently simulating small-room acoustics. J Acoust Soc Am *65*, 943-950.

Batra, R., Kuwada, S., and Fitzpatrick, D. C. (1997a). Sensitivity to interaural temporal disparities of low- and high-frequency neurons in the superior olivary complex. I. Heterogeneity of responses. J Neurophysiol *78*, 1222-1236.

Batra, R., Kuwada, S., and Fitzpatrick, D. C. (1997b). Sensitivity to interaural temporal disparities of low- and high-frequency neurons in the superior olivary complex. II. Coincidence detection. J Neurophysiol *78*, 1237-1247.

Batra, R., Kuwada, S., and Stanford, T. R. (1993). High-frequency neurons in the inferior colliculus that are sensitive to interaural delays of amplitude-modulated tones: evidence for dual binaural influences. J Neurophysiol *70*, 64-80.

Batra, R., Kuwada, S., Stanford, T.R. (1989). Temporal coding of envelopes and their interaural delays in the inferior colliculus of the unanesthetized rabbit. J Neurophysiol *61*, 257-268.

Beckius, G. E., Batra, R., and Oliver, D. L. (1999). Axons from anteroventral cochlear nucleus that terminate in medial superior olive of cat: observations related to delay lines. J Neurosci *19*, 3146-3161.

Beranek, L. (2004). Concert Halls and Opera Houses, 2nd edn (New York, Springer-Verlag).

Best, V., Gallun, F. J., Carlile, S., and Shinn-Cunningham, B. G. (2007). Binaural interference and auditory grouping. J Acoust Soc Am *121*, 1070-1076.

Bishop, B., Kim, D. O., Sterbing-D'Angelo, S., and Kuwada, S. (2009). Acoustic cues for sound localization measured in a rabbit and a tennis ball and computed using a rigid spherical model. Abstracts Assoc Res Otolaryn, 908.

Bock, G. R., Webster, W. R., and Aitkin, L. M. (1972). Discharge patterns of single units in inferior colliculus of the alert cat. J Neurophysiol *35*, 265-277.

Boehnke, S. E., Hall, S. E., and Marquardt, T. (2002). Detection of static and dynamic changes in interaural correlation. J Acoust Soc Am *112*, 1617-1626.

Borg, E., Engstrom, B., Linde, G., and Marklund, K. (1988). Eighth nerve fiber firing features in normal-hearing rabbits. Hearing Research *36*, 191-201.

Boudreau, J. C., and Tsuchitani, C. (1968). Binaural interaction in the cat superior olive S segment. J Neurophysiol *31*, 442-454.

Brand, A., Behrand, O., Marquardt, T., McAlpine, D., and Grothe, B. (2002). Precise inhibition is essential for microsecond interaural time difference coding. Nature *417*, 543-547.

Breebaart, J., van de Par, S., and Kohlrausch, A. (2001). Binaural processing model based on contralateral inhibition. I. Model structure. J Acoust Soc Am *110*, 1074-1088.

Brugge, J. F., Anderson, D. J., and Aitkin, L. M. (1970). Responses of neurons in the dorsal nucleus of the lateral lemniscus of cat to binaural tonal stimulation. J Neurophysiol *33*, 441-458.

Cai, H., Carney, L. H., and Colburn, H. S. (1998a). A model for binaural response properties of inferior colliculus neurons. I. A model with interaural time difference-sensitive excitatory and inhibitory inputs. J Acoust Soc Am *103*, 475-493.

Cai, H., Carney, L. H., and Colburn, H. S. (1998b). A model for binaural response properties of inferior colliculus neurons. II. A model with interaural time difference-sensitive excitatory and inhibitory inputs and an adaptation mechanism. J Acoust Soc Am *103*, 494-506.

Caird, D., and Klinke, R. (1983). Processing of binaural stimuli by cat superior olivary complex neurons. Exp Brain Res *52*, 385-399.

Caird, D., and Klinke, R. (1987). Processing of interaural time and intensity differences in the cat inferior colliculus. Exp Brain Res *68*, 379-392.

Cant, N. B., and Casseday, J. H. (1986). Projections from the anteroventral cochlear nucleus to the lateral and medial superior olivary nuclei. J Comp Neurol *247*, 457-476.

Carney, L. H., and Yin, T. C. (1989). Responses of low-frequency cells in the inferior colliculus to interaural time differences of clicks: excitatory and inhibitory components. J Neurophysiol *62*, 144-161.

Chase, S. M., and Young, E. D. (2005). Limited Segregation of Different Types of Sound Localization Information among Classes of Units in the Inferior Colliculus. J Neurosci *25*, 7575-7585.

Coffey, C. S., Ebert, J., Charles S., Marshall, A. F., Skaggs, J. D., Falk, S. E., Crocker, W. D., Pearson, J. M., and Fitzpatrick, D. C. (2006). Detection of interaural correlation by neurons in the superior olivary complex, inferior colliculus and auditory cortex of the unanesthetized rabbit. Hearing Research *221*, 1-16.

Colburn, H. S. (1973). Theory of binaural interaction based on auditory-nerve data. I. General strategy and preliminary results on interaural discrimination. J Acoust Soc Am *54*, 1458-1470.

Cover, T. M., and Thomas, J. A. (1991). Elements of Information Theory (New York, Wiley).

Culling, J. F., Colburn, H. S., and Spurchise, M. (2001). Interaural correlation sensitivity. Journal of the Acoustical Society of America *110*, 1020-1029.

D'Angelo, W. R., Sterbing, S. J., Ostapoff, E.-M., and Kuwada, S. (2003). Effects of Amplitude Modulation on the Coding of Interaural Time Differences of Low-Frequency Sounds in the Inferior Colliculus. II. Neural Mechanisms. J Neurophysiol *90*, 2827-2836.

D'Angelo, W. R., Sterbing, S. J., Ostapoff, E.-M., and Kuwada, S. (2005). Role of GABAergic Inhibition in the Coding of Interaural Time Differences of Low-Frequency Sounds in the Inferior Colliculus. J Neurophysiol *93*, 3390-3400.

Darwin, C. J. (2008). Spatial hearing and perceiving sources. In Auditory Perception of Sound Sources, W. A. Yost, ed. (New York, Springer).

Davis, K. A. (2002). Evidence of a functionally segregated pathway from dorsal cochlear nucleus to inferior colliculus. J Neurophysiol *87*, 1824-1835.

Davis, K. A., Ramachandran, R., and May, B. J. (1999). Single-unit responses in the inferior colliculus of decerebrate cats. II. Sensitivity to interaural level differences. J Neurophysiol *82*, 164-175.

Dean, I., Harper, N. S., and McAlpine, D. (2005). Neural population coding of sound level adapts to stimulus statistics. Nature Neuroscience *8*, 1684-1689.

Delgutte, B., Joris, P. X., Litovsky, R. Y., and Yin, T. C. (1995). Relative importance of different acoustic cues to the directional sensitivity of inferior colliculus neurons. In Advances in Hearing Research, G. A. Manley, G. M. Klump, C. Koeppl, H. Fastl, and H. Oeckinghaus, eds. (Singapore, World Scientific Pub.), pp. 288-299.

Delgutte, B., Joris, P. X., Litovsky, R. Y., and Yin, T. C. T. (1999). Receptive Fields and Binaural Interactions for Virtual-Space Stimuli in the Cat Inferior Colliculus. J Neurophysiol *81*, 2833-2851.

Devore, S., and Delgutte, B. (2008). Does spike rate adaptation mediate robust encoding of ITD in reverberation? Paper presented at: Society for Neuroscience (Washington, DC).

Finlayson, P. G. (1999). Post-stimulatory suppression, facilitation and tuning for delays shape responses of inferior colliculus neurons to sequential pure tones. Hear Res *131*, 177-194.

Finlayson, P. G., and Adam, T. J. (1997). Short-term adaptation of excitation and inhibition shapes binaural processing. Acta Otolaryngol *117*, 187-191.

Fitzpatrick, D. C., Batra, R., Stanford, T. R., and Kuwada, S. (1997). A neuronal population code for sound localization. Nature *388*, 871-874.

Fitzpatrick, D. C., Kuwada, S., and Batra, R. (2000). Neural sensitivity to interaural time differences: beyond the Jeffress model. J Neurosci *20*, 1605-1615.

Fitzpatrick, D. C., Kuwada, S., and Batra, R. (2002). Transformations in processing interaural time differences between the superior olivary complex and inferior colliculus: beyond the Jeffress model. Hear Res *168*, 79-89.

Fitzpatrick, D. C., Kuwada, S., Kim, D. O., Parham, K., and Batra, R. (1999). Responses of neurons to click-pairs as simulated echoes: Auditory nerve to auditory cortex. J Acoust Soc Am *106*, 3460-3472.

Geisler, C. D., Rhode, W. S., and Hazelton, D. W. (1969). Responses of inferior colliculus neurons in the cat to binaural acoustic stimuli having wide-band spectra. J Neurophysiol *32*, 960-974.

Giguere, C., and Abel, S. M. (1993). Sound localization: effects of reverberation time, speaker array, stimulus frequency, and stimulus rise/decay. J Acoust Soc Am *94*, 769-776.

Glendenning, K. K., and Masterton, R. B. (1983). Acoustic chiasm: efferent projections of the lateral superior olive. J Neurosci *3*, 1521-1537.

Goldberg, J. M., and Brown, P. B. (1969). Response of binaural neurons of dog superior olivary complex to dichotic tonal stimuli: some physiological mechanisms of sound localization. J Neurophysiol *32*, 613-636.

Grantham, D. W., and Wightman, F. L. (1978). Detectability of varying interaural temporal differences. J Acoust Soc Am *63*, 511-523.

Griffin, S. J., Bernstein, L. R., Ingham, N. J., and McAlpine, D. (2005). Neural sensitivity to interaural envelope delays in the inferior colliculus of the guinea pig. J Neurophysiol *93*, 3463-3478.

Grothe, B., and Sanes, D. H. (1994). Synaptic inhibition influences the temporal coding properties of medial superior olivary neurons: an in vitro study. J Neurosci *14*, 1701-1709.

Guinan, J. J., Jr., Norris, B. E., and Guinan, S. S. (1972). Single auditory units in the superior olivary complex. II: Locations of unit categories and tonotopic organization. Int J Neurosci *4*, 147-166.

Han, X., and Boyden, E. S. (2007). Multiple-Color Optical Activation, Silencing, and Desynchronization of Neural Activity, with Single-Spike Temporal Resolution. PLoS ONE *2*, e299.

Han, X., Qian, X., Bernstein, J. G., Zhou, H., Franzesi, G. T., Stern, P., Bronson, R. T., Graybiel, A. M., Desimone, R., and Boyden, E. S. (2009). Millisecond-Timescale Optical Control of Neural Dynamics in the Nonhuman Primate Brain. Neuron *62*, 191-198.

Hancock, K. E. (2007). A physiologically-based population rate code for interaural time differences predicts bandwidth-dependent lateralization. In Hearing - from sensory processing to perception, B. Kollmeier, G. Klump, V. Hohmann, U. Langemann, M. Mauermann, S. Uppenkamp, and J. Verhey, eds. (Berlin, Springer Verlag), pp. 389-398.

Hancock, K. E., and Delgutte, B. (2004). A Physiologically Based Model of Interaural Time Difference Discrimination. J Neurosci *24*, 7110-7117.

Harper, N. S., and McAlpine, D. (2004). Optimal neural population coding of an auditory spatial cue. Nature *430*, 682-686.

Hartmann, W. M. (1983). Localization of sound in rooms. Journal of the Acoustical Society of America *74*, 1380-1391.

Hartmann, W. M., Rakerd, B., and Koller, A. (2005). Binaural Coherence in Rooms. Acta Acustica United With Acustica *91*, 451-462.

Heffner, H., and Masterton, B. (1980). Hearing in Glires: Domestic rabbit, cotton rat, feral house mouse, and kangaroo rat. The Journal of the Acoustical Society of America *68*, 1584-1599.

Heffner, R., and Heffner, H. (1985). Hearing range of domestic cat. Hearing Research *19*, 85-88.

Houtgast, T., and Steeneken, H. J. M. (1973). The modulation transfer function in room acoustics as a predictor of speech intelligibility. Acustica *28*, 66-73.

Huber, D., Petreanu, L., Ghitani, N., Ranade, S., Hromadka, T., Mainen, Z., and Svoboda, K. (2008). Sparse optical microstimulation in barrel cortex drives learned behaviour in freely moving mice. *451*, 61-64.

Huisman, W. H. T., and Attenborough, K. (1991). Reverberation and attenuation in a pine forest. The Journal of the Acoustical Society of America *90*, 2664-2677.

Ihlefeld, A., and Shinn-Cunningham, B. G. (2004). Effect of source locations and listener location on ILD cues in a reverberant room. J Acoust Soc Am *115*, 2598.

Ingham, N. J., and McAlpine, D. (2004). Spike-Frequency Adaptation in the Inferior Colliculus. J Neurophysiol *91*, 632-645.

Ingham, N. J., and McAlpine, D. (2005). GABAergic Inhibition Controls Neural Gain in Inferior Colliculus Neurons Sensitive to Interaural Time Differences. J Neurosci *25*, 6187-6198.

Jeffress, L. A. (1948). A place theory of sound localization. J Comp Physiol Psychol *41*, 35-39.

Jenkins, W. M., and Masterton, R. B. (1982). Sound localization: effects of unilateral lesions in central auditory system. J Neurophysiol *47*, 987-1016.

Johnson, D. H. (1980). The relationship between spike rate and synchrony in responses of auditory-nerve fibers to single tones. J Acoust Soc Am *68*, 1115-1122.

Joris, P., and Yin, T. C. (2007). A matter of time: internal delays in binaural processing. Trends Neurosci *30*, 70-78.

Joris, P. X. (2003). Interaural time sensitivity dominated by cochlea-induced envelope patterns. J Neurosci *23*, 6345-6350.

Joris, P. X., and Yin, T. C. (1995). Envelope coding in the lateral superior olive. I. Sensitivity to interaural time differences. J Neurophysiol *73*, 1043-1062.

Kelly, J. B., and Kidd, S. A. (2000). NMDA and AMPA receptors in the dorsal nucleus of the lateral lemniscus shape binaural responses in rat inferior colliculus. J Neurophysiol *83*, 1403-1414.

Kelly, J. B., and Li, L. (1997). Two sources of inhibition affecting binaural evoked responses in the rat's inferior colliculus: the dorsal nucleus of the lateral lemniscus and the superior olivary complex. Hear Res *104*, 112-126.

Kiang, N. Y.-s. (1965). Discharge patterns of single fibers in the cat's auditory nerve (Cambridge, Mass.,, M.I.T. Press).

Kiang, N. Y. S., and Moxon, A. C. (1974). Tails of tuning curves of auditory-nerve fibers. Journal of the Acoustical Society of America *55*, 620-630.

Kidd, G., Jr., Arbogast, T. L., Mason, C. R., and Gallun, F. J. (2005a). The advantage of knowing where to listen. J Acoust Soc Am *118*, 3804-3815.

Kidd, G., Mason, C. R., Brughera, A., and Hartmann, W. M. (2005b). The Role of Reverberation in Release from Masking Due to Spatial Separation of Sources for Speech Identification. Acta Acustica united with Acustica *91*, 526-536.

Kidd, S. A., and Kelly, J. B. (1996). Contribution of the dorsal nucleus of the lateral lemniscus to binaural responses in the inferior colliculus of the rat: interaural time delays. J Neurosci *16*, 7390-7397.

Kiggins, J., Ihlefeld, A., and Shinn-Cunningham, B. G. (2005). How does reverberation affect the accuracy of sound localization? Paper presented at: BMES.

Kolarik, A. J., and Culling, J. F. (2009). Measurement of the binaural temporal window using a lateralisation task. Hear Res *248*, 60-68.

Kollmeier, B., and Gilkey, R. H. (1990). Binaural forward and backward masking: evidence for sluggishness in binaural detection. J Acoust Soc Am *87*, 1709-1719.

Krishna, B. S., and Semple, M. N. (2000). Auditory temporal processing: responses to sinusoidally amplitude-modulated tones in the inferior colliculus. J Neurophysiol *84*, 255-273.

Kuhn, G. F. (1977). Model for the interaural time differences in the azimuthal plane. The Journal of the Acoustical Society of America *62*, 157-167.

Kuwada, S., Batra, R., and Stanford, T. R. (1989). Monaural and binaural response properties of neurons in the inferior colliculus of the rabbit: effects of sodium pentobarbital. J Neurophysiol *61*, 269-282.

Kuwada, S., Stanford, T. R., and Batra, R. (1987). Interaural phase sensitive units in the inferior colliculus of the unanesthetized rabbit. Effects of changing frequency. Journal of Neurophysiology *57*, 1338-1360.

Kuwada, S., and Yin, T. C. (1983). Binaural interaction in low-frequency neurons in inferior colliculus of the cat. I. Effects of long interaural delays, intensity, and repetition rate on interaural delay function. J Neurophysiol *50*, 981-999.

Lane, C. C., and Delgutte, B. (2005). Neural correlates and mechanisms of spatial release from masking: single-unit and population responses in the inferior colliculus. J Neurophysiol, 1180-1198.

Le Beau, F. E., Rees, A., and Malmierca, M. S. (1996). Contribution of GABA- and glycine-mediated inhibition to the monaural temporal response properties of neurons in the inferior colliculus. J Neurophysiol *75*, 902-919.

Li, L., and Kelly, J. B. (1992). Binaural responses in rat inferior colliculus following kainic acid lesions of the superior olive: interaural intensity difference functions. Hear Res *61*, 73-85.

Liewald, J. F., Brauner, M., Stephens, G. J., Bouhours, M., Schultheis, C., Zhen, M., and Gottschalk, A. (2008). Optogenetic analysis of synaptic function. *5*, 895-902.

Litovsky, R. Y., Colburn, H. S., Yost, W. A., and Guzman, S. J. (1999). The precedence effect. The Journal of the Acoustical Society of America *106*, 1633-1654.

Litovsky, R. Y., and Delgutte, B. (2002). Neural Correlates of the Precedence Effect in the Inferior Colliculus: Effect of Localization Cues. J Neurophysiol *87*, 976-994.

Litovsky, R. Y., Fligor, B. J., and Tramo, M. J. (2002). Functional role of the human inferior colliculus in binaural hearing. Hear Res *165*, 177-188.

Litovsky, R. Y., and Yin, T. C. T. (1998). Physiological Studies of the Precedence Effect in the Inferior Colliculus of the Cat. I. Correlates of Psychophysics. J Neurophysiol *80*, 1285-1301.

Loftus, W. C., Bishop, D. C., Saint Marie, R. L., and Oliver, D. L. (2004). Organization of binaural excitatory and inhibitory inputs to the inferior colliculus from the superior olive. The Journal of Comparative Neurology *472*, 330-344.

Longworth-Reed, L., Brandewie, E., and Zahorik, P. (2009). Time-forward speech intelligibility in time-reversed rooms. J Acoust Soc Am *125*, EL13-EL19.

Louage, D. H., van der Heijden, M., and Joris, P. X. (2004). Temporal properties of responses to broadband noise in the auditory nerve. J Neurophysiol *91*, 2051-2065.

Macpherson, E. A., and Middlebrooks, J. C. (2002). Listener weighting of cues for lateral angle: The duplex theory of sound localization revisited. J Acoust Soc Am *111*, 2219-2236.

Masterton, R. B., Jane, J. A., and Diamond, I. T. (1968). Role of brain-stem auditory structures in sound localization. II. Inferior colliculus and its brachium. J Neurophysiol *31*, 96-108.

McAlpine, D., Jiang, D., and Palmer, A. R. (2001). A neural code for low-frequency sound localization in mammals. Nature Neuroscience *4*, 396-401.

McAlpine, D., Jiang, D., Shackleton, T. M., and Palmer, A. R. (1998). Convergent Input from Brainstem Coincidence Detectors onto Delay-Sensitive Neurons in the Inferior Colliculus. J Neurosci *18*, 6026-6039.

McAlpine, D., Jiang, D., Shackleton, T. M., and Palmer, A. R. (2000). Responses of Neurons in the Inferior Colliculus to Dynamic Interaural Phase Cues: Evidence for a Mechanism of Binaural Adaptation. J Neurophysiol *83*, 1356-1365.

McAlpine, D., and Palmer, A. R. (2002). Blocking GABAergic Inhibition Increases Sensitivity to Sound Motion Cues in the Inferior Colliculus. J Neurosci *22*, 1443-1453.

Musicant, A. D., Chan, J. C., and Hind, J. E. (1990). Direction-dependent spectral properties of cat external ear: new data and cross-species comparisons. J Acoust Soc Am *87*, 757-781.

Nelson, B. S., and Takahashi, T. T. (2008). Independence of echo-threshold and echo-delay in the barn owl. PLoS ONE *3*, e3598.

Nelson, P. C., and Carney, L. H. (2004). A phenomenological model of peripheral and central neural responses to amplitude-modulated tones. J Acoust Soc Am *116*, 2173-2186.

Nelson, P. C., and Carney, L. H. (2007). Neural rate and timing cues for detection and discrimination of amplitude-modulated tones in the awake rabbit inferior colliculus. J Neurophysiol *97*, 522-539.

Nelson, P. G., and Erulkar, S. D. (1963). Synaptic Mechanisms of Excitation and Inhibition in the Central Auditory Pathway. J Neurophysiol *26*, 908-923.

Nuding, S. C., Chen, G. D., and Sinex, D. G. (1999). Monaural response properties of single neurons in the chinchilla inferior colliculus. Hear Res *131*, 89-106.

Oliver, D. L., Beckius, G. E., Bishop, D. C., Loftus, W. C., and Batra, R. (2003). Topography of interaural temporal disparity coding in projections of medial superior olive to inferior colliculus. J Neurosci *23*, 7438-7449.

Oliver, D. L., Beckius, G. E., and Shneiderman, A. (1995). Axonal projections from the lateral and medial superior olive to the inferior colliculus of the cat: a study using electron microscopic autoradiography. J Comp Neurol *360*, 17-32.

Osen, K. K. (1972). Projection of the cochlear nuclei on the inferior colliculus in the cat. J Comp Neur *144*, 355-372.

Palmer, A. R., Liu, L. F., and Shackleton, T. M. (2007). Changes in interaural time sensitivity with interaural level differences in the inferior colliculus. Hear Res *223*, 105-113.

Pecka, M., Zahn, T. P., Saunier-Rebori, B., Siveke, I., Felmy, F., Wiegrebe, L., Klug, A., Pollak, G. D., and Grothe, B. (2007). Inhibiting the Inhibition: A Neuronal Network for Sound Localization in Reverberant Environments. J Neurosci *27*, 1782-1790.

Pollak, G. D., Burger, R. M., and Klug, A. (2003). Dissecting the circuitry of the auditory system. Trends Neurosci *26*, 33-39.

Pollak, G. D., Burger, R. M., Park, T. J., Klug, A., and Bauer, E. E. (2002). Roles of inhibition for transforming binaural properties in the brainstem auditory system. Hearing Research
A collection of papers presented at the Symposium on The Inferior Colliculus: From Past To Future *168*, 60-78.

Rakerd, B., and Hartmann, W. M. (2005). Localization of noise in a reverberant environment. In Auditory signal processing: Physiology, Psychophysics, and models, D. Pressnitzer, A. de Chevigne, S. McAdams, and L. Collet, eds. (Springer-Verlag), pp. 348-354.

Rakerd, B., Hartmann, W. M., and Pepin, E. (2006). Localizing noise in rooms via stead state interaural time differences. J Acoust Soc Am *120*, 3082-3083.

Rayleigh, L. (1907). On our perception of sound direction. Phil Mag *13*, 214-232.

Rees, A., and Moller, A. R. (1983). Responses of neurons in the inferior colliculus of the rat to AM and FM tones. Hear Res *10*, 301-330.

Rees, A., Sarbaz, A., Malmierca, M. S., and Le Beau, F. E. (1997). Regularity of firing of neurons in the inferior colliculus. J Neurophysiol *77*, 2945-2965.

Rose, J. E., Greenwood, D. D., Goldberg, J. M., and Hind, J. E. (1963). Some discharge characteristics of single neurons in the inferior colliculus of the cat. II. Timing of the discharges and observations on binaural stimulation. J Neurophysiol *26*, 321-341.

Rose, J. E., Gross, N. B., Geisler, C. D., and Hind, J. E. (1966). Some neural mechanisms in the inferior colliculus of the cat which may be relevant to localization of a sound source. J Neurophysiol *29*, 288-314.

Sakai, H., Sato, S.-i., and Ando, Y. (1998). Orthogonal acoustical factors of sound fields in a forest compared with those in a concert hall. J Acoust Soc Am *104*, 1491-1497.

Sally, S. L., and Kelly, J. B. (1992). Effects of superior olivary complex lesions on binaural responses in rat inferior colliculus. Brain Res *572*, 5-18.

Sanes, D. H., Malone, B. J., and Semple, M. N. (1998). Role of synaptic inhibition in processing of dynamic binaural level stimuli. J Neurosci *18*, 794-803.

Sayles, M., and Winter, I. M. (2008). Reverberation challenges the temporal representation of the pitch of complex sounds. Neuron *58*, 789-801.

Schwartz, A., Devore, S., and Delgutte, B. (2009). Effects of reverberation on directional sensitivity of auditory neurons: Periperal factors. Abstr Assoc Otolaryn, 622.

Scott, L. L., Mathews, P. J., and Golding, N. L. (2005). Posthearing Developmental Refinement of Temporal Processing in Principal Neurons of the Medial Superior Olive. J Neurosci *25*, 7887-7895.

Semple, M. N., and Kitzes, L. M. (1987). Binaural processing of sound pressure level in the inferior colliculus. J Neurophysiol *57*, 1-18.

Shackleton, T. M., Arnott, R. H., and Palmer, A. R. (2005). Sensitivity to Interaural Correlation of Single Neurons in the Inferior Colliculusof Guinea Pigs. JARO *6*, 244-259.

Shackleton, T. M., McAlpine, D., and Palmer, A. R. (2000). Modelling convergent input onto interaural-delay-sensitive inferior colliculus neurones. Hearing Research *149*, 199-215.

Shackleton, T. M., Meddis, R., and Hewitt, M. J. (1992). Across frequency integration in a model of lateralization. J Acoust Soc Am *91*, 2276-2279.

Shaw, E. A. G. (1974). Transformation of sound pressure level from the free field to the eardrum in the horizontal plane. Journal of the Acoustical Society of America *56*, 1848-1861.

Shinn-Cunningham, B. G. (2008). Object-based auditory and visual attention. Trends Cogn Sci *12*, 182-186.

Shinn-Cunningham, B. G., Desloge, J. G., and Kopco, N. (2001). Empirical and modeled acoustic transfer functions in a simple room: Effects of distance and direction. Paper

presented at: 2001 IEEE Workshop on Applications of Signal Prcessing to Audio and Acoustics (New Pfaltz, New York).

Shinn-Cunningham, B. G., and Kawakyu, K. (2003). Neural representation of source direction in reverberant space. Paper presented at: 2003 IEEE Workshop on Applications of Signal Processing to Audio and Acoustics (New Pfaltz, NY).

Shinn-Cunningham, B. G., Kopco, N., and Martin, T. J. (2005a). Localizing nearby sound sources in a classroom: Binaural room impulse responses. J Acoust Soc Am *117*, 3100-3115.

Shinn-Cunningham, B. G., Lin, I. F., and Streeter, T. (2005b). Trading directional accuracy for realism. Paper presented at: Human-Computer Interaction International / 1st International Conference on Virtual Reality.

Singh, N. C., and Theunissen, F. E. (2003). Modulation spectra of natural sounds and ethological theories of auditory processing. J Acoust Soc Am *114*, 3394-3411.

Sivaramakrishnan, S., and Oliver, D. L. (2001). Distinct K currents result in physiologically distinct cell types in the inferior colliculus of the rat. J Neurosci *21*, 2861-2877.

Smith, P. H. (1995). Structural and functional differences distinguish principal from nonprincipal cells in the guinea pig MSO slice. J Neurophysiol *73*, 1653-1667.

Smith, R. L., and Zwislocki, J. J. (1975). Short-term adaptation and incremental responses of single auditory-nerve fibers. Biol Cybernetics *17*, 169-182.

Smith, Z. M., and Delgutte, B. (2007). Sensitivity to interaural time differences in the inferior colliculus with bilateral cochlear implants. J Neurosci *27*, 6740-6750.

Spitzer, M. W., Bala, A. D. S., and Takahashi, T. T. (2004). A Neuronal Correlate of the Precedence Effect Is Associated With Spatial Selectivity in the Barn Owl's Auditory Midbrain. J Neurophysiol *92*, 2051-2070.

Spitzer, M. W., and Semple, M. N. (1991). Interaural phase coding in auditory midbrain: influence of dynamic stimulus features. Science *254*, 721-724.

Spitzer, M. W., and Semple, M. N. (1993). Responses of inferior colliculus neurons to time-varying interaural phase disparity: Effects of shifting the locus of virtual motion. J Neurophysiol *69*, 1245-1263.

Spitzer, M. W., and Semple, M. N. (1998). Transformation of Binaural Response Properties in the Ascending Auditory Pathway: Influence of Time-Varying Interaural Phase Disparity. J Neurophysiol *80*, 3062-3076.

Stecker, G. C., Harrington, I. A., and Middlebrooks, J. C. (2005). Location coding by opponent neural populations in the auditory cortex. PLoS Biol *3*, e78.

Stillman, R. D. (1971a). Characteristic delay neurons in the inferior colliculus of the kangaroo rat. Exp Neurol *32*, 404-412.

Stillman, R. D. (1971b). Pattern responses of low-frequency inferior colliculus neurons. Exp Neurol *33*, 432-440.

Stillman, R. D. (1971c). Pattern Responses of Low-Frequency Inferior Colliculus Neurons. Experimental Neurology *33*, 432-440.

Stillman, R. D. (1972). Responses of high-frequency inferior colliculus neurons to interaural intensity differences. Exp Neurol *36*, 118-126.

Svirskis, G., Kotak, V., Sanes, D. H., and Rinzel, J. (2004). Sodium along with low-threshold potassium currents enhance coincidence detection of subthreshold noisy signals in MSO neurons. J Neurophysiol *91*, 2465-2473.

Takahashi, T. T., Bala, A. D. S., Spitzer, M. W., Euston, D. R., Spezio, M. L., and Keller, C. H. (2003). The synthesis and use of the owl's auditory space map. Biological Cybernetics *89*, 378-387.

Tan, M. L., and Borst, J. G. G. (2007). Comparison of Responses of Neurons in the Mouse Inferior Colliculus to Current Injections, Tones of Different Durations, and Sinusoidal Amplitude-Modulated Tones 10.1152/jn.00174.2007. J Neurophysiol *98*, 454-466.

Ter-Mikaelian, M., Sanes, D. H., and Semple, M. N. (2007). Transformation of Temporal Properties between Auditory Midbrain and Cortex in the Awake Mongolian Gerbil. J Neurosci *27*, 6091-6102.

Thompson, G. C., and Masterton, R. B. (1978). Brain stem auditory pathways involved in reflexive head orientation to sound. J Neurophysiol *41*, 1183-1202.

Tollin, D. J., Populin, L. C., and Yin, T. C. T. (2004). Neural Correlates of the Precedence Effect in the Inferior Colliculus of Behaving Cats. J Neurophysiol *92*, 3286-3297.

Tollin, D. J., and Yin, T. C. (2002). The coding of spatial location by single units in the lateral superior olive of the cat. I. Spatial receptive fields in azimuth. J Neurosci *22*, 1454-1467.

Tollin, D. J., and Yin, T. C. (2005). Interaural phase and level difference sensitivity in low-frequency neurons in the lateral superior olive. J Neurosci *25*, 10648-10657.

Torterolo, P., Falconi, A., Morales-Cobas, G., and Velluti, R. A. (2002). Inferior colliculus unitary activity in wakefulness, sleep and under barbiturates. Brain Research *935*, 9-15.

Tsai, H.-C., Zhang, F., Adamantidis, A., Stuber, G. D., Bonci, A., de Lecea, L., and Deisseroth, K. (2009). Phasic Firing in Dopaminergic Neurons Is Sufficient for Behavioral Conditioning
10.1126/science.1168878. Science, 1168878.

van Adel, B. A., Kidd, S. A., and Kelly, J. B. (1999). Contribution of the commissure of Probst to binaural evoked responses in the rat's inferior colliculus: interaural time differences. Hear Res *130*, 115-130.

van Bergeijk, W. A. (1962). Variation on a Theme of Bekesy: A Model of Binaural Interaction. The Journal of the Acoustical Society of America *34*, 1431-1437.

Wallach, H., Newman, E. B., and Rosenzweig, M. R. (1949). The precedence effect in sound localization. J Am Psychol *57*, 315-336.

Wang, X., Lu, T., Snider, R. K., and Liang, L. (2005). Sustained firing in auditory cortex evoked by preferred stimuli. *435*, 341-346.

Wightman, F. L., and Kistler, D. J. (1992). The dominant role of low-frequency interaural time differences in sound localization. The Journal of the Acoustical Society of America *91*, 1648-1661.

Wu, S. H., Ma, C. L., Sivaramakrishnan, S., and Oliver, D. L. (2002). Synaptic modification in neurons of the central nucleus of the inferior colliculus. Hear Res *168*, 43-54.

Xie, R., Gittelman, J. X., and Pollak, G. D. (2007). Rethinking tuning: in vivo whole-cell recordings of the inferior colliculus in awake bats. J Neurosci *27*, 9469-9481.

Yin, T. C., and Chan, J. C. (1990). Interaural time sensitivity in medial superior olive of cat. J Neurophysiol *64*, 465-488.

Yin, T. C., Chan, J. C., and Carney, L. H. (1987). Effects of interaural time delays of noise stimuli on low-frequency cells in the cat's inferior colliculus. III. Evidence for cross-correlation. J Neurophysiol *58*, 562-583.

Yin, T. C., Chan, J. C., and Irvine, D. R. (1986). Effects of interaural time delays of noise stimuli on low-frequency cells in the cat's inferior colliculus. I. Responses to wideband noise. J Neurophysiol *55*, 280-300.

Yin, T. C., and Kuwada, S. (1983). Binaural interaction in low-frequency neurons in inferior colliculus of the cat. III. Effects of changing frequency. J Neurophysiol *50*, 1020-1042.

Yin, T. C., Kuwada, S., and Sujaku, Y. (1984). Interaural time sensitivity of high-frequency neurons in the inferior colliculus. J Acoust Soc Am *76*, 1401-1410.

Yin, T. C. T. (1994). Physiological correlates of the precedence effect and summing localization in the inferior colliculus of the cat. J Neurosci *14*, 5170-5186.

Young, E. D., and Brownell, W. E. (1976). Responses to tones and noise of single cells in dorsal cochlear nucleus of unanesthetized cats. J Neurophysiol *39*, 282-300.

Zhang, F., Prigge, M., Beyriere, F., Tsunoda, S. P., Mattis, J., Yizhar, O., Hegemann, P., and Deisseroth, K. (2008). Red-shifted optogenetic excitation: a tool for fast neural control derived from Volvox carteri. *11*, 631-633.